Jewell J. Hargleroad (SBN 130285)
Law Office of Jewell J. Hargleroad
1090 B Street, No. 104
Hayward, California 94541
(510) 331- 2975
jewellhargleroad@mac.com

Attorneys for Group Petitioners California Pilots Association, San Lorenzo Village Homes Association, Hayward Area Planning Association



STATE OF CALIFORNIA

STATE ENERGY RESOURCES

Conservation and Development Commission

| | |
|---|---|
| In the Matter of: | Docket No.: 06-AFC-6 |
| APPLICATION FOR CERTIFICATION FOR THE EASTSHORE ENERGY CENTER | **AMENDMENT TO GROUP PETITIONERS EXHIBIT LIST** |

On December 6, 2007, Group petitioners California Pilots Association ("Calpilots"), San Lorenzo Village Homes Association and Hayward Area Planning Association ("Hapa"), collectively referred to as "Group petitioners" served their exhibits delivering hard copies for filing and the hearing officer on December 7, 2007.

On Monday, December 10, 2007, the applicant's attorney inquired into whether Michael Toth, whose declarations filed in the Russell proceeding were included as exhibits, was going to testify. On Tuesday, December 11, 2007, counsel for Group Petitioners responded that Mr. Toth was "a potential rebuttal witness in air and public health concerning the data which has been referred to in the Final Staff Assessment and the applicable public records which were included in our exhibits, including his declarations submitted in the Russell proceeding."

Yesterday, counsel for the CEC staff stated the following in an email directed to Group Petitioners: "The only testimony Mr. Toth will be offering at the hearing is what is contained in

the two declarations you identified last Friday. Therefore, I assume that you do not mean that he will be offering new testimony on the stand, but that his declarations are a rebuttal of the FSA. Staff plans to cross examine Mr. Toth on the statements made in those declarations." Based on this, Group petitioners amend their exhibit list to include those documents which support Mr. Toth's declarations upon which staff wishes to examine. Attached is that amendment to the exhibit list, including those supporting documents. Hard copies will follow in the overnight delivery for the hearing officer.

Dated: December 12, 2007

Respectfully Submitted,

Jewell J. Hargleroad, Attorney for
Group Petitioners California
Pilots Association, San Lorenzo Village
Homes Association, and Hayward Area
Planning Association

# AMENDMENT TO GROUP PETITIONERS' EXHIBIT LIST

CEC Evidentiary Hearing for 06-AFC-6, Eastshore Energy Center

Documents in support of cross examination of Michael Toth regarding content of declarations submitted on behalf of Group's Petition To Reconsider in case 01-AFC-7C, Russell City Energy Center.

| Ex. # | Title | Source/Date | Relevance |
|---|---|---|---|
| 719 | Scientific Journal Article: "Acrolein is a major cigarette-related lung cancer agent: Preferential binding at p53 mutational hotspots and inhibition of DNA repair", Feng et al., PNAS 103 (42): 15404. (2006) | http://www.pnas.org/cgi/reprint/103/42/15404 Published: 8/17/2006 Retrieved: 12/11/2007 | Scientific research finding * Carcinogenicity of acrolein * Relation to carcinogenicity of Tobacco smoke |
| 720 | Scientific Journal Article: "Lung cancer, cardiopulmonary mortality, and long-term exposure to fine particulate air pollution." Pope, et al., JAMA. 2002 Mar 6;287(9):1132-41. PMID: 11879110 [PubMed - indexed for MEDLINE] | http://jama.ama-assn.org/cgi/reprint/287/9/1132 Published: 3/6/2002 Retrieved: 12/11/2007 | Scientific research finding * Relationship between increased ambient PM2.5 levels and health effects |
| 721 | Scientific Journal Article: "Reduction in fine particulate air pollution and mortality: Extended follow-up of the Harvard Six Cities study.", Laden, et al., Am J Respir Crit Care Med Vol 173. pp 667–672, 2006 | http://ajrccm.atsjournals.org/cgi/reprint/173/6/667 Published: 1/17/2006 Retrieved: 12/11/2007 | Scientific research finding * Relationship between decreased ambient PM2.5 levels and decreased health effects |
| 722 | Commissioned study: "IN-SITU ENGINE EMISSIONS TESTING AND COMPARISON FOR A HIGH SPEED FERRY AND COMPETING LAND TRANSIT VEHICLE, PHASE I: TASK 7.0: Final Report", Seaworthy Systems Inc., P.O. Box 965, Essex, CT 06426, prepared for Center for Commercial Deployment of Transportation Technologies (CCDoTT) California State University, Long Beach 6300 State University Drive, Long Beach, CA 90815 | http://www.ccdott.org/Deliverables/2001/task1.16/task%201.16.pdf Published: June 2002 Retrieved: 12/11/2007 | Documentation program for real-time, in-situ use of EPA test method 320 FTIR using a commercial subcontractor for detecting acrolein and other emissions in large maritime reciprocating internal combustion engines. |
| 723 | Product literature: "Gasmet In Situ Continuous Gas Monitoring analyzer", Avensys Inc. 400 Montpellier, Montreal, Quebec H4N 2G7, Tel: (514) 428-6766, Fax: (514) 428-8999 | http://www.avensyssolutions.com/data/File/Solutions/GASMET-In-Situ.pdf Retrieved: 12/11/2007 | Commercial in-situ real-time FTIR emissions monitoring product |
| 724 | Product literature: "Extractive FTIR Air Emissions Testing", GE Energy, 4200 Wildwood Parkway, Atlanta, GA 30339 | http://www.gepower.com/prod_serv/serv/env_serv/en/downloads/gea14569_ftir_techoverview.pdf Retrieved: 12/11/2007 | Commercial in-situ real-time FTIR emissions testing service, includes measurement of acrolein and formaldehyde for reciprocating internal combustion engines. |
| 725 | Scientific Journal Article: "Origin, Occurrence, and Source Emission Rate of | http://pubs.acs.org/cgi-bin/article.cgi/esthag/2007/41/ | Typical indoor and outdoor acrolein concentrations and activities |

| | | | |
|---|---|---|---|
| | Acrolein in Residential Indoor Air", Seaman, et al., Environ. Sci. Technol. 2007, 41, 6940-6946 | i20/pdf/es0707299.pdf Published: 10/2007 Retrieved: 11/17/2007 | associated with indoor concentrations. |
| 726 | "Source contributions to the mutagenicity of urban particulate air pollution.", Hannigan, et al., J Air Waste Manag Assoc. 2005 Apr;55(4):399-410. | http://secure.awma.org/journal/GetPdf.asp?id=1359 Published: 4/2005 Retrieved: 11/24/2007 | Largest source contributions to PM mutagenicity are natural gas combustion and diesel fueled vehicles. |

TECHNICAL PAPER

ISSN 1047-3289 J. Air & Waste Manage. Assoc. 55:399–410


# Source Contributions to the Mutagenicity of Urban Particulate Air Pollution

**Michael P. Hannigan**
*Mechanical Engineering Department, University of Colorado, Boulder, CO*

**William F. Busby, Jr.**
*Center for Environmental Health Sciences, Massachusetts Institute of Technology, Cambridge, MA*

**Glen R. Cass**
*Environmental Engineering Science Department, California Institute of Technology, Pasadena, CA*

## ABSTRACT

Using organic compounds as tracers, a chemical mass balance model was employed to investigate the relationship between the mutagenicity of the urban organic aerosol sources and the mutagenicity of the atmospheric samples. The fine particle organic mass concentration present in the 1993 annual average Los Angeles-area composite sample was apportioned among eight emission source types. The largest source contributions to fine particulate organic compound mass concentration were identified as smoke from meat cooking, diesel-powered vehicle exhaust, wood smoke, and paved road dust. However, the largest source contributions to the mutagenicity of the atmospheric sample were natural gas combustion and diesel-powered vehicles. In both the human cell and bacterial assay systems, the combined mutagenicity of the composite of primary source effluents predicted to be present in the atmosphere was statistically indistinguishable from the mutagenicity of the actual atmospheric sample composite. Known primary emissions sources appear to be capable of emitting mutagenic organic matter to the urban atmosphere in amounts sufficient to account for the observed mutagenicity of the ambient samples. The error bounds on this analysis, however, are wide enough to admit to the possible importance of additional mutagenic organics that are formed by atmospheric reaction (e.g., 2-nitrofluoranthene has been identified as an important human cell mutagen in the atmospheric composite studied here, accounting for ~1% of the total sample mutagenic potency).

**IMPLICATIONS**

Currently, regulations exist to control the total mass concentration of fine particulate matter (PM) in the ambient air. The ambient particle mixture is incredibly complex, and it is likely that different portions of the mixture exert different environmental stresses. Future regulations may need to focus on specific portions of the mixture. This study demonstrates a method of determining which portions of the particle mixture are responsible for a specific environmental stress. The method was employed to investigate the origin of the mutagenicity of the ambient PM, and it was found that further study of natural gas combustion emissions may be warranted.

## INTRODUCTION

A major aim of most air pollution control programs is to limit the atmospheric concentrations of pollutants that could cause adverse effects on human health. Careful design of an emission control program requires knowledge about the connections between pollutant source emissions, atmospheric transport and chemical transformation, and the ambient pollutant concentrations to which people are exposed. Such source-to-receptor relationships often are determined through computer-based air quality models by solving continuity equations for individual compounds or compound classes, and often the pollutant species being tracked is essentially a simplified index for the presence of a much more complex pollutant mixture. In the case of particulate air pollution, the presently regulated indices of pollutant exposure in the United States are defined in terms of the airborne particle mass concentration contributed by particles with a diameter smaller than 10 μm ($PM_{10}$) and by particles with a diameter smaller than 2.5 μm ($PM_{2.5}$).

Urban particulate air pollution contains an extremely complex mixture of thousands of different organic compounds, many present in only trace amounts, along with acid aerosols and trace metals, plus a much larger amount of likely harmless but bulky material from other sources,

such as airborne soil dust and sea salt. By focusing attention on particle mass concentration, even the $PM_{2.5}$ mass concentration, it is entirely likely that those chemical components of the particulate air pollution mixture that actually are capable of inducing the sort of biological changes that could affect health will be missed entirely.

Certain chemical components of the particulate air pollution mixture are capable of inducing genetic damage. Particulate air pollution has been shown to be mutagenic to bacteria[1–7] and human cells[8,9] and carcinogenic to mice.[10] Using bioassay-directed chemical analysis and bacterial mutagenicity as the biological endpoint, several studies[4,11–13] have attempted to identify the specific chemical species present in atmospheric particles that can cause genetic damage. In a program of bioassay-directed chemical analysis, the organic extracts of atmospheric particles containing complex mixtures of compounds are fractionated chemically and tested for mutagenicity in an iterative process until the mutagenic fractions are amenable to chemical analysis. In this way, the most important mutagens in the complex atmospheric sample can be identified and quantified. PM emissions from sources such as diesel engine exhaust also have been studied using bioassay-directed chemical analysis.[13–15] The effluents from automobile exhaust, coal-fired furnaces, and kerosene flames have been examined using different biological endpoints, such as carcinogenicity in mice[16–18] and human cell mutagenicity.[19]

Determining the effect of air pollution sources on the mutagenic potency of atmospheric PM based on the existing scientific literature is difficult at best. Several biological endpoints have been used to create the existing database on emission source characteristics. Furthermore, important differences exist in the procedures used by different laboratories to collect and analyze air pollution samples even when the bioassay procedures to be applied to the samples are nominally similar.[20–22] These differences between laboratories can significantly obscure comparisons between the properties of source samples and atmospheric samples that were analyzed by different research groups. In addition, the list of air pollutant emission sources studied to determine their mutagenic potency is quite short, with much of the previous work being focused on one source, diesel engine exhaust.

The present study seeks to establish methods for determining the contributions of specific fine particle emissions sources to the human cell mutagenicity of ambient particulate air pollution. Methods developed were tested in the Los Angeles area using data on the organic chemical composition and human cell mutagenicity of a comprehensive set of atmospheric fine particle samples and a comprehensive set of urban organic aerosol source samples, both collected specifically for use in this study. The analysis proceeds by first determining the contribution of specific fine particle emission sources to the ambient fine particle organic compound mass concentration, using a previously developed chemical mass balance receptor modeling technique that uses organic compounds as tracers.[23–25] The calculated source contributions were used along with the human cell mutagenic potency values [mutant fraction per μg of fine particulate organic carbon (OC) emitted from the source] for each emission source to determine the mutagenic density (mutant fraction per $m^3$ of air) of the ambient aerosol that would exist if atmospheric chemical reactions were unimportant to transformation of the ambient mixture. This calculated mutagenic density of the ambient fine particle mixture then can be compared with the measured value, and the importance of specific sources and secondary chemical reactions can be evaluated.

Filter samples collected throughout the course of 1993 at four air monitoring sites in southern California were used here to create a composite fine particulate air pollution sample that is representative of long-term exposure conditions in southern California. A comprehensive set of urban fine particle emission source samples, which represent ~80% of the fine organic PM emissions in the Los Angeles area,[26] is analyzed in the present study to describe the character of primary source emissions. The human cell mutation assay[27] used in this study tests for mutagenic activity at the thymidine kinase locus in the h1A1v2 cell line (AHH-1 TK± cells bearing the plasmid pHSRAA, which contains two copies of the human CYP1A1 cDNA). For purposes of comparison against earlier studies, the bacterial mutagenicity of the source and ambient samples also will be explored. The bacterial mutation assay used is a version of the *S. typhimurium* TM677 forward mutation assay developed by Skopek and coworkers,[28] which measures resistance to 8-azaguanine.

## EXPERIMENTAL METHODS

### Ambient Samples

An urban particulate air pollution sample representative of exposure conditions in the greater Los Angeles area was created by compositing a portion of every urban fine particulate filter sample collected during a 1993 southern California air monitoring campaign. This air monitoring campaign was described in more detail elsewhere.[8,29] Individual urban particulate air pollution samples were taken for 24 hr every sixth day for the entire year of 1993 at four urban sites. These urban sites were chosen in an attempt to capture the variety of typical PM exposures seen in the South Coast air basin: a highly industrialized area, Long Beach; a location that experiences dense freeway traffic, central Los Angeles; a downwind residential area with high ozone and secondary

aerosol concentrations, Azusa; and a site even farther downwind with even more secondary aerosol, Rubidoux.

To collect a large volume of size-separated organic aerosol in a 24-hr period, a high-volume dichotomous virtual impactor was employed at each site. Details of the design of this sampler are given by Solomon and co-workers,[30] and a description of its use for this sampling campaign can be found elsewhere.[8,29] When operated at a nominal flow rate of 175 L/min, this sampler produced a size cut between fine and coarse particles at ~3–4 μm aerodynamic diameter. Quartz fiber filters were used for the PM collection, and details of the filter-handling procedures are given by Hannigan et al.[29] One-sixth of each fine particle filter was extracted to form the composite sample used here. This composite physically represented the annual average ambient fine PM concentration averaged over all four urban sites. All sample and organic aerosol extract mass is reported in units of μg of equivalent OC (EOC), which is defined as the amount of OC present on the filter sections before extraction as determined by thermal evolution and combustion analysis[31,32] of separate sections cut from the same quartz fiber filters. The EOC measure provides a link from the assay results to the ambient organic aerosol concentrations.

In addition to the high-volume dichotomous sampler, a low-volume fine particle sampler employing an Air and Industrial Hygiene Laboratory (AIHL)-design cyclone separator[33] was located at each sampling site during the 1993 field measurement campaign. For the collection of fine PM (diameter less than 2 μm), the sampler was equipped with two quartz fiber filters, each operated at a flow rate of 10 L/min, and two polytetrafluoroethylene (PFTE) filters operated at flow rates of 3 L/min and 5 L/min. Samples collected on the PFTE filters were used for inorganic chemical analysis as well as for the determination of the total fine particle mass concentration. Details of the operation of this sampler can be found elsewhere.[29] To examine the differences associated with the slightly different size cuts of each type of sampler, elemental carbon (EC) and OC were measured on all quartz fiber filters collected using the low-volume sampler as well as the high-volume sampler. Plotting the pollutant concentration measured with the high-volume sampler versus the concentration measured over the same time period with the low-volume sampler yields a slope of 1.03 ± 0.02 for EC and a slope of 0.90 ± 0.02 for OC. The high-volume sampler actually collected slightly less OC than the low-volume sampler even though the size cut for the high-volume sampler is slightly larger. The artifacts associated with volatilization and adsorption affect the mass of organics collected more than a small-size cut difference. An excellent discussion of these artifacts is presented by Turpin and co-workers.[34] Both samplers collect essentially the same amount of EC.

### Source Samples

The aerosol source samples used in the present study were collected by Hildemann and co-workers[26,35] using a portable dilution source sampling system. The sampling strategy focused on obtaining representative samples from 15 source types that collectively accounted for ~80% of the fine organic aerosol emissions to the atmosphere in the Los Angeles area. All 15 source types are shown in Table 1. All samples were collected on quartz fiber filters, which were prepared and stored by the same procedures as those used for ambient samples. Variability between sources of the same type is addressed by compositing samples from several sources (e.g., a small fleet of different motor vehicles) before extraction and bioassay (Table 1). In a previous study using bacterial mutation assays, five non-combustion sources from among the 15 source types studied here were determined to be non-mutagenic at dose levels at which the other 10 were active.[36] Further biological analysis using the human cell assay in the present study was conducted only for that group of 10 mutagenic source types. During the course of the human cell bioassays, the diesel sample was fully consumed and was replaced by extract prepared from the SRM 1650 diesel exhaust aerosol sample distributed by the National Institute of Standards and Technology. Concurrently with the execution of the new human cell assays of these source samples, sample extracts were retested in the bacterial assay system to obtain further direct comparison of the mutagenic potency of the source and ambient samples in both the bacterial and human cell systems.

### Extract Preparation

All source and ambient PM filter samples used in this study were extracted in soxhlets with dichloromethane for at least 16 hr. Extracts were concentrated in a vacuum centrifuge. Further concentration or solvent exchange into dimethyl sulfoxide (DMSO) for assay testing was accomplished by blowing a gentle stream of dry ultrapure nitrogen over the sample. The extracted mass from a portion of the composited ambient aerosol sample was measured by a microscale evaporation method[37] and was compared with the mass of OC (EOC) originally present on the filter samples before extraction as determined by thermal evolution and combustion analysis.[31,32] The results of this test showed 0.93 ± 0.07 μg of extracted mass per μg of EOC. For a more detailed description of the filter extraction procedure, see Hannigan et al.[36]

### Human Cell Mutation Assay

The procedures for the routine use of the h1A1v2 cell line for mutagenicity testing at the thymidine kinase (*tk*) locus were given by Penman et al.[27] and Busby et al.[38] Allquots of sample extract were tested by exposing duplicate

**Table 1.** Summary of bioassay results for the particle emission sources.

| Source Sample | Human Cell Mutagenic Potency[a] [IMF (×10⁶) per μg EOC] | Bacterial Assay Mutagenic Potency[b] −PMS [IMF (×10⁶) per μg EOC] | Bacterial Assay Mutagenic Potency[b] +PMS [IMF (×10⁶) per μg EOC] | Lumped Source Type[c] |
|---|---|---|---|---|
| Catalyst-equipped automobiles | 0.11 ± 0.04 | 2.8 ± 0.95 | 0.37 ± 0.03 | 1 |
| Noncatalyst automobiles | 0.40 ± 0.07 | 2.3 ± 0.10 | 0.83 ± 0.07 | 1 |
| Heavy-duty diesel trucks | 0.18 ± 0.04[d] | 5.1 ± 2.9 | 0.76 ± 0.08 | 2 |
| Fuel oil-fired boiler | 0.07 ± 0.02 | 1.0 ± 0.61 | 0.70 ± 0.27 | |
| Natural gas home appliances | 4.1 ± 1.4 | 13 ± 4.7 | 16 ± 2.9 | 3 |
| Fireplace, pine combustion | 0.08 ± 0.03 | 1.4 ± 0.15 | 0.15 ± 0.04 | 4 |
| Fireplace, oak combustion | 0.08 ± 0.08 | 2.9 ± 0.43 | 0.11 ± 0.10 | 4 |
| Fireplace, synthetic log | 0.00 ± 0.01 | 0.39 ± 0.07 | 0.00 ± 0.09 | |
| Cigarette smoke | 0.01 ± 0.01 | 0.10 ± 0.05 | 0.07 ± 0.02 | 5 |
| Roofing tar pot | 0.10 ± 0.07 | 0.07 ± 0.01 | 0.07 ± 0.05 | |
| Meat charbroiling | ND | – | – | 6 |
| Paved road dust | ND | – | – | 7 |
| Brake wear dust | ND | – | – | |
| Tire wear debris | ND | – | – | 8 |
| Urban vegetative detritus | ND | – | – | 9 |

[a]The human cell mutagenic potency value represents an estimate of the initial slope of the dose/response relationship obtained using a least-squares linear fit to the data that was forced through the origin (zero dose by definition yields zero IMF). Only those source samples that tested positive in the bacterial assay were tested in the human cell assay; the human cell mutagenic potency for the other source samples is labeled not determined (ND); [b]The bacterial assay mutagenic potency was estimated under two assay conditions, with the addition of PMS (referred to elsewhere as S9) and in the absence of PMS. The potency value is determined by calculating the initial slope of the dose/response curve using a least-squares linear fit to the data. A dash indicates that the sample was not mutagenic at the dose levels tested; [c]Lumped source type numbers indicate which source sample chemical fingerprints were combined to form a single lumped source type for use in the chemical mass balance model. No number indicates that these sources were not used in the chemical mass balance model; [d]Human cell mutagenic potency value for heavy-duty diesel trucks is based on testing extract of the NBS SRM 1650 diesel exhaust PM sample.

12-mL cultures of $1.8 \times 10^6$ exponentially growing cells for 72 hr. Exposure was terminated by centrifuging and resuspending the cells in fresh media (30 mL). One day after the exposure was terminated, the cultures were counted and diluted to 80 mL at $2 \times 10^5$ cells/mL. After the 3-day phenotypic expression period, cultures were plated in 96-well microtiter plates in the presence of the selective agent to determine mutagenicity ($n = 3$ with 20,000 cells per well) and in the absence of the selective agent to determine plating efficiency ($n = 2$ with two cells per well). The selective agent used for this forward mutation assay was trifluorothymidine. After an additional 13-day incubation period, the plates were scored for the presence of a colony in each well. The positive control sample consisted of 1 μg/mL benzo[*a*]pyrene (BaP), and DMSO was used as the negative control.

Plating efficiencies, mutant fractions, and their associated confidence intervals (standard deviations) were calculated using methods described by Furth et al.[39] Each sample was tested in a minimum of two independent assays to ensure test reproducibility, and the results of each independent assay were pooled. To control for varying background mutation rates (i.e., variations in the concurrent negative controls from one experiment to another), the results from all experiments were converted to induced mutant fraction (IMF) by subtracting the mean mutant fraction of the concurrent negative control from the mean mutant fraction observed for the sample extracts. The mutagenic potency of a sample was defined as the IMF per μg EOC supplied to the test. The mutagenic potency of each sample was estimated by pooling all experimental points for each sample and then computing the initial slope of the dose/response relationship using a least-squares fit to the data that was forced through the origin (because at zero dose, there is, by definition, zero IMF). This technique was used previously to evaluate the seasonal and spatial variation of the human cell mutagenicity of southern California airborne fine particle samples.[8]

### Bacterial Mutation Assay

A detailed description of the procedures for the routine use of the *S. typhimurium* forward mutation assay can be found elsewhere.[28,40] Briefly, the suspended bacteria underwent a 2-hr exposure to several dilutions of the sample. The exposure was done under two conditions, with or

without the presence of 5% (v/v) Aroclor-induced post-mitochondrial supernatant preparation (PMS, also referred to elsewhere as S9). After the exposure period, the reaction was quenched and aliquots were plated in the presence and absence of 50 μg/mL of 8-azaguanine. The results from a minimum of four independent cultures, each plated in triplicate, were averaged to estimate toxicity and mutagenicity at each sample dilution. Colonies were counted after 48 hr. The mutant fraction (i.e., mutagenicity) was determined as the number of colonies formed in the presence of 8-azaguanine divided by the number of colonies formed in its absence, multiplied by a dilution factor. Positive concurrent control samples (BaP for +PMS and 4-nitroquinoline oxide for −PMS) and negative concurrent control samples (DMSO, both +PMS and −PMS) were processed in parallel with each sample. The bacterial mutagenic potency was determined by calculating the initial slope of the dose-response curve using a least squares linear fit to the data. It is known that the TM677 strain used for this study does possess nitroreductase; 1-nitropyrene (1-NP), 4-NP, 1,3-dinitropyrene (1,3-DNP), 1,6-DNP, and 1,8-DNP are all potent −PMS mutagens in this strain of TM677.[40]

### Chemical Analysis

Organic chemical analysis by gas chromatography/mass spectrometry (GC/MS) was conducted to quantify mutagenic compounds in both the source and ambient samples as well as to quantify the concentration of organic compounds that act as tracers for the presence of the effluent from specific sources when found in an ambient sample.[23,24] Procedures used for GC/MS analysis in the present study are given in detail elsewhere.[41] All GC/MS analyses used in the source apportionment phase of this study were done in full scan mode using co-injection of a known amount of 1-phenyl dodecane as a measure of instrument response. For quantification of each organic compound, relative response factors were obtained from multiple injections of an authentic standard or from multiple injections of a compound with a similar molecular weight (MW) and functionality. A 45-component standard mixture was injected periodically between sample injections to ensure that instrument performance was stable throughout the long series of analyses.

The concentration of the trace elements aluminum (Al) and silicon (Si) required for use by the source apportionment technique[23] were determined by X-ray fluorescence analysis[42] applied to samples collected on 47-mm-diameter PFTE filters collected in parallel with each of the quartz fiber filters used for source and ambient measurements. EC and OC concentrations present on sections cut from the source sample filters were determined by the thermal evolution and combustion method.[31,32]

### Chemical Mass Balance Model

A previously published chemical mass balance model that uses organic compounds as tracers for the presence in the atmosphere of the emissions from specific sources[23–25] was used in this study. Details of this source apportionment technique were given by Schauer and co-workers.[23] Briefly, the concentration of a specific compound in the ambient sample is described as a linear combination of emissions of that specific compound from the various emission sources. Using strict chemical species selection criteria, Schauer and co-workers[23] developed a list of organic chemical species, plus EC, Al, and Si, to apportion the fine organic aerosol concentration and fine particle mass concentration in the Los Angeles-area atmosphere between the contributing sources considered herein. This compound list was used as a starting point for the present study.

The selection of emission source types also was important. If two emission source types had similar chemical fingerprints, then they would have been indistinguishable. Therefore, some grouping of similar source types occurred for the model to generate useful results. For the Los Angeles-area source samples used here, the pine and oak wood combustion source profiles were combined to produce an emissions-weighted average source profile for wood smoke, and the catalyst plus noncatalyst gasoline-powered motor vehicle exhaust profiles were combined to produce an emissions-weighted average profile for gasoline-powered vehicles. The composite woodsmoke profile was assembled exactly as described by Schauer and co-workers.[23] The gasoline-powered motor vehicle exhaust composite profile was recalculated as a weighted average of the catalyst and noncatalyst engine exhaust samples assembled to reflect a 1993 mixture of emissions from catalyst versus noncatalyst vehicles according to the 1993 vehicle mileage tables published by the South Coast Air Quality Management District[43] plus estimates of off-road gasoline engine use.

Diesel engine emissions were distinguished from gasoline-powered vehicle engine emissions in part by the larger fraction of black EC in diesel exhaust. In recent years, diesel engine emission control technology has improved greatly, creating a vehicle fleet in current use that represents a mixture of old and newer technology engines with varying emissions ratios of EC to organic compounds. In the present study, a fleet average ratio of EC to particulate organic compounds from on-road diesel vehicles first was computed from the literature review of diesel engine emissions characteristics as a function of production era reported by Sawyer and Johnson[44] combined with estimates of relative annual mileage accumulation by trucks and autos of different ages.[45,46] The analysis suggests that diesel engine emissions in the South Coast

Air Basin surrounding Los Angeles in 1993 should consist of ~33% EC and 31% organic compounds by mass, plus trace amounts of Si and Al, as measured in diesel exhaust by Hildemann and co-workers.[26] The combined diesel engine profile used in the present study thus consists of EC, Al, Si, and total organics in those proportions, with the relative composition of the organic compounds taken from the GC/MS analysis of filter samples taken during the source tests of Hildemann and co-workers.[26]

The completed source profiles for the nine emissions source types showing the relative concentration of tracer compounds that were supplied to the chemical mass balance model are given in Figures 1–5. All chemical compound concentrations in the source samples supplied to the human cell assay in this study were based on new GC/MS analyses of high-volume filter samples collected by Hildemann and co-workers[26,35,47] because those high-volume filters were the source of the organic material used in the new human cell bioassays and because the ambient samples used here were taken with high-volume dichotomous samplers. Analysis of the five source samples that were found to be nonmutagenic in previous work consisted solely of quantification of tracer compounds used in the source apportionment calculations, and therefore, previously generated extracts of these samples were used. A description of the sample extraction and concentration protocol used for the five nonmutagenic source samples can be found in Mazurek et al.[48] Elimination of variation in analytical conditions and techniques made it necessary to quantify the organic compound concentrations in all source and ambient samples used in the chemical mass balance model on the same instrument, with the same protocol, over a short period of time. By processing both source and ambient samples by GC/MS simultaneously, any biases caused by chemical analysis procedures were equalized between the source and ambient samples, which in turn aided the matching of source profiles to the ambient samples.

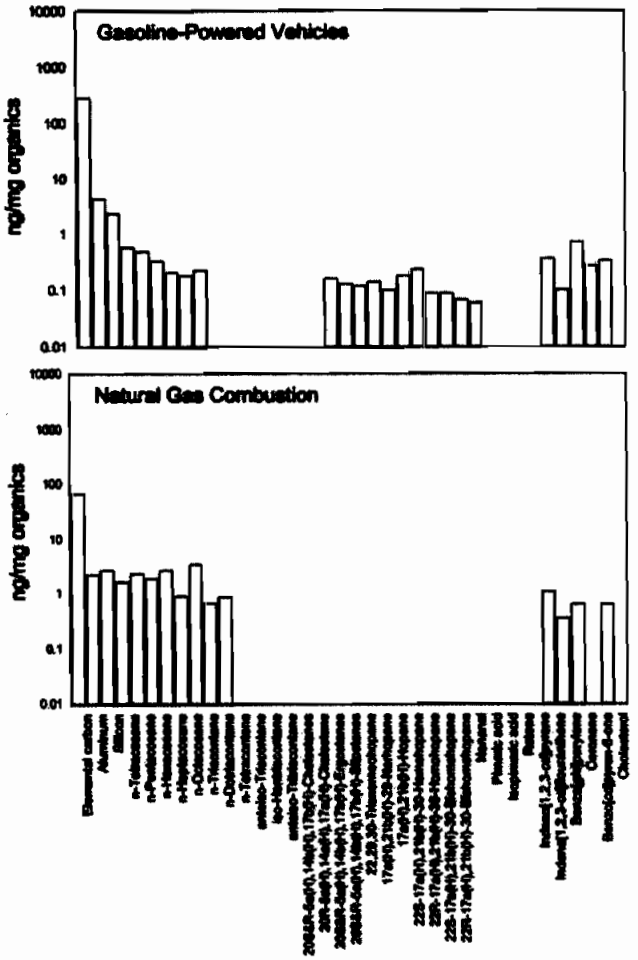


**Figure 1.** Source profiles for gasoline-powered vehicle exhaust aerosol and natural gas combustion particles.

## RESULTS

### Apportionment of Fine Particulate Organic Mass

The chemical mass balance model constructed previously by Schauer and co-workers[23,24] was used to apportion the fine organic PM in the Los Angeles-area 1993 annual composite sample between nine source types. These source types include diesel vehicles, gasoline-powered vehicles, paved road dust, tire wear debris, wood combustion, cigarette smoke, meat cooking, urban vegetative detritus, and natural gas combustion. Improvements were made to the model based on the more extensive set of chemical species available from the present series of chemical analyses. The most volatile polyaromatic hydrocarbons (PAHs) and oxy-polyaromatic hydrocarbons used by Schauer et al.,[23] benzo[*k*]fluoranthene, benzo[*b*]fluoranthene, benzo[*e*]pyrene, 7H-benzo[*de*]-anthracen-7-one, and benz[*a*]anthracen-7,12-dione, were removed from the model and replaced with a very nonvolatile PAH, coronene. The most volatile n-alkane used by Schauer et al.,[23] n-tricosane, was also removed from the calculation because it has been determined to partition significantly into the vapor phase.[49] The potentially reactive olefinic acid, oleic acid, previously used as part of the mass balance for detecting meat smoke, was replaced by a better meat smoke tracer, cholesterol, which is now quantifiable in the ambient samples. Base case (i.e., use of the chemical mass balance as prescribed by Schauer et al.[23] with these improvements) mass balance calculations yielded a result in which one of the minor source types, urban vegetative detritus, did not contribute a statistically significant portion of fine particle organic mass. Therefore, the chemical mass balance model was reconstructed in such a way that any compound in the mass balance calculation that could be coming in significant amounts

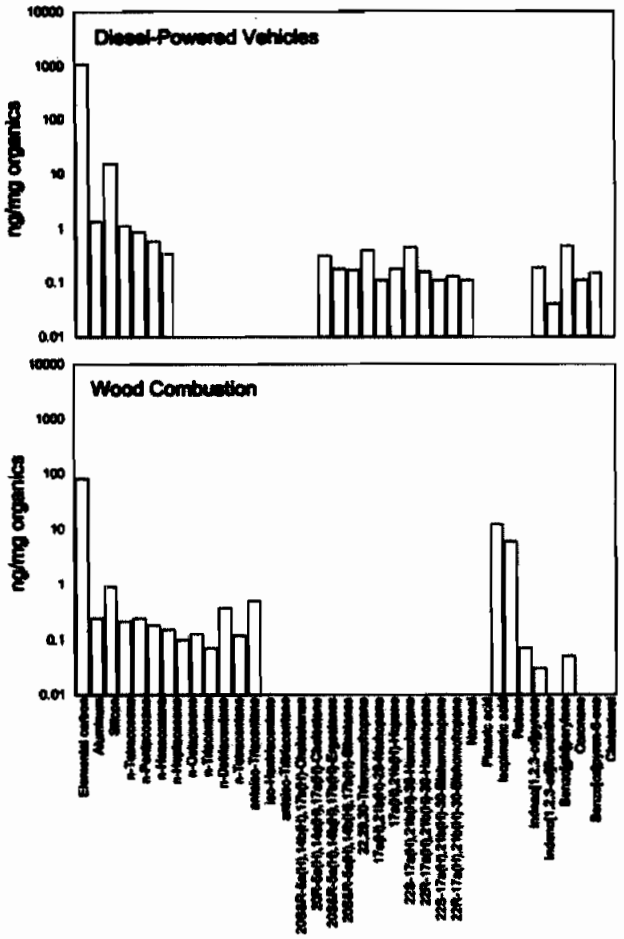


**Figure 2.** Source profiles for diesel-powered vehicle exhaust aerosol and wood combustion particles.

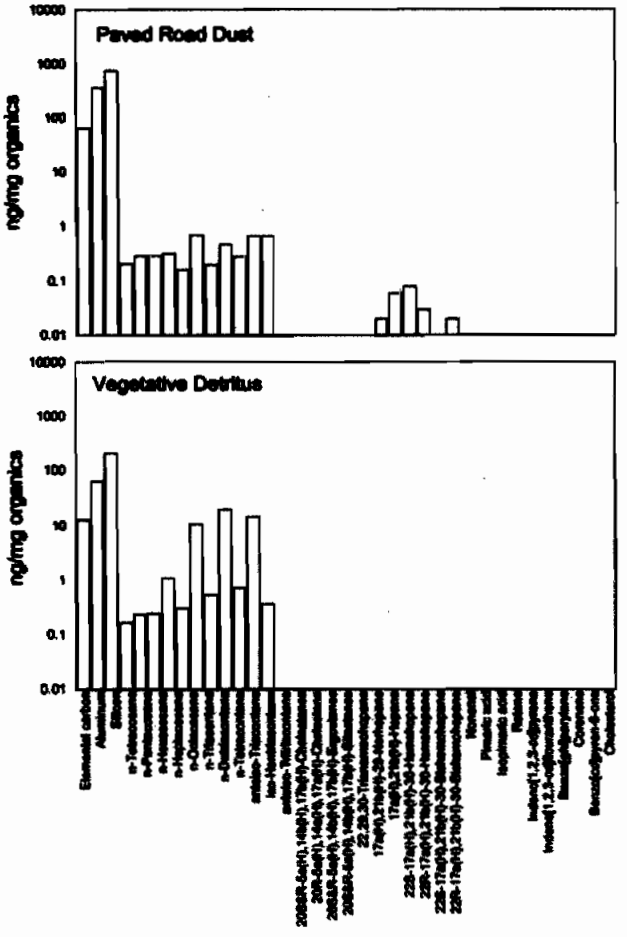


**Figure 3.** Source profiles for paved road dust and vegetative detritus.

from vegetative detritus is not used in fitting the model to the ambient data. The model then was fit to the eight remaining source types.

A comparison of the calculated and measured ambient concentrations for each of the mass balance chemical species is shown in Figure 6. There is generally good agreement among the calculated and measured values across the 34 diverse compounds and three elements used in the chemical mass balance. The mean (± standard deviation of the population) of the ratio of calculated to measured concentrations for each chemically distinct tracer group is 0.83 (±0.32) for the n-alkanes, 1.15 (±0.33) for the iso- and anteiso-alkanes, 1.01 (±0.23) for the steranes and hopanes, 1.13 (±0.51) for the conifer resin acids and their thermal alteration products, and 1.01 (±0.38) for the PAH.

The calculated source contributions to the Los Angeles-area 1993 annual average particulate organics mass concentration are given in Table 2. The largest contributors to the fine particulate organics mass are meat cooking, wood combustion, diesel engine exhaust, tire wear, and gasoline-powered vehicles. These results generally agree with the previous work by Schauer et al.,[23] which apportioned the fine particulate organic mass in the Los Angeles-area atmosphere based on data collected in 1982. These researchers found fine particle tire wear to account for 0.00–0.13 μg organics/$m^3$ (versus 0.62 ± 0.20 μg/$m^3$ in the present study), fine particle paved road dust to account for 0.49–0.89 μg organics/$m^3$ (versus 0.46 ± 0.09 μg/$m^3$ in the present study), cigarette smoke to account for 0.13–0.19 μg organics/$m^3$ (versus 0.39 ± 0.06 μg/$m^3$ in the present study), meat cooking to account for 1.22–1.69 μg organics/$m^3$ (versus 2.77 ± 0.55 μg/$m^3$ in the present study), wood combustion to account for 0.31–1.57 μg organics/$m^3$ (versus 0.95 ± 0.42 μg/$m^3$ in the present study), gasoline-powered vehicles to account for 0.25–1.56 μg organics/$m^3$ (versus 0.61 ± 0.29 μg/$m^3$ in the present study), and diesel vehicles to account for 1.02–2.72 μg organics/$m^3$ (versus 0.84 ± 0.20 μg/$m^3$ in the present study). The main differences between the 1982 and 1993 results are the increase in the tire wear

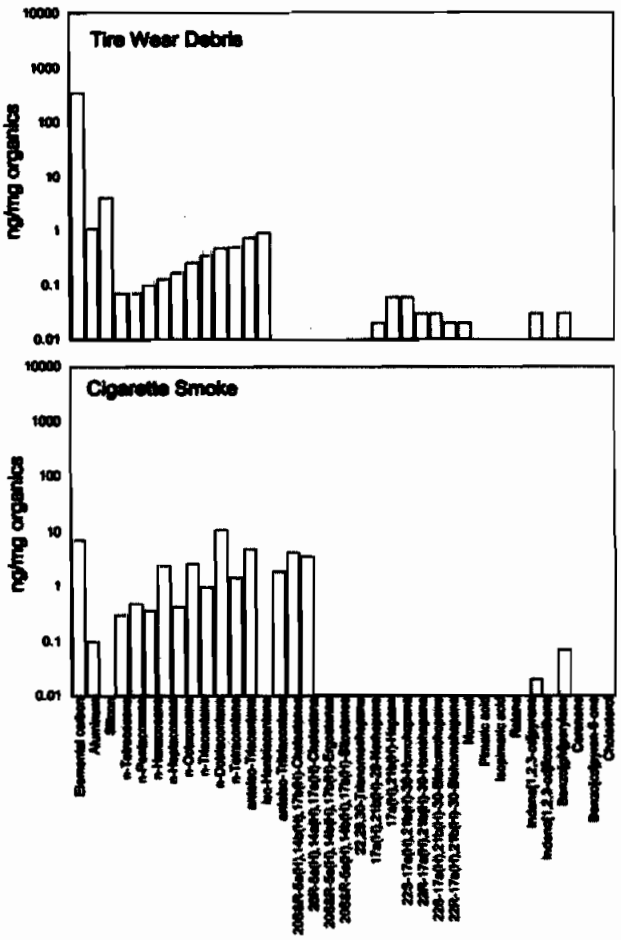


**Figure 4.** Source profiles for tire wear debris and cigarette smoke.

contribution, the increase in the meat cooking contribution, and the reduction in the contribution from diesel vehicles. Tire wear is present in the paved road dust sample,[50] and these two sources can be difficult to resolve separately. The combination of the two contributions is similar to the previous study. The increase in the contribution from meat cooking is caused by the use of a more atmospherically stable compound (cholesterol) in the model. The reduction in the contribution from diesel vehicles has been documented by Christoforou and coworkers,[51] who illustrate the decline in black EC concentration in the Los Angeles atmosphere over the period 1982–1993. That decline is consistent with the introduction of cleaner diesel engine technologies and cleaner diesel fuels over the period 1982–1993.[44] Each of the source contributions calculated in the 1993 study is significantly different from 0 with 95% confidence.

The sum of the calculated source contributions to ambient fine particulate organics mass can be compared with the measured ambient fine particulate organics mass concentration. The observed 1993 annual average fine

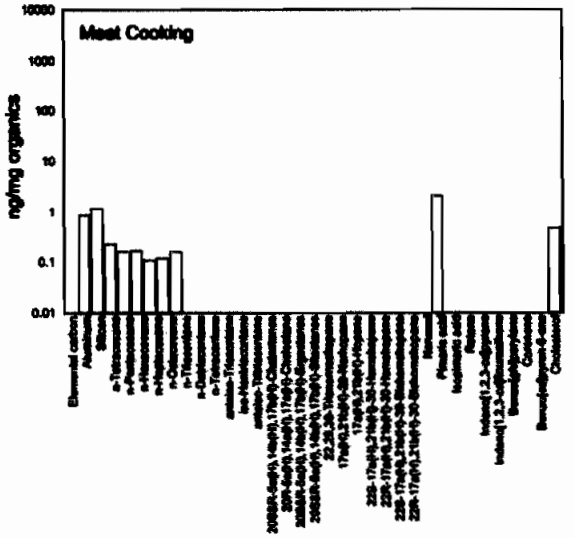


**Figure 5.** Source profile for meat cooking aerosol.

particulate organics mass concentration measured by high-volume sampling is 10.67 ± 0.98 $\mu g/m^3$ as calculated by multiplying the fine particulate OC concentration by 1.2 to account for the mass of elements other than carbon. The use of the 1.2 factor for ambient samples is open for debate; see refs 52 and 53 for further discussion. Conversion of fine particulate OC mass concentration to organics mass concentration for primary emissions typically involves the use of the 1.2 factor.[50,54–58] The focus of this study is the apportionment of the fine particulate organics mass concentration via chemical mass balance, not calculating organics mass closure via summation of individual species mass concentrations. Using the same OC to organics conversion factor for the source and ambient samples is vital to the successful application of the

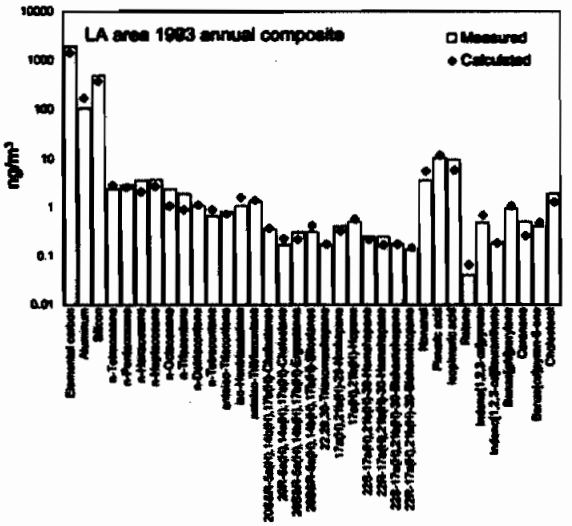


**Figure 6.** Comparison of model predictions to measured ambient concentrations for the chemical mass balance compounds.

**Table 2.** Summary of source contributions to fine ambient organic aerosol annual average mass concentration and mutagen density in the Los Angeles study area during 1993.

| Source Type | Source Type Contribution ($\mu$g organics per m$^3$) | Human Cell Mutagen Density Contribution[a] IMF ($\times 10^6$) per m$^3$ | Bacterial Assay Mutagen Density Contribution[b] +PMS [MF ($\times 10^6$) per m$^3$] | −PMS [MF ($\times 10^6$) per m$^3$] |
|---|---|---|---|---|
| Diesel-powered vehicles | 0.84 ± 0.20 | 0.15 ± 0.05 | 0.84 ± 0.17 | 4.30 ± 2.65 |
| Tire wear debris | 0.62 ± 0.20 | ND | 0 | 0 |
| Paved road dust | 0.46 ± 0.09 | ND | 0 | 0 |
| Urban vegetative detritus[c] | 0 | ND | 0 | 0 |
| Natural gas combustion | 0.24 ± 0.10 | 0.98 ± 0.53 | 4.78 ± 2.12 | 3.11 ± 1.72 |
| Cigarette smoke | 0.39 ± 0.06 | 0.004 ± 0.004 | 0.03 ± 0.01 | 0.04 ± 0.02 |
| Meat cooking | 2.77 ± 0.52 | ND | 0 | 0 |
| Gasoline-powered vehicles | 0.61 ± 0.29 | 0.12 ± 0.06 | 0.31 ± 0.15 | 1.62 ± 0.87 |
| Wood combustion | 0.95 ± 0.42 | 0.08 ± 0.04 | 0.13 ± 0.07 | 1.61 ± 0.73 |
| Sum | 6.89 ± 0.80 | 1.33 ± 0.54 | 5.89 ± 2.13 | 10.67 ± 3.36 |
| Measured | 10.67 ± 0.98 | 1.60 ± 0.35 | 2.67 ± 0.40 | 14.08 ± 4.56 |
| Ratio | 0.65 ± 0.10 | 0.83 ± 0.38 | 2.21 ± 0.87 | 0.76 ± 0.34 |

[a]The human cell mutagen density contribution is calculated by multiplying the relative source contribution ($\mu$g EOC per m$^3$ air) by the source's human cell mutagenic potency [IMF ($\times 10^6$) per $\mu$g EOC]. Only those source samples that tested positive in the bacterial assay were tested in the human cell assay; therefore, the human cell mutagenic potency contribution for the other source samples is labeled not determined (ND), even though it is expected to be close to zero; [b]The bacterial assay mutagen density contribution is calculated by multiplying the relative source contribution ($\mu$g EOC per m$^3$ air) by the source's bacterial mutagenic potency; [c]The contribution of this source to the ambient sample fine particle organic compound concentration in 1993 is not significantly different from zero; therefore, this source was removed from the model calculations.

chemical mass balance model and, therefore, the 1.2 factor was chosen.

The sum of the calculated source contributions is 6.89 ± 0.80 $\mu$g/m$^3$, or 65 ± 10% of the measured value. The remaining 35% places an upper limit on the amount of secondary organic PM that could be present because of gas-to-particle conversion processes in the atmosphere. Schauer and co-workers,[23] using the same technique, found this upper limit on secondary organic aerosol to range from 13% to 31% in the Los Angeles area in 1982. Because the sources used in the mass balance are expected to account for only 80% of the primary organic aerosol emissions in the Los Angeles area,[26] the best estimate would be that secondary organic aerosol concentrations are lower, in the vicinity of 20% of the fine organic aerosol on an annual basis in 1993. Several studies have used EC as a tracer for primary OC.[59–62] While these studies show that secondary organic aerosol concentration can reach 80+% during some episodes, they also suggest that a 20% secondary organic aerosol contribution for an annual average urban sample is realistic.

The relative contribution of the source types to the concentration of the individual chemical species also can be calculated from the mass balance model. The percentages of the calculated concentrations of each chemical species in the model that originate from the individual source types are shown in Figure 7.

## Apportionment of Ambient Particulate Mutagenicity

Each of the 15 source samples shown in Table 1 was tested previously[36] in a bacterial mutagenicity assay (the *S. typhimurium* forward mutation assay of Skopek et al.[28]). These source samples represent emission source types that accounted for ~80% of the fine particle emissions in the

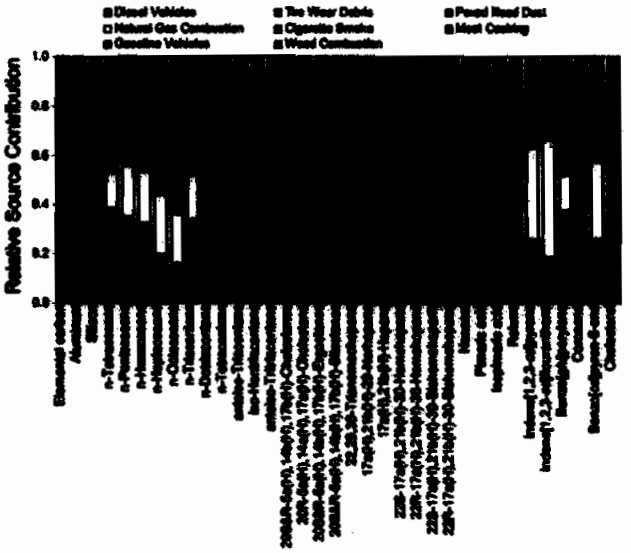


**Figure 7.** Relative source contribution to modeled ambient concentrations of organic compounds in the mass balance.

Los Angeles area in 1982. Of these 15 source samples, 10 were found to be mutagenic at the doses tested, and further biological analyses using both bacterial[28] and human cell[27] mutation assays were performed on the 10 mutagenic source samples. The mutagenic potency values shown in Table 1 represent the mutagenic strength (mutagenicity per mass of organics emitted) of a source sample in the mutation assay systems studied. In all three assay systems, the natural gas home appliance emissions sample showed the highest mutagenic potency. Other researchers have observed strong mutagenic activity for the PM emissions from natural gas combustion.[63] In the human cell mutation assay, the source type showing the second highest mutagenic potency was noncatalyst automobile exhaust aerosol, followed by diesel engine exhaust aerosol, and then followed by several other samples having approximately the same mutagenic potency: catalyst-equipped automobile exhaust, fuel oil-fired boiler emissions, smoke from fireplace combustion of pine wood, smoke from fireplace combustion of oak wood, and roofing tar pot emissions. In the bacterial assay system with addition of PMS, noncatalyst auto exhaust aerosol, heavy-duty diesel truck exhaust particles, and fuel oil-fired boiler emissions exhibited approximately equal mutagenic potency, followed by catalyst-equipped auto exhaust particles, smoke from fireplace combustion of pine and oak wood, as well as cigarette smoke and roofing tar pot emissions. In the bacterial assay system without addition of PMS, the source sample with the second-highest mutagenic potency is heavy-duty diesel truck exhaust, followed in order of potency by smoke from fireplace combustion of oak wood, catalyst and noncatalyst-equipped automobile exhaust aerosol, smoke from fireplace combustion of pine wood, fuel oil-fired boiler emissions, smoke from fireplace combustion of synthetic logs, and then cigarette smoke and roofing tar pot emissions.

The product of the mutagenic potency of an emission source times the contribution of that source type to the ambient fine organics mass concentration provides an estimate of the contribution of that source type to the mutagenicity of the ambient aerosol composite. The assumptions are that (1) there are linearly additive mutagenic contributions to the atmospheric sample, and (2) mutagenicity of the source effluents is not transformed by atmospheric chemical reactions. This multiplication of mutagenic potency (mutagenicity per unit organics mass) times the quantity of organics contributed from the source (organic mass per $m^3$) yields a quantity that previously has been defined as the mutagen density, which is the induced mutant fraction per $m^3$ ambient air sampled to supply organics to the standard bioassays. These source contributions to mutagen density are shown in Table 2. The mutagenic potency of the gasoline-powered vehicle composite sample is estimated as a linear combination of the potencies of the catalyst and noncatalyst gasoline-powered engine exhaust fine particle samples assembled in proportion to their contribution to fine particle organics mass emissions from the 1993 Los Angeles fleet, as calculated earlier. The sum of the mutagen density contributions from each source can be compared with the mutagen density observed in the ambient sample.

In the human cell assay, the sum of the mutagen density contributions from the source types used in this analysis accounts for an IMF of 1.33 ($\pm$0.56) $\times$ $10^{-6}$ per $m^3$ air, or 83% $\pm$ 38% of the mutagen density of the composite ambient sample. The overall contribution of the primary source effluents is statistically indistinguishable from the total human cell mutagenicity of the ambient sample, 45–121% using the uncertainty bounds. This is consistent with previous inferences drawn from the seasonal and spatial patterns of the mutagenic potency of ambient samples taken in the Los Angeles area during 1993, which also suggest that mutagenic potency values do not vary seasonally and do not increase with downwind transport away from the primary source areas, as might be expected if the most important human cell mutagens were being created by atmospheric chemical reactions.[8] The natural gas home appliance emissions estimate is by far the largest predicted primary source contributor to the mutagen density of the atmospheric sample, even though the mass concentration of the natural gas source material is extraordinarily low. This occurs because the mutagenic potency of the natural gas combustion aerosol is very high. The PAHs in the natural gas sample are not accompanied by a large amount of particle-phase hydrocarbons from unburned fuel that contribute to the mass concentration but not to the mutagenicity of many of the other samples.[55,57] To reiterate, the natural gas combustion emissions sample used for this study was a composite sample of only a few natural gas home appliances. Still, further investigation into the nature of natural gas combustion emissions is warranted.

In a previous study,[36] the bacterial mutagenicity of different extracts from these same source samples was weighted by their relative Los Angeles-area emissions for 1982, and the mutagenicity of this emissions-weighted source effluent composite was compared with the bacterial mutagenicity measured in 1982 ambient fine particle samples taken in Los Angeles. When the bacterial mutagenicity measured in the ambient sample was compared with the bacterial mutagenicity of the emissions-weighted source composite, it was found that this simple approximation generated rough agreement between the mutagenicity of the two types of samples.

Given the new ambient samples from 1993 and the newly calculated 1993 source contributions, it is now

possible to repeat that earlier study for a more recent year. The sum of the mutagen density contributions in the bacterial assay from the source types used in this analysis accounts for 221% ± 87% of the ambient mutagen density in the presence of PMS and 76% ± 34% in the absence of PMS. Again, the bacterial mutagenicity of a source contribution-weighted composite of the primary source samples is approximately large enough to account for nearly all of the bacterial mutagenicity of the ambient samples.

## CONCLUSIONS

The primary fine particle organic mass concentration in the Los Angeles-area atmosphere in 1993 has been apportioned between eight emission source types. The largest primary contributors to organic aerosol mass are meat cooking, wood combustion, and diesel vehicles. This result agrees with a previous analysis performed by Schauer and co-workers[23] using ambient samples taken during 1982. The major difference between the two studies is a decrease in the source contribution from diesel vehicles. That decrease in diesel engine exhaust aerosol concentration is believed to be consistent with the introduction of cleaner diesel engines and cleaner-burning diesel fuels between 1982 and 1993.

The fine particle mutagenicity of the Los Angeles-area atmospheric aerosol in 1993 also has been apportioned between the same eight source types using both a human cell assay system as well as a bacterial assay system. In both the human cell and bacterial assay systems, a linear combination of the mutagenicity values of the primary source samples assembled in proportion to their calculated contribution to the atmospheric sample composite is statistically indistinguishable from the measured mutagenicity of the atmospheric sample itself. In both the human cell assay system and bacterial assay system (+PMS), the largest source of the predicted contribution to the mutagenicity of the atmospheric sample is caused by natural gas combustion in residential appliances, with smaller contributions from diesel exhaust, gasoline-powered vehicle exhaust, and wood smoke. In the bacterial assay system (−PMS), diesel exhaust is the largest contributor, followed by natural gas appliances, gasoline-powered vehicles, and wood smoke.

Known primary emissions sources are clearly capable of emitting mutagenic organic matter to the urban atmosphere in amounts sufficient to account for the observed mutagenicity of the ambient samples. The error bounds on this analysis, however, are wide enough to admit to the possible presence of additional mutagenic organics that are formed by atmospheric chemical reaction (e.g., 2-nitrofluoranthene, which has been identified as one of the more important single human cell mutagens in the atmospheric composite studied here, accounting for ~1% of the total sample mutagenic potency[8]).

The compounds that have thus far been identified as the important mutagens in this ambient fine PM sample include cyclopenta[*cd*]pyrene, benzo[*a*]pyrene, benzo[*k*]fluoranthene, and benzo[*b*]fluoranthene. These compounds account for ~10–15% of the whole sample mutagenicity. These compounds also have been identified in several source samples.[50,54–58] The interesting point is that a linear combination of the emissions of these PAHs according to the source contributions computed in this article will overpredict the atmospheric concentration of these PAHs.[64] If these PAHs were reacting to form non-mutagenic compounds, then the linear combination of the mutagenic potencies from the sources should overpredict the atmospheric mutagenic potency. This does not occur. Likely, there is conversion of mutagenic PAH to mutagenic PAC (polycyclic aromatic compounds) and formation of mutagenic PAC from secondary aerosol generation involving gas-phase PAH. Still, the important source of the ambient mutagens is the source that emits the PAH.

Interestingly, the major contributors to the particulate air pollution mass are not necessarily the major contributors to the mutagenicity of the particulate air pollution. This may be true of other environmental stresses. The general method employed herein, which combines source apportionment with environmental assays of source and ambient samples, can be used to investigate the origin of other environmental stresses such as asthma, as long as a viable assay can be identified.

## ACKNOWLEDGMENTS

The authors thank Bruce Penman and Charlie Crespi at Gentest Corp. and Bill Thilly at MIT for the overseeing of the human cell mutation assay system. Those individuals who performed the mutation assays, Lawerence Donhoffner and Lita Doza-Corpus at Gentest, plus Henny Smith, Xia He, Woody Bishop, and Clo Butcher at MIT, are also greatly appreciated. Much of the analytical prep work was done in the Analytical Laboratory at the Center for Environmental Health Sciences, MIT, and the authors are indebted to the director, Art Lafleur, for providing space and knowledge. The authors also would like to thank all those individuals associated with the ambient sampling campaign, specifically Matt Fraser and Lynn Salmon, and the fine particle source sample archives, specifically Lynn Hildemann and Monica Mazurek. Thanks also go to Jamie Schauer for his valuable guidance with the chemical mass balance calculations. This research has been supported by Center Grant P30-ES02109 and Program Grant P01-ES07168 from the National Institute of Environmental Health Sciences.

## REFERENCES


1. Dehnen, W.; Pitz, N.; Tomingas, R. *Cancer Lett.* **1978**, *4*, 5-12.
2. Pitts, J.N.; Grosjean, D.; Mischke, T.M.; Simmon, V.F.; Poole, D. *Toxicol. Lett.* **1977**, *1*, 65-70.
3. Tokiwa, H.; Morita, K.; Takeyoshi, H.; Takahashi, K.; Ohnishi, Y. *Mutat. Res.* **1977**, *48*, 237-248.
4. Wise, S.A.; Chesler, S.N.; Hilpert, L.R.; May, W.E.; Rebbert, R.E.; Vogt, C.R.; Nishioka, M.G.; Austin, A.; Lewtas, J. *Environ. Int.* **1985**, *11*, 147-160.
5. Pagano, P.; DeZaiacomo, T.; Scarcella, E.; Bruni, S.; Calamosca, M. *Environ. Sci. Technol.* **1996**, *30*, 3512-3516.
6. Adonis, M.; Gil, L. *Mutat. Res.* **1993**, *292*, 51-61.
7. Villalobospietrini, R.; Blanco, S.; Gomezarroyo, S. *Atmos. Environ.* **1995**, *29*, 517-524.
8. Hannigan, M.P.; Cass, G.R.; Penman, B.W.; Crespi, C.L.; Lafleur, A.L.; Busby, W.F.; Thilly, W.G. *Environ. Sci. Technol.* **1997**, *31*, 438-447.
9. Durant, J.L.; Lafleur, A.L.; Plummer, E.F.; Taghizadeh, K.; Busby, W.F.; Thilly, W.G. *Environ. Sci. Technol.* **1998**, *32*, 1894-1906.
10. Asahina, S.; Arnold, E.; Andrea, J.; Carmel, A.; Bishop, Y.; Epstein, S.S.; Coffin, D.; Joshi, S. *Cancer Res.* **1972**, *32*, 2263.
11. Helmig, D.; Lopezcancio, J.; Arey, J.; Harger, W.P.; Atkinson, R. *Environ. Sci. Technol.* **1992**, *26*, 2207-2213.
12. Arey, J.; Zielinska, B.; Harger, W.P.; Atkinson, R.; Winer, A.M. *Mutat. Res.* **1988**, *207*, 45-51.
13. Savard, S.; Otson, R.; Douglas, G.R. *Mutat. Res.* **1992**, *276*, 101-115.
14. Salmeen, I.T.; Pero, A.M.; Zator, R.; Schuetzle, D.; Riley, T.L. *Environ. Sci. Technol.* **1984**, *18*, 375-382.
15. Nishioka, M.G.; Petersen, B.A.; Lewtas, J. *Comparison of NitroAromatic Content and Direct-Acting Mutagenicity of Diesel Emissions*; Batelle Press: Columbus, OH, 1982.
16. Grimmer, G.; Naujack, K.W.; Dettbarn, G.; Brune, H.; Deutschwenzel, R.; Misfeld, J. *Erdol Kohle Erdgas P* **1982**, *35*, 466-472.
17. Grimmer, G.; Brune, H.; Deutschwenzel, R.; Naujack, K.W.; Misfeld, J.; Timm, J. *Cancer Lett.* **1983**, *21*, 105-113.
18. Grimmer, G.; Brune, H.; Deutschwenzel, R.; Dettbarn, G.; Misfeld, J.; Abel, U.; Timm, J. *Cancer Lett.* **1984**, *23*, 167-176.
19. Skopek, T.R.; Liber, H.L.; Kaden, D.A.; Hites, R.A.; Thilly, W.G. *J. Natl. Cancer I.* **1979**, *63*, 309-312.
20. Lewtas, J.; Claxton, L.D.; Rosenkranz, H.S.; Schuetzle, D.; Shelby, M.; Matsushita, H.; Wurgler, F.E.; Zimmermann, F.K.; Lofroth, G.; May, W.E.; Krewski, D.; Matsushima, T.; Ohnishi, Y.; Gopalan, H.N.G.; Sarin, R.; Becking, G.C. *Mutat. Res.* **1992**, *276*, 3-9.
21. May, W.E.; Benner, B.A.; Wise, S.A.; Schuetzle, D.; Lewtas, J. *Mutat. Res.* **1992**, *276*, 11-22.
22. Claxton, L.D.; Douglas, G.; Krewski, D.; Lewtas, J.; Matsushita, H.; Rosenkranz, H. *Mutat. Res.* **1992**, *276*, 61-80.
23. Schauer, J.J.; Rogge, W.F.; Hildemann, L.M.; Mazurek, M.A.; Cass, G.R; *Atmos. Environ.* **1996**, *30*, 3837-3855.
24. Schauer, J.J.; Cass, G.R. *Environ. Sci. Technol.* **2000**, *34*, 1821-1832.
25. Zheng, M.; Cass, G. R.; Schauer, J.J.; Edgerton, E.S. *Environ. Sci. Technol.* **2002**, *36*, 2361-2371.
26. Hildemann, L.M.; Markowski, G.R.; Cass, G.R. *Environ. Sci. Technol.* **1991**, *25*, 744-759.
27. Penman, B.W.; Chen, L.P.; Gelboin, H.V.; Gonzalez, F.J.; Crespi, C.L. *Carcinogenesis* **1994**, *15*, 1931-1937.
28. Skopek, T.R.; Liber, H.L.; Krolewski, J.J.; Thilly, W.G. *P. Natl. Acad. Sci. USA* **1978**, *75*, 410-414.
29. Hannigan, M.P.; Cass, G.R.; Lafleur, A.L.; Busby, W.F.; Thilly, W.G. *Environ. Health Persp.* **1996**, *104*, 428-436.
30. Solomon, P.A.; Moyers, J.L.; Fletcher, R.A. *Aerosol Sci. Tech.* **1983**, *2*, 455-464.
31. Birch, M.E.; Cary, R.A. *Aerosol Sci. Tech.* **1996**, *25*, 221-241.
32. Johnson, R.I.; Shaw, J.J.; Cary, R.A.; Huntzicker, J.J. in *Atmospheric Aerosol: Source/Air Quality Relationships*; Macias, E.S., Hopke, P.K., Eds.; American Chemical Society: Washington, DC, 1981; pp 223-233.
33. John, W.; Reischl, G. *J. Air & Waste Manage. Assoc.* **1980**, *30*, 872-876.
34. Turpin, B.J.; Saxena, P.; Andrews, E. *Atmos. Environ.* **2000**, *34*, 2983-3013.
35. Hildemann, L.M.; Cass, G.R.; Markowski, G.R. *Aerosol Sci. Tech.* **1989**, *10*, 193-204.
36. Hannigan, M.P.; Cass, G.R.; Lafleur, A.L.; Longwell, J.P.; Thilly, W.G. *Environ. Sci. Technol.* **1994**, *28*, 2014-2024.
37. Lafleur, A.L.; Monchamp, P.A.; Plummer, E.F.; Kruzel, E.L. *Anal. Lett.* **1986**, *19*, 2103-2119.
38. Busby, W.F.; Penman, B.W.; Crespi, C.L. *Mutat. Res.—Genet. Tox.* **1994**, *322*, 233-242.
39. Furth, E.E.; Thilly, W.G.; Penman, B.W.; Liber, H.L.; Rand, W.M. *Anal. Biochem.* **1981**, *110*, 1-8.
40. Busby, W.F.; Smith, H.; Bishop, W.W.; Thilly, W.G. *Mutat. Res.—Genet. Tox.* **1994**, *322*, 221-232.
41. Hannigan, M.P.; Cass, G.R.; Penman, B.W.; Crespi, C.L.; Lafleur, A.L.; Busby, W.F.; Thilly, W.G.; Simoneit, B.R.T. *Environ. Sci. Technol.* **1998**, *32*, 3502-3514.
42. Dzubay, T.G. *X-Ray Fluorescence Analysis of Environmental Samples*; Ann Arbor Science: Ann Arbor, MI, 1977.
43. *1997 Air Quality Management Plan*; South Coast Air Quality Management District: Diamond Bar, CA, 1996.
44. Sawyer, R.F.; Johnson, J.J. in *Diesel Exhaust: A Critical Analysis of Emissions, Exposure, and Health Effects: A Special Report of the Institute's Diesel Working Group*; Health Effects Institute: Cambridge, MA, 1995; pp 65-82.
45. Compilation of Air Pollution Emission Factors. Volume 2: Mobile Sources; EPA/AP-42; Office of Mobile Sources, U.S. Environmental Protection Agency: Research Triangle Park, NC, 1985.
46. Singer, B.C.; Harley, R.A. *J. Air & Waste Manage. Assoc.* **1996**, *46*, 581-593.
47. Hildemann, L.M.; Markowski, G.R.; Jones, M.C.; Cass, G.R. *Aerosol Sci. Tech.* **1991**, *14*, 138-152.
48. Mazurek, M.A.; Simoneit, B.R.T.; Cass, G.R.; Gray, H.A. *Int. J. Environ. Ch.* **1987**, *29*, 119-139.
49. Fraser, M.P.; Cass, G.R.; Simoneit, B.R.T.; Rasmussen, R.A. *Environ. Sci. Technol.* **1997**, *31*, 2356-2367.
50. Rogge, W.F.; Hildemann, L.M.; Mazurek, M.A.; Cass, G.R.; Simoneit, B.R.T. *Environ. Sci. Technol.* **1993**, *27*, 1892-1904.
51. Christoforou, C.S.; Salmon, L.G.; Hannigan, M.P.; Solomon, P.A.; Cass, G.R. *J. Air & Waste Manage. Assoc.* **2000**, *50*, 43-53.
52. Turpin, B.J.; Lim, H.J. *Aerosol Sci. Tech.* **2001**, *35*, 602-610.
53. Russell, L.M. *Environ. Sci. Technol.* **2003**, *37*, 2982-2987.
54. Rogge, W.F.; Hildemann, L.M.; Mazurek, M.A.; Cass, G.R.; Simoneit, B.R.T. *Environ. Sci. Technol.* **1991**, *25*, 1112-1125.
55. Rogge, W.F.; Hildemann, L.M.; Mazurek, M.A.; Cass, G.R.; Simoneit, B.R.T. *Environ. Sci. Technol.* **1993**, *27*, 636-651.
56. Rogge, W.F.; Hildemann, L.M.; Mazurek, M.A.; Cass, G.R.; Simoneit, B.R.T. *Environ. Sci. Technol.* **1993**, *27*, 2700-2711.
57. Rogge, W.F.; Hildemann, L.M.; Mazurek, M.A.; Cass, G.R.; Simoneit, B.R.T. *Environ. Sci. Technol.* **1993**, *27*, 2736-2744.
58. Rogge, W.F.; Hildemann, L.M.; Mazurek, M.A.; Cass, G.R. *Environ. Sci. Technol.* **1994**, *28*, 1375-1388.
59. Turpin, B.J.; Huntzicker, J.J. *Atmos. Environ. A–Gen.* **1991**, *25*, 207-215.
60. Turpin, B.J.; Huntzicker, J.J. *Atmos. Environ.* **1995**, *29*, 3527-3544.
61. Lim, H.J.; Turpin, B.J. *Environ. Sci. Technol.* **2002**, *36*, 4489-4496.
62. Strader, R.; Lurmann, F.; Pandis, S.N. *Atmos. Environ.* **1999**, *33*, 4849-4863.
63. Lapin, C.A.; Gautam, M.; Zielinska, B.; Wagner, V.O.; McClellan, R.O. *Mutat. Res.–Gen. Tox. En.* **2002**, *519*, 205-209.
64. Rogge, W.F.; Hildemann, L.M.; Mazurek, M.A.; Cass, G.R.; Simoneit, B.R.T. *J. Geophys. Res.–Atmos.* **1996**, *101*, 19379-19394.



**About the Authors**

Michael P. Hannigan is a research associate in the Mechanical Engineering Department at the University of Colorado in Boulder. William F. Busby, Jr., (deceased) was on the faculty of the Center for Environmental Health Sciences at the Massachusetts Institute of Technology. Glen R. Cass (deceased) was on the faculty of the California Institute of Technology and the Georgia Institute of Technology. Address correspondence to: Michael Hannigan, University of Colorado, UCB 427, Boulder, CO 80309; e-mail: hannigan@colorado.edu.

# Acrolein is a major cigarette-related lung cancer agent: Preferential binding at *p53* mutational hotspots and inhibition of DNA repair

Zhaohui Feng[†], Wenwei Hu[†], Yu Hu, and Moon-shong Tang[‡]

Departments of Environmental Medicine, Pathology, and Medicine, New York University School of Medicine, Tuxedo, NY 10987

Communicated by Richard B. Setlow, Brookhaven National Laboratory, Upton, NY, August 14, 2006 (received for review June 22, 2006)

**The tumor suppressor gene *p53* is frequently mutated in cigarette smoke (CS)-related lung cancer. The *p53* binding pattern of carcinogenic polycyclic aromatic hydrocarbons (PAHs) found in CS coincides with the *p53* mutational pattern found in lung cancer, and PAHs have thus been considered to be major culprits for lung cancer. However, compared with other carcinogenic compounds, such as aldehydes, the amount of PAHs in CS is minute. Acrolein (Acr) is abundant in CS, and it can directly adduct DNA. Acr–DNA adducts, similar to PAH–DNA adducts, induce predominantly G-to-T transversions in human cells. These findings raise the question of whether Acr–DNA adducts are responsible for *p53* mutations in CS-related lung cancer. To determine the role of Acr–DNA adducts in *p53* mutagenesis in CS-related lung cancer we mapped the distribution of Acr–DNA adducts at the sequence level in the *p53* gene of lung cells using the UvrABC incision method in combination with ligation-mediated PCR. We found that the Acr–DNA binding pattern is similar to the *p53* mutational pattern in human lung cancer. Acr preferentially binds at CpG sites, and this enhancement of binding is due to cytosine methylation at these sequences. Furthermore, we found that Acr can greatly reduce the DNA repair capacity for damage induced by benzo[*a*]pyrene diol epoxide. Together these results suggest that Acr is a major etiological agent for CS-related lung cancer and that it contributes to lung carcinogenesis through two detrimental effects: DNA damage and inhibition of DNA repair.**

DNA damage

The tumor suppressor gene *p53* is frequently mutated in human cancers (1, 2), and its mutational patterns often bear the fingerprints of the etiological carcinogens. Most notably it has been found that >50% of alfatoxin B1-associated liver cancers have mutations in codon 249 of the *p53* gene and that *p53* mutations are concentrated at contiguous pyrimidines in sunlight-associated skin cancers (3, 4). Previously we demonstrated that DNA adducts induced by diol epoxides of polycyclic aromatic hydrocarbons (PAHs), a major category of cigarette smoke (CS) carcinogens, preferentially occur at *p53* mutational hotspots in CS-related lung cancers and that adducts formed at these locations are poorly repaired (5–7). The *p53* gene is the most frequently mutated tumor suppressor gene in CS-related lung cancers, and its mutational pattern is distinctly different from that found in lung cancers of nonsmokers (Fig. 5, which is published as supporting information on the PNAS web site); PAHs have been shown to be strong carcinogens, and thus PAH-induced DNA damage may shape the *p53* mutational pattern in lung cancer and may also represent a strong molecular link between lung cancer and cigarette smoking (1, 2, 5–7). The question of whether PAHs are the major culprits in CS smoke that cause human cancer remains unsettled because CS contains >4,000 compounds, many of which, particularly aldehydes, are not only more cytotoxic than PAHs but can also cause similar kinds of mutations (8, 9).

Acrolein (Acr) is one of the most abundant, reactive, and mutagenic aldehydes in CS; it is found in amounts up to 1,000-fold higher than those of PAHs in CS [10–500 $\mu$g per cigarette compared with 0.01–0.05 $\mu$g of benzo[*a*]pyrene (BP) per cigarette] (8). It can be taken up reasonably efficiently by human cells and react directly without metabolic activation with guanine residues in DNA to produce exocyclic DNA adducts, 6-hydroxy-1,$N^2$-propanodeoxyguanosine and 8-hydroxy-1,$N^2$-propanodeoxyguanosine adducts (Acr–dG) (Fig. 1), which are mutagenic and induce predominantly G:C-to-T:A transversion mutations similar to PAHs (9). Although Acr has been shown to be cytotoxic and genotoxic in human cells, as a suspected carcinogen its carcinogenicity in animal models has not been adequately evaluated because of its extremely potent toxic effects, which often result in death (9–11). Nonetheless, it has been found that Acr treatment greatly enhances urinary bladder papilloma occurrence in rats (9). Acr is one of the two major toxic metabolites of the chemotherapeutic agents cyclophosphamide and ifosfamide, and Acr has been long suspected to be an important factor in the induction of secondary human bladder tumors in cyclophosphamide-treated patients (9). Acr–dG DNA adducts have been detected in animal and human tissues (12), and it has been shown that the oral tissues of cigarette smokers have significantly higher Acr–dG levels than those of nonsmokers (13). These findings raise the possibility that Acr may contribute greatly to CS-related mutagenesis and carcinogenesis. To determine this possibility we developed a method using the UvrABC nuclease incision method in combination with the ligation-mediated PCR (LMPCR) technique (UvrABC/LMPCR) to map the Acr–dG adduct distribution at the sequence level in the *p53* gene in normal human lung cells and compared it to the *p53* binding pattern of BP diol epoxide (BPDE), a major carcinogenic form of BP, in the same cells (5, 8).

Acr is very reactive toward nucleophiles, including thiol-containing proteins; intracellularly the majority of Acr is covalently bonded with proteins (9). Two major endogenously produced aldehydes, *trans*-4-hydroxy-2-nonenal (4-HNE) and malondialdehyde, can bond with proteins and have been found to cause an inhibitory effect on nucleotide excision repair (NER) (14, 15). We therefore also examined the effect of Acr on DNA repair using host cell reactivation and *in vitro* DNA damage-specific repair synthesis assays (14, 15).

---

Author contributions: Z.F., W.H., Y.H., and M.-s.T. designed research; Z.F., W.H., and Y.H. performed research; Z.F., W.H., Y.H., and M.-s.T. contributed new reagents/analytic tools; Z.F., W.H., Y.H., and M.-s.T. analyzed data; and Z.F., W.H., Y.H., and M.-s.T. wrote the paper.

The authors declare no conflict of interest.

Freely available online through the PNAS open access option.

Abbreviations: CS, cigarette smoke; PAH, polycyclic aromatic hydrocarbon; Acr, acrolein; Acr–dG, 6- or 8-hydroxy-1,$N^2$-propanodeoxyguanosine; BP, benzo[*a*]pyrene; BPDE, BP diol epoxide; 4-HNE, *trans*-4-hydroxy-2-nonenal; MDA, malondialdehyde; NHBE, normal human bronchial epithelial; NHLF, normal human lung fibroblast; LMPCR, ligation-mediated PCR; NER, nucleotide excision repair.

[†]Present address: Cancer Institute of New Jersey/University of Medicine and Dentistry of New Jersey, New Brunswick, NJ 08903.

[‡]To whom correspondence should be addressed. E-mail: tang@env.med.nyu.edu.





www.pnas.org/cgi/doi/10.1073/pnas.0607031103

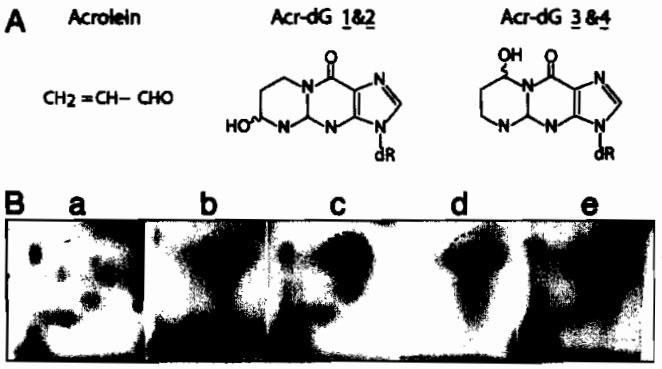


**Fig. 1.** Chemical structures and detections of Acr–dG. (*A*) Chemical structure of Acr and Acr–dG adducts. (*B*) Identification of $^{32}$P-labeled Acr–DNA adducts by 2D TLC. Acr-modified DNA isolated from Acr-treated human cells and Acr-treated purified genomic DNA were digested with phosphodiesterase and nuclease P1, labeled with [$\gamma$-$^{32}$P]ATP, and subjected to 2D TLC, as described in *Materials and Methods*. The standard Acr–dG adducts were obtained by reaction of Acr (0.2 M) with dGMP (2 mM) and then labeled with [$\gamma$-$^{32}$P]ATP, and the major Acr–dG 3 adducts are indicated by circles. (*a*) DNA isolated from control cells. (*b*) Acr-modified genomic DNA. (*c*) DNA from Acr-treated cells. (*d*) Acr-modified dGMP. (*e*) Mixture of *c* and *d*.

## Results

**Acr Can Directly Modify DNA to Form Propanodeoxyguanine Adducts *In Vitro* and *In Vivo*.** It is well known that Acr can react directly with guanine residues in purified DNA to produce four isomeric exocyclic DNA adducts, two minor stereoisomeric Acr–dG adducts (Acr–dG 1 and 2), and two major stereoisomeric 8-hydroxy-1,$N^2$-propanodexoyguaosine adducts (Acr–dG 3 and 4) (16) (F. L. Chung and C. Rizzo, personal communication) (Fig. 1). To ensure that the Acr–DNA adducts formed *in vivo* resulted from the direct interaction of Acr with genomic DNA, we identified the type of DNA adducts formed in cultured lung cells treated with Acr and in purified genomic DNA treated with Acr using the $^{32}$P postlabeling and 2D TLC method. The results in Fig. 1 show that Acr–dG 3 is the major Acr–dG adduct found both in Acr-treated purified genomic DNA and in DNA from cells treated with Acr. Three isomeric Acr–dG adducts are found in Acr-modified dGMP, with the major adduct (Acr–dG 3) being the same as that found in Acr-treated cells and genomic DNA. No Acr–dG 1 or Acr–dG 2 adducts were found in Acr-treated cells or Acr-modified genomic DNA. Although a small quantity of Acr–dG 4 adducts was found in Acr-treated cells, this type of adduct was not found in Acr-modified genomic DNA. Using relatively high concentrations of Acr (1.1 M) for modifications of calf thymus DNA, Chung *et al.* (16) detected Acr–dG 1 and 2 adducts. These two types of adducts were not evident in Acr-cultured Chinese hamster ovary cells, liver samples from mice and rats, and human liver and oral tissue samples; in contrast, Acr–dG 3 adducts were detected in these samples (12, 13, 17). Structural constraints in genomic DNA and chromatin structure may hinder formation of Acr–dG 1 and 2 adduct isomers. Our results are consistent with well established findings that Acr can react directly without metabolic activation with guanine residues in DNA to produce exocyclic propanodeoxyguanosine DNA adducts (12, 13, 16–18).

**UvrABC Is Able to Incise Acr–dG Adducts Quantitatively and Specifically.** To assess the contribution of Acr-induced DNA damage to the *p53* mutation pattern in lung cancer it is necessary to map the Acr–DNA adduct distribution at the sequence level in the *p53* gene of lung cells treated with Acr. Previously, using the UvrABC/LMPCR method, we successfully mapped various types of bulky carcinogen-induced DNA damage at the sequence level in the *p53* and *ras* genes (5, 19–21). The rationale of this approach is based on the finding that, under proper conditions, UvrABC can incise bulky DNA adducts specifically and quantitatively, and the extent of UvrABC incision therefore represents the extent of adduct formation rather than UvrABC sequence preferences (22). Because radioactively labeled Acr is not available, we assessed the quantitative relationship between UvrABC incision and Acr–DNA adduct formation in supercoiled DNA. We found that the number of UvrABC incisions was proportional to the concentration of Acr used for DNA modification, indicating that UvrABC is able to cut Acr–dG adducts quantitatively (Fig. 6*A*, which is published as supporting information on the PNAS web site). To determine the specificity of UvrABC cutting, 5′ or 3′ single-end, $^{32}$P-labeled *p53* DNA fragments were reacted with UvrABC nuclease, and the resultant DNAs were separated by electrophoresis in a denatured DNA sequencing gel. The results show that UvrABC makes the typical dual incisions 7 nt 5′ and 4 nt 3′ to an Acr–dG adduct, similar to what we have found for most bulky carcinogen-induced DNA damage (22) (Fig. 6 *B* and *C*). The results also show that the kinetics of UvrABC cutting at different sequences are similar, if not identical (Fig. 7 *A* and *C*, which is published as supporting information on the PNAS web site). It should be noted that we have found that at the end of incubation UvrABC remains active. Based on these results we concluded that UvrABC is able to cut Acr–dG adducts quantitatively and specifically and that the extent of UvrABC cutting at different sequences represents the extent of Acr–DNA adduct formation at the sequence.

**Acr–DNA Adducts Are Preferentially Formed at the Lung Cancer *p53* Mutational Hotspots.** Having established that the UvrABC nuclease is able to incise Acr–dG adducts specifically and quantitatively, we then used the UvrABC/LMPCR method to map the Acr–DNA binding spectrum in the coding strand of exons 5, 7, and 8 of the *p53* gene in normal human lung cells. Normal human bronchial epithelial (NHBE) cells and normal human lung fibroblasts (NHLF) were treated with different concentrations of Acr for 6 h, and genomic DNA was isolated to map the Acr–DNA binding pattern. For comparison purposes we also mapped the distribution of BPDE–DNA adducts in the *p53* gene of NHBE cells treated with BPDE using the same UvrABC/LMPCR method. The results in Fig. 2*A*, lanes 3–5, show that Acr–dG preferentially formed at codons 152, 154, 156, 157, and 158 in exon 5; codons 248 and 249 in exon 7; and codons 273 and 282 in exon 8 of the *p53* gene. The Acr–DNA adduct distributions in exons 5, 7, and 8 of the *p53* gene in the NHBE cells are very similar, but not quite identical, to the BPDE–DNA adduct distribution, as shown in Fig. 2*B*. BPDE preferentially forms DNA adducts at only CpG sites in codons 156, 157, and 158 of exon 5; codon 248 of exon 7; and codon 273 of exon 8 in the *p53* gene in NHBE cells, which is consistent with previously published reports (5, 6). Codons 157, 158, 248, 249, 273, and 282 of the *p53* gene are the mutational hotspots in CS-related lung cancer, and codons 249 and 273 of the *p53* gene are mutational hotspots in lung cancers of both cigarette smokers and nonsmokers (Fig. 5). Whereas Acr–dG adducts preferentially form at codon 249, BPDE–dG adducts do not (Fig. 2). It is worth noting that we have previously found that six of the activated cigarette PAHs either do not bind or weakly bind to this codon (5, 7).

We also mapped the distribution of Acr–DNA adducts along the *p53* gene in NHLF treated with Acr. The results show that the Acr–DNA adduct distribution pattern in the *p53* gene in NHLF was almost identical to that found in NHBE cells (Fig. 2*A*). These results clearly demonstrate that the specific binding spectrum of Acr in NHBE cells is due to the intrinsic binding specificity of Acr rather than the specificity of cell types.

The levels of Acr–dG formation in exons 5, 7, and 8 of the *p53* gene of NHBE cells were compared with the mutation distribution in this gene in CS-related lung cancer obtained from the *p53* database (Fig. 2*C*). The histograms of both show remarkable resemblance, which indicates that Acr–dG adducts may contribute

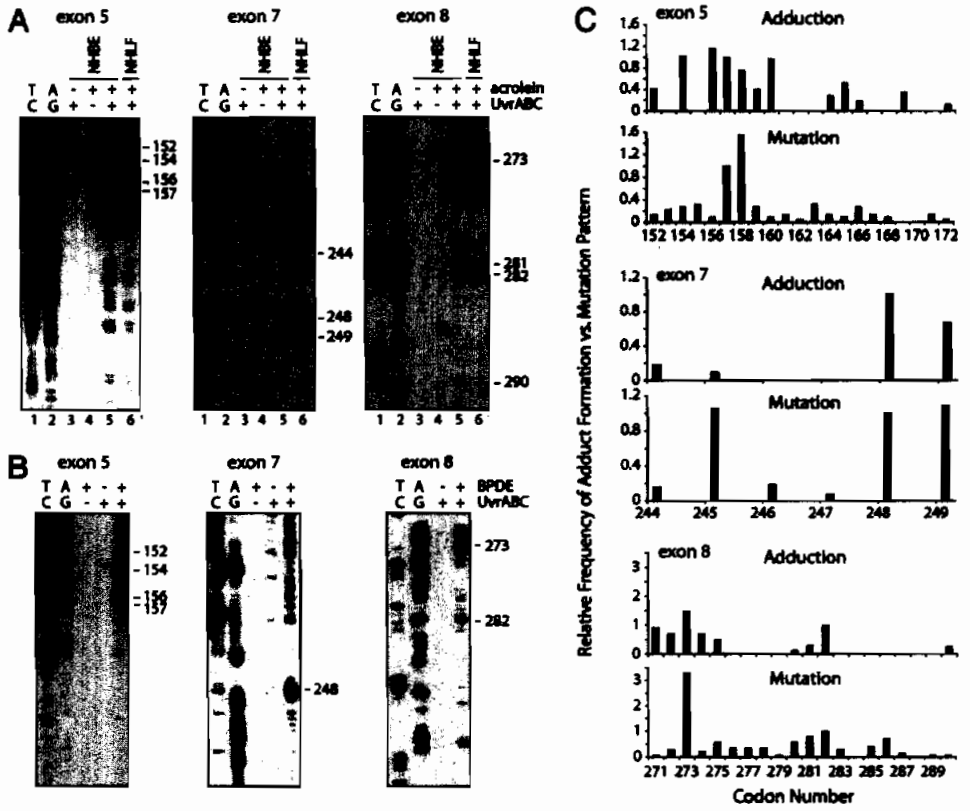


**Fig. 2.** Acr–dG and BPDE–dG distributions in the *p53* gene. (*A* and *B*) Acr–dG and BPDE–dG adduct distribution in exons 5, 7, and 8 of the *p53* gene of normal human lung cells treated with Acr (*A*) and BPDE (*B*). In *A*, NHBE cells and NHLF were treated with 20 μM Acr for 6 h, and in *B*, NHBE cells were treated with 1 μM BPDE for 30 min. Genomic DNA was then isolated, the DNA adduct distribution was mapped by the UvrABC/LMPCR method, and the DNA was separated by electrophoresis. A/G and T/C are Maxam and Gilbert reaction products (26). (*C*) Comparisons of the frequency of Acr–dG adduct distribution along the *p53* gene in NHBE cells with the frequency of the *p53* mutations in CS-related lung cancer (International Agency for Research on Cancer *p53* Mutation database, http://www-p53.iarc.fr).

to CS-related lung cancer and that Acr, instead of PAHs, from CS may be the etiological agent that causes mutations at codon 249 of the *p53* in lung cancers of both cigarette smokers and nonsmokers. Acr is abundant in secondhand smoke and is also rich in cooking fumes (8, 9), which may be the major sources of Acr exposure for nonsmokers.

**C5 Cytosine Methylation Enhances Acr–dG Binding at CpG Sites in the *p53* Gene.** Results in Fig. 2 show that, except for codon 249, all of the preferential sites of Acr–dG binding are guanines within CpG sites. Why does Acr preferentially bind at codons containing CpG sequences? In human genomic DNA cytosines at CpG sequences are frequently methylated at the C5 position, and this methylation may affect the stereostructure of DNA and/or nucleosomal structure in a manner that consequently affects bulky carcinogen binding (23–25). Indeed, we have found that C5 cytosine methylation at CpG sites enhances the binding of bulky chemicals at the adjacent guanines (25). Two approaches were undertaken to ascertain the reason behind the selectivity of Acr binding at CpG-containing codons in the *p53* gene. First, we determined the Acr–dG binding pattern in the *p53* gene by directly modifying NHBE genomic DNA and compared it to the pattern that resulted from treating intact NHBE cells; we found that both patterns of Acr–dG formation in the *p53* gene are very similar, if not identical (Fig. 8, which is published as supporting information on the PNAS web site). These results thus rule out nucleosomal structure playing a major role in determining the Acr–dG binding pattern in the *p53* gene. Second, we determined the Acr binding pattern in *p53* DNA fragments with or without C5 cytosine methylation at CpG sequences. 3′ $^{32}$P-end-labeled DNA fragments of exon 7 and 5′ $^{32}$P-end-labeled DNA fragments of exon 5 of the *p53* gene obtained by PCR amplification were subjected to SssI methylase treatment in the presence of *S*-adenosylmethionine to methylate all cytosines at CpG sites. DNA fragments with and without methylation treatment were then modified with Acr, and the adduct distributions were mapped by the UvrABC incision method. The extent of cytosine methylation was determined by Maxam and Gilbert chemical cleavage reactions (26). Because hydrazine is unable to modify C5-methylated cytosines, both the 5′- and 3′-phosphodiester bonds of each methylated cytosine are refractory to piperidine hydrolysis and no cytosine ladders are observed at methylated cytosines (26). As shown in Fig. 3 *A* and *B*, under the methylation conditions we used all of the CpG sites in the DNA fragments are methylated, and the intensities of the UvrABC incision bands of Acr–DNA adducts are enhanced 2- to 4-fold at almost all CpG-containing codons, such as codons 152, 154, 156, 157, 158, and 159 (Fig. 3*A*) and codons 245 and 248 (Fig. 3*B*) in methylated versus unmethylated *p53* DNA fragments. In contrast, the intensities of UvrABC incision bands of Acr–DNA adducts did not change significantly at the non-CpG-containing codons in methylated DNA fragments. To rule out the possibility that this enhancement of UvrABC cutting at methylated CpG sites is due to UvrABC having a higher cutting efficiency toward Acr adducts at methylated CpG sites versus other non-CpG sequences, the kinetics of UvrABC cutting for methylated CpG sequences and other sequences was determined in methylated *p53* exon 7 DNA fragments to determine whether the kinetics of UvrABC incision was in fact different for methylated CpG sites versus other sequences. We found UvrABC incision at all Acr-binding sites, in

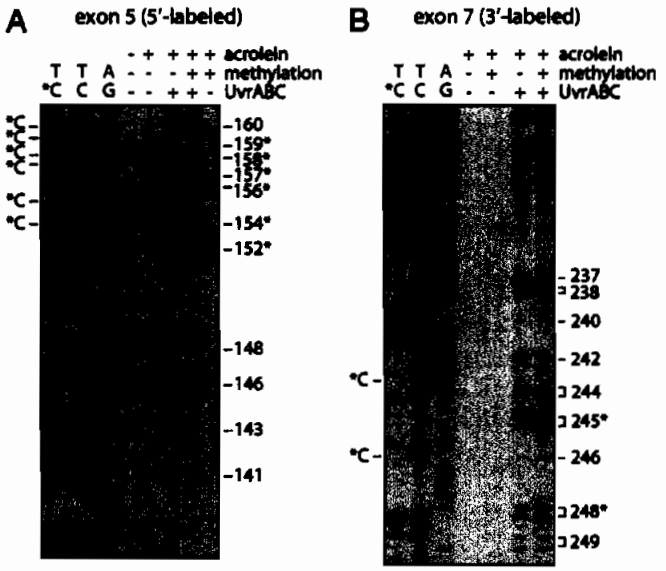


**Fig. 3.** The effect of $^5$C cytosine methylation at CpG sites on Acr–dG adduct formation. Cytosines at CpG sites of 5′ $^{32}$P-labeled exon 5 (*A*) and 3′ $^{32}$P-labeled exon 7 (*B*) of *p53* DNA fragments were methylated by SssI CpG methylase, and the DNA fragments with and without methylation treatment were modified with Acr (30 μM, 10-h incubation), treated with UvrABC nucleases, and separated by electrophoresis as previously described (25). A/G and T/C are Maxam and Gilbert reaction products. T/*C represents Maxam and Gilbert reaction products from methylated DNA fragments. *C represents the methylated cytosine, and the codon number of the bands corresponding to CpG sites is indicated by an asterisk.

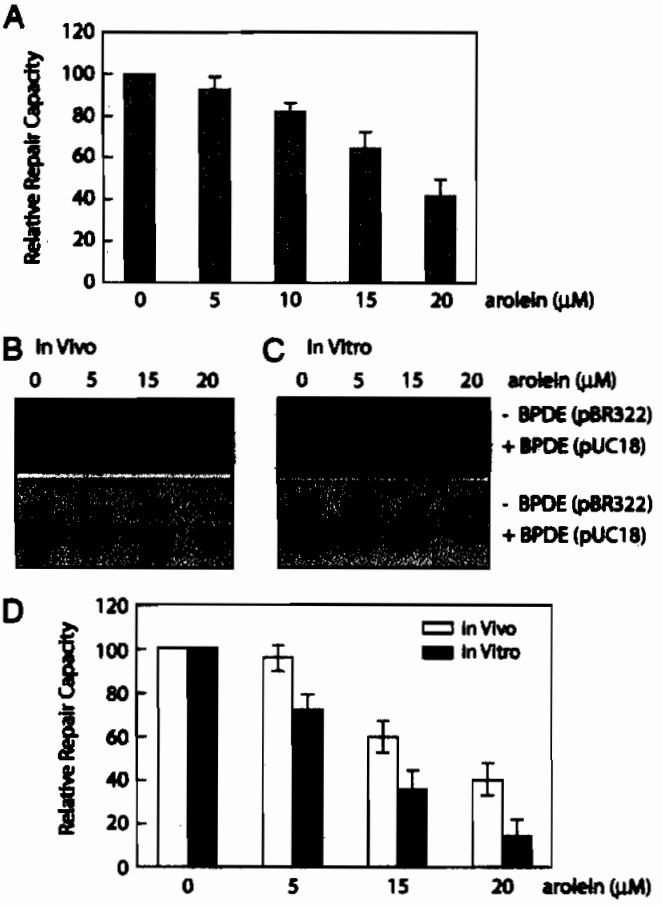


**Fig. 4.** Inhibition of the repair of BPDE–DNA adducts in human cells by Acr. (*A*) Repair inhibition determined by host cell reactivation assay. BPDE-modified luciferase reporter and unmodified β-galactosidase plasmids were cotransfected into NHLF treated with different concentrations of Acr for 1 h, and luciferase and β-galectosidase activities were measured 20 h after transfection. The relative repair capacity was calculated as the percentage of the relative luciferase activity of the plasmids in Acr-treated cells compared with untreated cells after normalization of the transfection frequency with β-galactosidase activity. (*B–D*) Repair inhibition determined by *in vitro* DNA repair synthesis assay. BPDE-modified pUC18 and unmodified pBR322 plasmids were used as DNA substrates for *in vitro* DNA repair synthesis assay. (*B*) NHLF were treated with different concentrations of Acr for 1 h, and the cell extracts were used for repair assay. (*C*) Different concentrations of Acr were added directly into cell extracts prepared from untreated NHLF immediately before the start of repair assay. (*Upper*) Photograph of an ethidium bromide-stained gel. (*Lower*) Autoradiograph of the same gel. (*D*) The relative repair capacity was calculated as the percentage of the repair activity in Acr-treated samples to untreated samples. The data represent three independent experiments, and the error bars represent the standard deviation.

both methylated CpG sequences (codons 245 and 248) and other unmethylated sequences, to be a function of incubation time and to plateau after 30 min of incubation, which leads us to conclude that the enhancement of UvrABC cutting at methylated CpG sites is due to preferential Acr binding as opposed to preferential UvrABC cutting for Acr adducts at methylated CpG sites (Fig. 7). Taken together, these results suggest that the strong binding of Acr at CpG-containing codons in the *p53* gene in human lung cells is due to 5-C cytosine methylation at these sequences. The results also suggest that the weaker Acr–dG formation at codons such as 158, 175, and 245 that contain CpG sequences is likely due to cytosines at these sequences not being methylated.

**Acr Treatment Reduces the Ability of Cells to Repair BPDE–DNA Adducts.** The carbonyl group and olefinic bond of Acr make this molecule reactive toward not only nucleic acids but also thiol-containing proteins (9). It is conceivable that Acr binding may or may not affect the functions of the proteins. Previously we have found that aldehydes, such as 4-HNE and malondialdehyde, can greatly reduce cellular NER capacity (14, 15). We therefore determined the effect of Acr treatment on NER capacity using the well established host cell reactivation assay and *in vitro* DNA damage-specific repair synthesis assay (14, 15). We found that, similar to 4-HNE and malondialdehyde, Acr can greatly inhibit NER for BPDE-induced DNA damage (Fig. 4). This inhibitory effect is much more pronounced in cell lysates directly treated with Acr than in whole cells treated with Acr (Fig. 4), suggesting that the Acr may interact with components in growth medium, that the cellular membrane may serve as a barrier to the uptake of Acr, and that the inhibitory effect is due to the interactions of Acr with repair proteins.

**Acr–dG Adducts Induce G-to-T Transversion Mutations in Human Cells.** It has long been recognized that CS-related lung cancers are rich in G-to-T transversions in the *p53* gene (>30% versus 10% in other human cancers) (2). This phenomenon has been attributed to mutations induced by bulky carcinogens in CS, including PAHs (5–7, 27). To determine the types of mutations induced by Acr–dG, we modified shuttle vector pSP189 DNA containing the *supF* gene with Acr (100 μM) and transfected the plasmid into NHLF for replication. Replicated plasmid was then transformed into indicator *Escherichia coli* cells, mutant white colonies were collected, and Acr-induced mutations in the *supF* gene were sequenced. We found that Acr modification resulted in greatly enhancing mutation frequency (from $4 \times 10^{-4}$ to $120 \times 10^{-4}$) and that >50% of the base substitutions induced by Acr–dG adducts are G-to-T transversions (28 of 55 total base substitution mutants sequenced). These results further support the hypothesis that Acr in CS contributes significantly to *p53* mutagenesis in lung cancer.

## Discussion

CS is the major cause of lung cancer deaths, and 90% of all lung cancers in the United States are CS-related (28, 29). CS contains >4,000 compounds, many of which, including PAHs, N-nitrosamines, aromatic amines, and metals, are not only mutagenic but also well established carcinogens in animal models (8, 29, 30). Therefore, it is reasonable to assume that these compounds contribute to CS-related lung carcinogenesis in humans. Previously, using the UvrABC/LMPCR method, we found that diol epoxides of potent PAH carcinogens found in CS preferentially form DNA adducts at *p53* mutational hotspots in CS-related lung cancer, such as codons 156, 157, 158, 245, 273, and 282 (5, 7). In addition, BPDE–DNA adducts formed at these sites are poorly repaired (6). Because the *p53* gene is the most frequently mutated gene in CS-related lung cancer and the *p53* mutational spectra in lung cancer of smokers and nonsmokers are distinctly different (1, 2) (Fig. 5), our findings strongly suggest that targeted DNA damage determines the *p53* mutational spectrum in CS-related lung cancer. These results, however, do not exclude the possibility that many other CS compounds also contribute to lung carcinogenesis. In fact, these results raise the possibility that any DNA-damaging compounds present in CS that preferentially bind to the CS-related lung cancer *p53* mutational hotspots are lung cancer etiological agents.

Acr is one of the most abundant compounds generated in CS; the amount of Acr in a single cigarette, depending on the manufacturer, ranges from 10 to 500 $\mu$g (8, 31). The total amount of PAHs present in CS, in contrast, is in the range of just a few micrograms (8). Acr has been shown to interact with nucleophiles, including DNA and proteins in cells (32). Unlike PAHs, where only metabolically activated forms can form adducts with DNA, Acr can directly interact with DNA and form DNA adducts (18, 23). Similar to PAH–DNA adducts, Acr–DNA adducts induce mainly G:C-to-T:A transversion mutations (10, 33–35), the major type of mutations found in the *p53* gene in CS-related lung cancer. Although the carcinogenicity of Acr in the lung has not been studied because of the severe toxicity associated with Acr treatment in animals, i.p. injection of Acr has been shown to cause bladder cancer in rats (36). These results indicate that Acr is indeed a carcinogenic substance. Although the effects of CS on Acr–dG formation in the lung tissue of cigarette smokers has not been determined, it has been reported that the level of Acr–dG DNA adducts in the oral tissue of smokers is in the range of a few micromoles per mole of guanine, which is far above the level of PAH–DNA adducts found in the oral or lung tissue of cigarette smokers (12, 13). It is very likely that the level of Acr–dG in lung tissue is similar to that found in the oral tissues of cigarette smokers. If this is the case, then, based on Acr abundance in CS, its reactivity toward DNA, and mutagenicity of Acr–DNA adducts, Acr is potentially one of the major etiological agents of CS-induced lung cancer. Our current results demonstrate that, similar to PAHs, Acr preferentially binds to *p53* mutational hotspots of CS-related lung cancer in human cells, including NHBE cells. These results strongly suggest that Acr–dG adducts, as well as PAH–DNA adducts, contribute greatly to these mutations in lung cancer.

We have found that all of the Acr preferential binding guanines, except for codon 249, in the *p53* gene are located at CpG sequences and that C5 cytosine methylation at CpG sites can greatly enhance Acr–dG adduct formation. This C5 cytosine methylation has been previously shown to also enhance guanine adduction at CpG sites by BPDE, aflatoxin B1 8,9-epoxide, and *N*-acetoxy-acetylaminofluorene, even though the binding positions by these agents on guanines are different (25). The precise mechanism of how C5 methylation enhances adduction to guanines at these sites has yet to be elucidated. It is worth noting that these CpG sites are in the coding region of the *p53* gene and are also very distant from promoter region. The function and the extent of methylation at these CpG sites in the *p53* gene in NHBE and lung fibroblasts are also unknown and may vary among different individuals. If this is the case perhaps these variations may contribute to the different susceptibilities of individuals to CS-induced lung cancer.

We found that codon 249 in the *p53* gene is a preferential binding site for Acr even though it is not a CpG-containing site and the Acr binding at this position is not affected by CpG methylation at the surrounding sequences (codon 248). Codon 249 is a mutational hotspot in lung and liver cancers (2) (Fig. 5). Intriguingly, we found that all of the PAHs we tested and AFB1–8,9-epoxides, the etiological agents for liver cancer, do not preferentially bind to codon 249 (3, 5, 7, 25). Recently, however, we found that 4-HNE, another $\alpha,\beta$-unsaturated aldehyde and a major lipid peroxidation product that is also able to interact with DNA to form exocyclic propanodeoxyguanosine adducts, preferentially forms DNA adducts at this codon (37). 4-HNE–dG adducts have been found to induce G:C-to-T:A mutations in human cells (38). Increasing evidence suggests that lipid peroxidation and chronic oxidative stress play important roles in human carcinogenesis; although the mechanisms involved are unclear, it is possible that aldehydes resulting from endogenous lipid peroxidation and other sources, such as Acr, 4-HNE, malondialdehyde, and crotonaldehyde, may contribute greatly to mutations at codon 249 in human cancer.

We have also found that Acr can greatly reduce the NER capacity. NER is the major repair pathway for bulky DNA damage, including PAH–DNA adducts and exocyclic propanodeoxyguanine adducts (22, 39). It has been found that the NER capacity in individuals who have a genetic defect in NER genes, such as xeroderma pigmentosum patients, is reduced to 10–20% that of normal individuals; these patients have 2,000-fold and 20- to 30-fold higher cancer incidence in skin and internal organs, respectively (40). NER gene knockout animals have a predisposition for spontaneous and chemically induced carcinogenesis (41). It has been strongly suggested that PAHs present in CS and in the environment are the agents responsible for the lung carcinogenesis, and the DNA damage induced by activated metabolites of PAHs initiate carcinogenesis (5, 7, 42). Our findings that Acr greatly inhibit cellular repair capacity to remove BPDE–DNA adducts in human lung cells strongly suggest that Acr also contributes significantly to lung carcinogenesis by its inhibitory effects on DNA repair in addition to damaging DNA directly. Our findings that the Acr–dG adduct distribution is similar to the mutational spectrum in CS-related lung cancer and that Acr can cause a significant inhibitory effect on DNA repair raise the possibility that Acr is an equally potent, if not more potent, lung cancer etiological agent as PAHs, considering the abundant amount of Acr in CS and in the environment. We propose that the carcinogenicity of Acr is derived from two detrimental effects: damaging DNA and reducing DNA repair capacity. These two effects may in turn lead to more mutations, which can be induced by both PAHs and Acr, to trigger carcinogenesis.

Worldwide, >2 million people die of CS-related cancer annually (43). Although smoking cessation is the most effective way to reduce these cigarette-induced deaths, this approach is unrealistic in the short term. Identifying the etiological agents for CS-induced cancer and designing methods to eliminate them from CS provide us with the simplest and most realistic solution. Although Acr carcinogenicity requires further epidemiological confirmation and studies in proper animal models, immediate measures to reduce this contaminant both in CS and in the environment seem warranted.

## Materials and Methods

**Cell Culture, Carcinogen Treatment, and Genomic DNA Isolation.** NHBE cells were cultured in medium provided by Clonetics (San Diego, CA). NHLF (CCL-202) and lung adenocarcinoma cells (A549) (American Type Culture Collection, Manassas, VA) were grown in MEM supplemented with 10% FBS. Stock solutions of Acr (Sigma-Aldrich, St. Louis, MO) and BPDE (Chemsyn Science Laboratories, Lenexa, KS) were prepared immediately before use. Cells at 70% confluency were washed with phosphate buffer

(PBS/70 mM NaCl/2 mM KCl/1 mM $KH_2PO_4$, pH 7.4) and treated with different concentrations of Acr (0–100 $\mu$M) in serum-free culture medium for 6 h or different concentrations of BPDE for 30 min at 37°C in the dark. After treatment, the genomic DNA was isolated as previously described (5–7). For *in vitro* modifications, genomic DNA was isolated from untreated cells and dissolved in $H_2O$, mixed with different concentrations of Acr, and incubated at 37°C for 12 h. After repeated phenol and diethyl ether extractions, the DNA was then precipitated with ethanol and dissolved in TE buffer (10 mM Tris, pH 7.5/1 mM EDTA).

**Acr–DNA Adduct Analysis.** Acr–DNA adducts formed in cells treated with Acr (0–100 $\mu$M) and in purified genomic DNA modified with Acr (0–100 $\mu$M) were analyzed by the $^{32}$P postlabeling and the 2D TLC method on polyethyleneimine cellulose sheets (Anatech, Newark, DE), as described by Eder and Budiawan (44). The solvents used were as follows: D1, 0.7 M ammonium formate (pH 3.5); D2, 0.3 M ammonium sulfate (pH 7.5). The chromatograms were visualized by autoradiography, the Acr–DNA adducts (although all $^{32}$P-labeled Acr–dG adducts were in 3′,5′-bisphosphate forms, for the sake of simplicity they remain labeled as Acr–dG adducts) were excised, and the radioactivity was measured. Acr–DNA adduct levels were calculated by determining the relative adduct labeling, which is the ratio of labeled adduct nucleotides to labeled total nucleotides. The specific radioactivity of [$\gamma$-$^{32}$P]ATP, determined by labeling a known amount of dGMP (deoxyadenosine 3′-phosphate) (Sigma), was used for the relative labeling calculations. The well characterized Acr–dG 2 and Acr–dG 3 adducts and oligomer containing Acr–dG 3 [kindly provided by Fung-Lung Chung (Georgetown University, Washington, DC) and Carmelo Rizzo and Larry Marnett (Vanderbilt University, Nashville, TN), respectively] were used as standards (16).

**Preparation of $^{32}$P End-Labeled *p53* DNA Fragments and C5 Cytosine Methylation at CpG Sites.** DNA fragments of 247-bp 5′ $^{32}$P-end-labeled *p53* exon 5 and 141-bp 3′ $^{32}$P-end-labeled *p53* exon 7 were prepared according to the previously described method (19). These $^{32}$P-end-labeled *p53* DNA fragments were subjected to SssI methylase (New England Biolabs, Beverly, MA) treatment in the presence of *S*-adenosylmethionine according to the manufacturer's instructions to methylate all cytosines at CpG sites.

**Acr Modification of Supercoiled Plasmids and DNA Fragments and UvrABC Incision Assay of Acr–dG Adducts.** Supercoiled pGEM plasmids, purified as described previously (14), and $^{32}$P-labeled DNA fragments were modified with different concentrations of Acr solution and purified as described above; after ethanol precipitation DNA was dissolved in TE buffer. Methods for UvrA, UvrB, and UvrC protein purifications, UvrABC nuclease incision assays, separations of the resultant DNA, and quantification of band intensity were the same as previously described (5–7, 22).

**Mapping DNA Adduct Distribution in the *p53* Gene in Human Genomic DNA by Using the UvrABC/LMPCR Method.** The UvrABC/LMPCR method was the same as described previously (5, 20). Each experiment was repeated three times with very similar results. The calculation of the relative intensities of DNA adduct formation at different codons in the *p53* gene was performed as previously described (5, 20). We used various concentrations of Acr for treating cells in this study and found that concentrations did not qualitatively affect the Acr–DNA binding patterns. Thus, for the sake of clarity, results from one concentration were used for the quantitative determinations.

**Determination of the Effect of Acr Treatment on DNA Repair.** Host cell reactivation and *in vitro* DNA repair synthesis assays were performed as previously described to determine the effects of Acr treatment on DNA repair in human cells (14, 15).

**Determination of Mutations Induced by Acr–DNA Adducts.** The methods used for mutation detection and for mutational spectrum determination were the same as previously described (38). Briefly, shuttle vector pSP189 plasmid DNA was modified with different concentrations of Acr and transfected into NHLF for replication. Plasmids were recovered 72 h after transfection, and replicated plasmids were then transformed into MB7070 *E. coli* indicator cells. The *supF* gene in plasmids isolated from mutant white colonies were then sequenced.

We thank Drs. Yen-Yee T. Nydam and Cathy Klein for critical review and Joyce Clemente and Helen Duss for manuscript preparation. This study was supported by National Institutes of Health Grants ES03124, ES10344, ES00260, CA99007, and CA114541.

1. Olivier M, Eeles R, Hollstein M, Khan MA, Harris CC, Hainaut P (2002) *Hum Mutat* 19:607–614.
2. Greenblatt MS, Bennett WP, Hollstein M, Harris CC (1994) *Cancer Res* 54:4855–4878.
3. Hsu IC, Metcalf RA, Sun T, Welsh JA, Wang NJ, Harris CC (1991) *Nature* 350:427–428.
4. Brash DE (1997) *Trends Genet* 13:410–414.
5. Denissenko MF, Pao A, Tang M-s, Pfeifer GP (1996) *Science* 274:430–432.
6. Denissenko M, Pao A, Pfeifer G, Tang M-s (1998) *Oncogene* 16:1241–1249.
7. Smith LE, Denissenko MF, Bennett WP, Amin S, Tang M-s, Pfeifer GP (2000) *J Natl Cancer Inst* 92:803–811.
8. Hoffman D, Hecht SS (1990) in *Handbook of Experimental Pharmacology*, eds Cooper CS, Grover PL (Springer, Heidelberg), pp 70–74.
9. Gomes R, Meek ME, Eggleton M (2002) *Concise International Chemical Assessment Document No 43* (World Health Organization, Geneva).
10. Curren RD, Yang LL, Conklin PM, Grafstrom RC, Harris CC (1988) *Mutat Res* 209:17–22.
11. Grafstrom RC, Dypbukt JM, Willey JC, Sundqvist K, Edman C, Atzori L, Harris CC (1988) *Cancer Res* 48:1717–1721.
12. Nath RG, Chung F-L (1994) *Proc Natl Acad Sci USA* 91:7491–7495.
13. Nath RG, Ocando JE, Guttenplan JB, Chung F-L (1998) *Cancer Res* 58:581–584.
14. Feng Z, Hu W, Tang M-s (2004) *Proc Natl Acad Sci USA* 101:8598–8602.
15. Feng Z, Hu W, Marnett L, Tang M-s (2006) *Mutat Res*, in press.
16. Chung F-L, Young R, Hecht SS (1984) *Cancer Res* 44:990–995.
17. Foiles PG, Akerkar SA, Miglietta LM, Chung F-L (1990) *Carcinogenesis* 11:2059–2061.
18. Nath RG, Chen HJC, Nishikawa A, Young-Sciame R, Chung F-L (1994) *Carcinogenesis* 15:979–984.
19. Feng Z, Hu W, Rom WN, Beland FA, Tang M-s (2002) *Biochemistry* 41:6414–6421.
20. Feng Z, Hu W, Chen JX, Pao A, Li H, Rom W, Hung MC, Tang M-S (2002) *J Natl Cancer Inst* 94:1527–1536.
21. Feng Z, Hu W, Rom WN, Beland FA, Tang M-s (2002) *Carcinogenesis* 23:1721–1727.
22. Tang M-s (1996) in *Technologies for Detection of DNA Damage and Mutation*, ed Pfeifer G (Plenum, New York), pp 139–152.
23. Tornaletti S, Pfeifer GP (1995) *Oncogene* 10:1493–1499.
24. Johnson WS, He QY, Tomasz M (1995) *Bioorg Med Chem* 3:851–860.
25. Chen JX, Zheng Y, West M, Tang M-s (1998) *Cancer Res* 58:2070–2075.
26. Maxam AM, Gilbert W (1980) *Methods Enzymol* 65:499–560.
27. Pfeifer GP, Hainaut P (2003) *Mutat Res* 526:39–43.
28. World Health Organization (1997) *Tobacco or Health: A Global Status Report* (World Health Organization, Geneva).
29. Hoffmann D, Hoffmann I, El-Bayoumy K (2001) *Chem Res Toxicol* 14:767–790.
30. Hecht SS, Carmella SG, Murphy SE, Foiles PG, Chung F-L (1993) *J Cell Biochem Suppl* 17F:27–35.
31. Fujioka K, Shibamoto T (2006) *Environ Toxicol* 21:47–54.
32. Esterbauer H, Schaur RJ, Zollner H (1991) *Free Radical Biol Med* 11:81–128.
33. Kawanishi M, Matsuda T, Nakayama A, Takebe H, Matsui S, Yagi T (1998) *Mutat Res* 417:65–73.
34. Kanuri M, Minko IG, Nechev LV, Harris TM, Harris CM, Lloyd RS (2002) *J Biol Chem* 21:18257–18265.
35. Yang IY, Chan G, Miller H, Huang Y, Torres MC, Johnson F, Moriya M (2002) *Biochemistry* 41:13826–13832.
36. Cohen SM, Garland EM, St John M, Okamura T, Smith RA (1992) *Cancer Res* 52:3577–3581.
37. Hu W, Feng Z, Eveleigh J, Iyer G, Pan J, Amin S, Chung F-L, Tang M-s (2002) *Carcinogenesis* 23:1781–1789.
38. Feng Z, Hu W, Amin S, Tang M-s (2003) *Biochemistry* 42:7848–7854.
39. Sancar A, Tang M-S (1993) *Photochem Photobiol* 57:905–921.
40. Cleaver JE (2005) *Nat Rev Cancer* 5:564–573.
41. van Steeg H, Mullenders LH, Vijg J (2000) *Mutat Res* 450:167–180.
42. Harvey RG (1991) in *Chemistry and Carcinogenicity* (Oxford Univ Press, Oxford), p 396.
43. Stewart BW, Kleihues P, eds (2003) World Cancer Report (IARC Press, World Health Organization, Geneva).
44. Eder E, Budiawan (2001) *Cancer Epidemiol* 10:883–888.

# Lung Cancer, Cardiopulmonary Mortality, and Long-term Exposure to Fine Particulate Air Pollution

C. Arden Pope III, PhD
Richard T. Burnett, PhD
Michael J. Thun, MD
Eugenia E. Calle, PhD
Daniel Krewski, PhD
Kazuhiko Ito, PhD
George D. Thurston, ScD

**Context** Associations have been found between day-to-day particulate air pollution and increased risk of various adverse health outcomes, including cardiopulmonary mortality. However, studies of health effects of long-term particulate air pollution have been less conclusive.

**Objective** To assess the relationship between long-term exposure to fine particulate air pollution and all-cause, lung cancer, and cardiopulmonary mortality.

**Design, Setting, and Participants** Vital status and cause of death data were collected by the American Cancer Society as part of the Cancer Prevention II study, an ongoing prospective mortality study, which enrolled approximately 1.2 million adults in 1982. Participants completed a questionnaire detailing individual risk factor data (age, sex, race, weight, height, smoking history, education, marital status, diet, alcohol consumption, and occupational exposures). The risk factor data for approximately 500 000 adults were linked with air pollution data for metropolitan areas throughout the United States and combined with vital status and cause of death data through December 31, 1998.

**Main Outcome Measure** All-cause, lung cancer, and cardiopulmonary mortality.

**Results** Fine particulate and sulfur oxide–related pollution were associated with all-cause, lung cancer, and cardiopulmonary mortality. Each 10-$\mu g/m^3$ elevation in fine particulate air pollution was associated with approximately a 4%, 6%, and 8% increased risk of all-cause, cardiopulmonary, and lung cancer mortality, respectively. Measures of coarse particle fraction and total suspended particles were not consistently associated with mortality.

**Conclusion** Long-term exposure to combustion-related fine particulate air pollution is an important environmental risk factor for cardiopulmonary and lung cancer mortality.

*JAMA. 2002;287:1132-1141* www.jama.com

BASED ON SEVERAL SEVERE AIR pollution events,[1-3] a temporal correlation between extremely high concentrations of particulate and sulfur oxide air pollution and acute increases in mortality was well established by the 1970s. Subsequently, epidemiological studies published between 1989 and 1996 reported health effects at unexpectedly low concentrations of particulate air pollution.[4] The convergence of data from these studies, while controversial,[5] prompted serious reconsideration of standards and health guidelines[6-10] and led to a long-term research program designed to analyze health-related effects due to particulate pollution.[11-13] In 1997, the Environmental Protection Agency adopted new ambient air quality standards that would impose regulatory limits on fine particles measuring less than 2.5 μm in diameter ($PM_{2.5}$). These new standards were challenged by industry groups, blocked by a federal appeals court, but ultimately upheld by the US Supreme Court.[14]

Although most of the recent epidemiological research has focused on effects of short-term exposures, several studies suggest that long-term exposure may be more important in terms of overall public health.[4] The new standards for long-term exposure to $PM_{2.5}$ were originally based primarily on 2 prospective cohort studies,[15,16] which evaluated the effects of long-term pollution exposure on mortality. Both of these studies have been subjected to much scrutiny,[5] including an extensive independent audit and reanalysis of the original data.[17] The larger of these 2 studies linked individual risk factor and vital status data with national ambient air pollution data.[16] Our analysis uses data from the larger study and

**Author Affiliations:** Brigham Young University, Provo, Utah (Dr Pope); Health Canada, Ottawa, Ontario (Dr Burnett); University of Ottawa, Ottawa, Ontario (Drs Burnett and Krewski); American Cancer Society, Atlanta, Ga (Drs Thun and Calle); and New York University School of Medicine, Tuxedo, NY (Drs Ito and Thurston).
**Corresponding Author and Reprints:** C. Arden Pope III, PhD, Department of Economics, Brigham Young University, 142 FOB, Provo, UT 84602 (e-mail: cap3@email.byu.edu).

(1) doubles the follow-up time to more than 16 years and triples the number of deaths; (2) substantially expands exposure data, including gaseous copollutant data and new $PM_{2.5}$ data, which have been collected since the promulgation of the new air quality standards; (3) improves control of occupational exposures; (4) incorporates dietary variables that account for total fat consumption, and consumption of vegetables, citrus, and high-fiber grains; and (5) uses recent advances in statistical modeling, including the incorporation of random effects and nonparametric spatial smoothing components in the Cox proportional hazards model.

## METHODS

### Study Population

The analysis is based on data collected by the American Cancer Society (ACS) as part of the Cancer Prevention Study II (CPS-II), an ongoing prospective mortality study of approximately 1.2 million adults.[18,19] Individual participants were enrolled by ACS volunteers in the fall of 1982. Participants resided in all 50 states, the District of Columbia, and Puerto Rico, and were generally friends, neighbors, or acquaintances of ACS volunteers. Enrollment was restricted to persons who were aged 30 years or older and who were members of households with at least 1 individual aged 45 years or older. Participants completed a confidential questionnaire, which included questions about age, sex, weight, height, smoking history, alcohol use, occupational exposures, diet, education, marital status, and other characteristics.

Vital status of study participants was ascertained by ACS volunteers in September of the following years: 1984, 1986, and 1988. Reported deaths were verified with death certificates. Subsequently, through December 31, 1998, vital status was ascertained through automated linkage of the CPS-II study population with the National Death Index.[19] Ascertainment of deaths was more than 98% complete for the period of 1982-1988 and 93% complete after 1988.[19] Death certificates or codes for cause of death were obtained for more than 98% of all known deaths. Cause of death was coded according to the *International Classification of Diseases, Ninth Revision (ICD-9)*. Although the CPS-II cohort included approximately 1.2 million participants with adequate questionnaire and cause-of-death data, our analysis was restricted to those participants who resided in US metropolitan areas with available pollution data. The actual size of the analytic cohort varied depending on the number of metropolitan areas for which pollution data were available. TABLE 1 provides the number of metropolitan areas and participants available for each source of pollution data.

### Air Pollution Exposure Estimates

Each participant was assigned a metropolitan area of residence based on address at time of enrollment and 3-digit ZIP code area.[20] Mean (SD) concentrations of air pollution for the metropolitan areas were compiled from various primary data sources (Table 1). Many of the particulate pollution indices, including $PM_{2.5}$, were available from data from the Inhalable Particle Monitoring Network for 1979-1983 and data from the National Aerometric Database for 1980-1981, periods just prior to or at the beginning of the follow-up period. An additional data source was the Environmental Protection Agency Aerometric Information Retrieval System (AIRS). The mean concentration of each pollutant from all available monitoring sites was calculated for each metropolitan area during the 1 to 2 years prior to enrollment.[17]

Additional information on ambient pollution during the follow-up period was extracted from the AIRS database as quarterly mean values for each routinely monitored pollutant for 1982 through 1998. All quarterly averages met summary criteria imposed by the Environmental Protection Agency and were based on observations made on at least 50% of the scheduled sampling days at each site. The quarterly mean values for all stations in each metropolitan area were calculated across the study years using daily average values for each pollutant except ozone. For ozone, daily 1-hour maximums were used and were calculated for the full year and for the third quarter only (ie, July, August, September). While gaseous pollutants generally had recorded data throughout the entire follow-up period of interest, the particulate matter monitoring protocol changed in the late 1980s from total suspended particles to particles measuring less than 10 μm in diameter ($PM_{10}$), resulting in the majority of total suspended particle data being available in the early to mid-1980s and $PM_{10}$ data being mostly available in the early to mid-1990s.

As a consequence of the new $PM_{2.5}$ standard, a large number of sites began collecting $PM_{2.5}$ data in 1999. Daily $PM_{2.5}$ data were extracted from the AIRS database for 1999 and the first 3 quarters of 2000. For each site, quarterly averages for each of the 2 years were computed. The 4 quarters were averaged when at least 1 of the 2 corresponding quarters for each year had at least 50% of the sixth-day samples and at least 45 total sampling days available. Measurements were averaged first by site and then by metropolitan area. Although no network of $PM_{2.5}$ monitoring existed in the United States between the early 1980s and the late 1990s, the integrated average of $PM_{2.5}$ concentrations during the period was estimated by averaging the $PM_{2.5}$ concentration for early and later periods.

Mean sulfate concentrations for 1980-1981 were available for many cities based on data from the Inhalable Particle Monitoring Network and the National Aerometric Database. Recognizing that sulfate was artifactually overestimated due to glass fiber filters used at that time, season and region-specific adjustments were made.[17] Since few states analyzed particulate samples for sulfates after the early 1980s, individual states were directly contacted for data regarding filter use. Ion chromatography was used to analyze $PM_{10}$ filters and this data could be obtained from metropolitan areas across the

United States. Filters were collected for a single reference year (1990) in the middle of the 1982-1998 study period. The use of quartz filters virtually eliminated the historical overestimation of sulfate. Mean sulfate concentrations for 1990 were estimated using sulfate from AIRS, data reported directly from individual states, and analysis of archived filters.

### Statistical Analysis

The basic statistical approach used in this analysis is an extension of the standard Cox proportional hazards survival model,[21] which has been used for risk estimates of pollution-related mortality in previous longitudinal cohort studies.[15,16] The standard Cox model implicitly assumes that observations are statistically independent after controlling for available risk factors, resulting in 2 concerns with regard to risk estimates of pollution-related mortality.[22] First, if the assumption of statistical independence is not valid, the uncertainty in the risk estimates of pollution-related mortality may be misstated. Second, even after controlling for available risk factors, survival times of participants living in communities closer together may be more similar than participants living in communities farther apart, which results in spatial autocorrelation. If this spatial autocorrelation is due to missing or systematically mismeasured risk factors that are spatially correlated with air pollution, then the risk estimates of pollution-related mortality may be biased due to inadequate control of these factors. Therefore, in this analysis, the Cox proportional hazards model was extended by incorporating a spatial random-effects component, which provided accurate es-

**Table 1.** Summary of Alternative Pollution Indices*

| Pollutant (Years of Data Collection) | Units | Source of Data | Data Compilation Team† | No. of Metropolitan Areas | No. of Participants, in Thousands | Mean (SD) |
|---|---|---|---|---|---|---|
| $PM_{2.5}$ | μg/m³ | | | | | |
| 1979-1983 | | IPMN | HEI | 61 | 359 | 21.1 (4.6) |
| 1999-2000 | | AIRS | NYU | 116 | 500 | 14.0 (3.0) |
| Average | | | | 51 | 319 | 17.7 (3.7) |
| $PM_{10}$ | μg/m³ | | | | | |
| 1982-1998 | | AIRS | NYU | 102 | 415 | 28.8 (5.9) |
| $PM_{15}$ | μg/m³ | | | | | |
| 1979-1983 | | IPMN | HEI | 63 | 359 | 40.3 (7.7) |
| $PM_{15-2.5}$ | μg/m³ | | | | | |
| 1979-1983 | | IPMN | HEI | 63 | 359 | 19.2 (6.1) |
| Total suspended particles | μg/m³ | | | | | |
| 1980-1981 | | NAD | HEI | 156 | 590 | 68.0 (16.7) |
| 1979-1983 | | IPMN | HEI | 56 | 351 | 73.7 (14.3) |
| 1982-1998 | | AIRS | NYU | 150 | 573 | 56.7 (13.1) |
| Sulfate | μg/m³ | | | | | |
| 1980-1981 | | IPMN and NAD, artifact adjusted | HEI | 149 | 572 | 6.5 (2.8) |
| 1990 | | Compilation and analysis of $PM_{10}$ filters | NYU | 53 | 269 | 6.2 (2.0) |
| Sulfur dioxide | ppb | AIRS | | | | |
| 1980 | | | HEI | 118 | 520 | 9.7 (4.9) |
| 1982-1998 | | | NYU | 126 | 539 | 6.7 (3.0) |
| Nitrogen dioxide | ppb | AIRS | | | | |
| 1980 | | | HEI | 78 | 409 | 27.9 (9.2) |
| 1982-1998 | | | NYU | 101 | 493 | 21.4 (7.1) |
| Carbon monoxide | ppm | AIRS | | | | |
| 1980 | | | HEI | 113 | 519 | 1.7 (0.7) |
| 1982-1998 | | | NYU | 122 | 536 | 1.1 (0.4) |
| Ozone | ppb | AIRS | | | | |
| 1980 | | | HEI | 134 | 569 | 47.9 (11.0) |
| 1982-1998 | | | NYU | 119 | 525 | 45.5 (7.3) |
| 1982-1998‡ | | | NYU | 134 | 557 | 59.7 (12.8) |

*$PM_{2.5}$ indicates particles measuring less than 2.5 μm in diameter; $PM_{10}$, particles measuring less than 10 μm in diameter; $PM_{15}$, particles measuring less than 15 μm in diameter; $PM_{15-2.5}$, particles measuring between 2.5 and 15 μm in diameter; μg/m³, micrograms per cubic meter; ppb, parts per billion; ppm, parts per million; IPMN, Inhalable Particle Monitoring Network; AIRS, Aerometric Information Retrieval System [Environmental Protection Agency]; and NAD, National Aerometric Database.
†HEI indicates data were compiled by the Health Effects Institute reanalysis team, which was previously published.[17] NYU indicates data were compiled at the New York University School of Medicine, Nelson Institute of Environmental Medicine (K.I. and G.D.T.).
‡Daily 1-hour maximums were used. Values were calculated only for the third quarter (ie, July, August, September).

timates of the uncertainty of effect estimates. The model also evaluated spatial autocorrelation and incorporated a nonparametric spatial smooth component (to account for unexplained spatial structure). A more detailed description of this modeling approach is provided elsewhere.[22]

The baseline analysis in this study estimated adjusted relative risk (RR) ratios for mortality by using a Cox proportional hazards model with inclusion of a metropolitan-based random-effects component. Model fitting involved a 2-stage process. In the first stage, survival data were modeled using the standard Cox proportional hazards model, including individual level covariates and indicator variables for each metropolitan area (without pollution variables). Output from stage 1 provided estimates of the metropolitan-specific logarithm of the RRs of mortality (relative to an arbitrary reference community), which were adjusted for individual risk factors. The correlation between these values, which was induced by using the same reference community, was then removed.[23] In the second stage, the estimates of adjusted metropolitan-specific health responses were related to fine particulate air pollution using a linear random-effects regression model.[24] The time variable used in the models was survival time from the date of enrollment. Survival times of participants who did not die were censored at the end of the study period. To control for age, sex, and race, all of the models were stratified by 1-year age categories, sex, and race (white vs other), which allowed each category to have its own baseline hazard. Models were estimated for all-cause mortality and for 3 separate mortality categories: cardiopulmonary (*ICD-9* 401-440 and 460-519), lung cancer (*ICD-9* 162), and all others.

Models were estimated separately for each of the 3 fine particle variables, $PM_{2.5}$ (1979-1983), $PM_{2.5}$ (1999-2000), and $PM_{2.5}$ (average). Individual level covariates were included in the models to adjust for various important individual risk factors. All of these variables were classified as either indicator (ie, yes/no, binary, dummy) variables or continuous variables. Variables used to control for tobacco smoke, for example, included both indicator and continuous variables. The smoking indicator variables included: current cigarette smoker, former cigarette smoker, and a pipe or cigar smoker only (all vs never smoking) along with indicator variables for starting smoking before or after age 18 years. The continuous smoking variables included: current smoker's years of smoking, current smoker's years of smoking squared, current smoker's cigarettes per day, current smoker's cigarettes per day squared, former smoker's years of smoking, former smoker's years of smoking squared, former smoker's cigarettes per day, former smoker's cigarettes per day squared, and the number of hours per day exposed to passive cigarette smoke.

To control for education, 2 indicator variables, which indicated completion of high school or education beyond high school, were included. Marital status variables included indicator variables for single and other vs married. Both body mass index (BMI) values and BMI values squared were included as continuous variables. Indicator variables for beer, liquor, and wine drinkers and nonresponders vs nondrinkers were included to adjust for alcohol consumption. Occupational exposure was controlled for using various indicator variables: regular occupational exposure to asbestos, chemicals/acids/solvents, coal or stone dusts, coal tar/pitch/asphalt, diesel engine exhaust, or formaldehyde, and additional indicator variables that indicated 9 different rankings of an occupational dirtiness index that has been developed and described elsewhere.[17,25] Two diet indices that accounted for fat consumption and consumption of vegetables, citrus, and high-fiber grains were derived based on information given in the enrollment questionnaire.[18] Quintile indicator variables for each of these diet indices were also included in the models.[18]

In addition to the baseline analysis, several additional sets of analysis were conducted. First, to more fully evaluate the shape of the concentration-response function, a robust locally weighted regression smoother[26] (within the generalized additive model framework[27]) was used to estimate the relationship between particulate air pollution and mortality in the second stage of model fitting. Second, the sensitivity of the fine particle mortality risk estimates compared with alternative modeling approaches and assumptions was evaluated. Standard Cox proportional hazards models were fit to the data including particulate air pollution as a predictor of mortality and sequentially adding (in a controlled forward stepwise process) groups of variables to control for smoking, education, marital status, BMI, alcohol consumption, occupational exposures, and diet.

In addition, to evaluate the sensitivity of the estimated pollution effect while more aggressively controlling for spatial differences in mortality, a 2-dimensional term to account for spatial trends was added to the models and was estimated using a locally weighted regression smoother. The "span" parameter, which controls the complexity of the surface smooth, was set at 3 different settings to allow for increasingly aggressive fitting of the spatial structure. These included a default span of 50%, the span that resulted in the lowest unexplained variance in mortality rate between metropolitan areas, and the span that resulted in the strongest evidence (highest $P$ value) to suggest no residual spatial structure. The risk estimates and SEs (and thus the confidence intervals) were estimated using generalized additive modeling[27] with S-Plus statistical software,[28] which provides unbiased effect estimates, but may underestimate SEs if there is significant spatial autocorrelation and significant correlations between air pollution and the smoothed surface of mortality. Therefore, evidence of spatial autocorrelation was carefully evaluated and tested using the Bartlett test.[29] The correlations of residual mortality

with distance between metropolitan areas were graphically examined.

Analyses were also conducted of effect modification by age, sex, smoking status, occupational exposure, and education. Finally, models were fit using a variety of alternative pollution indices, including gaseous pollutants. Specifically, models were estimated separately for each of the pollution variables listed in Table 1, while also including all of the other risk factor variables.

## RESULTS

Fine particulate air pollution generally declined in the United States during the follow-up period of this study. FIGURE 1 plots mean $PM_{2.5}$ concentrations for 1999-2000 over mean $PM_{2.5}$ concentrations for 1979-1983 for the 51 cities in which paired data were available. The concentrations of $PM_{2.5}$ were lower in 1999-2000 than in 1979-1983 for most cities, with the largest reduction observed in the cities with the highest concentrations of pollution during 1979-1983. Mean $PM_{2.5}$ levels in the 2 periods were highly correlated ($r$=0.78). The rank ordering of cities by relative pollution levels remained nearly the same. Therefore, the relative levels of fine particle concentrations were similar whether based on measurements at the beginning of the study period, shortly following the study period, or an average of the 2.

**Figure 1.** Mean Fine Particles Measuring Less Than 2.5 µm in Diameter ($PM_{2.5}$)

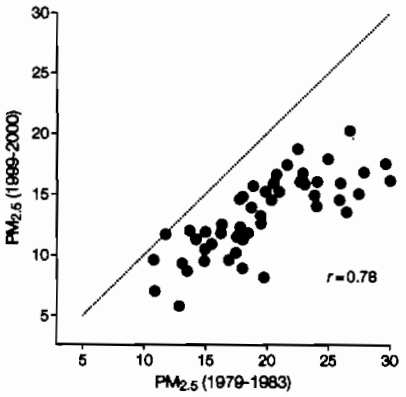


Mean $PM_{2.5}$ concentrations in micrograms per meters cubed for 1999-2000 are plotted along with concentrations for 1979-1983 for the 51 metropolitan areas with paired pollution data. The dotted line is a reference 45°-equality line.

As reported in TABLE 2, all 3 indices of fine particulate air pollution were associated with all-cause, cardiopulmonary, and lung cancer mortality, but not mortality from all other causes combined. FIGURE 2 presents the nonparametric smoothed exposure response relationships between cause-specific mortality and $PM_{2.5}$ (average). The log RRs for all-cause, cardiopulmonary, and lung cancer mortality increased across the gradient of fine particulate matter. Goodness-of-fit tests indicated that the associations were not significantly different from linear associations ($P$>.20).

The fine particle mortality RR ratios from various alternative modeling approaches and assumptions are presented in FIGURE 3. After controlling for smoking, education, and marital status, the controlled forward stepwise inclusion of additional covariates had little influence on the estimated associations with fine particulate air pollution on cardiopulmonary and lung cancer mortality. As expected, cigarette smoking was highly significantly associated with elevated risk of all-cause, cardiopulmonary, and lung cancer mortality ($P$<.001). Estimated RRs for an average current smoker (men and women combined, 22 cigarettes/day for 33.5 years, with initiation before age 18 years) were equal to 2.58, 2.89, and 14.80 for all-cause, cardiopulmonary, and lung cancer mortality, respectively. Statistically significant, but substantially smaller and less robust associations, were also observed for education, marital status, BMI, alcohol consumption, occupational exposure, and diet variables. Although many of these covariates were also statistically associated with mortality, the risk estimates of pollution-related mortality were not highly sensitive to the inclusion of these additional covariates.

Figure 3 also demonstrates that the introduction of the random-effects component to the model resulted in larger SEs of the estimates and, therefore, somewhat wider 95% confidence intervals. There was no evidence of statistically significant spatial autocorrelation in the survival data based on the Bartlett test ($P$>.20) after controlling for fine particulate air pollution and the various individual risk factors. Furthermore, graphical examination of the correlations of the residual mortality with distance between metropolitan areas did not reveal significant spatial autocorrelation (results not shown). Nevertheless, the incorporation of spatial smoothing was included to further investigate the robustness of the estimated particulate pollution effect. Effect estimates were not highly sensitive to the incorporation of spatial smoothing to account for regional clustering or other spatial patterns in the data.

FIGURE 4 presents fine particle air pollution–related mortality RR ratios after stratifying by age, sex, education, and smoking status, and adjusting for all other risk factors. The differences across age and sex strata were not generally consistent or statistically significant. However, a consistent pattern emerged from this stratified analysis: the association with particulate pollution was stronger for both cardiopulmo-

**Table 2.** Adjusted Mortality Relative Risk (RR) Associated With a 10-µg/m³ Change in Fine Particles Measuring Less Than 2.5 µm in Diameter

| | Adjusted RR (95% CI)* | | |
|---|---|---|---|
| Cause of Mortality | 1979-1983 | 1999-2000 | Average |
| All-cause | 1.04 (1.01-1.08) | 1.06 (1.02-1.10) | 1.06 (1.02-1.11) |
| Cardiopulmonary | 1.06 (1.02-1.10) | 1.08 (1.02-1.14) | 1.09 (1.03-1.16) |
| Lung cancer | 1.08 (1.01-1.16) | 1.13 (1.04-1.22) | 1.14 (1.04-1.23) |
| All other cause | 1.01 (0.97-1.05) | 1.01 (0.97-1.06) | 1.01 (0.95-1.06) |

*Estimated and adjusted based on the baseline random-effects Cox proportional hazards model, controlling for age, sex, race, smoking, education, marital status, body mass, alcohol consumption, occupational exposure, and diet. CI indicates confidence interval.

nary and lung cancer mortality for participants with less education. Also, for both cardiopulmonary and lung cancer mortality, the RR estimates were higher for nonsmokers.

FIGURE 5 summarizes the associations between mortality risk and air pollutant concentrations listed in Table 1. Statistically significant and relatively consistent mortality associations existed for all measures of fine particulate exposure, including $PM_{2.5}$ and sulfate particles. Weaker less consistent mortality associations were observed with $PM_{10}$ and $PM_{15}$. Measures of the coarse particle fraction ($PM_{15-2.5}$) and total suspended particles were not consistently associated with mortality. Of the gaseous pollutants, only sulfur dioxide was associated with elevated mortality risk. Interestingly, measures of $PM_{2.5}$ were associated with all-cause cardiopulmonary, and lung cancer mortality, but not with all other mortality. However, sulfur oxide pollution (as measured by sulfate particles and/or sulfur dioxide) was significantly associated with mortality from all other causes in addition to all-cause, cardiopulmonary, and lung cancer mortality.

## COMMENT

This study demonstrated associations between ambient fine particulate air pollution and elevated risks of both cardiopulmonary and lung cancer mortality. Each 10-$\mu g/m^3$ elevation in long-term average $PM_{2.5}$ ambient concentrations was associated with approximately a 4%, 6%, and 8% increased risk of all-cause, cardiopulmonary, and lung cancer mortality, respectively, although the magnitude of the effect somewhat depended on the time frame of pollution monitoring. In addition, this analysis addresses many of the important questions concerning the earlier, more limited analysis of the large CPS-II cohort, including the following issues.

First, does the apparent association between pollution and mortality persist with longer follow-up and as the cohort ages and dies? The present analysis more than doubled the follow-up time to more than 16 years, resulting in approximately triple the number of deaths, yet the associations between pollution and mortality persisted.

Second, can the association between fine particulate air pollution and increased cardiopulmonary and lung cancer mortality be due to inadequate control of important individual risk factors? After aggressively controlling for smoking, the estimated fine particulate pollution effect on mortality was remarkably robust. When the analysis was stratified by smoking status, the estimated pollution effect on both cardiopulmonary and lung cancer mortality was strongest for never smokers vs former or current smokers. This analysis also controlled for education, marital status, BMI, and alcohol consumption. This analysis used improved variables to control for occupational exposures and incorporated diet variables that accounted for total fat consumption, as well as for consumption of vegetables, citrus, and high-fiber grains. The mortality associations with fine particulate air pollution were largely unaffected by the inclusion of these individual risk factors in the models. The data on smoking and other individual risk factors, however, were obtained directly by questionnaire at time of enrollment and do not reflect changes that may have occurred following enrollment. The lack of risk factor follow-up data results in some misclassification of exposure, reduces the precision of control for risk factors, and constrains our ability to differentiate time dependency.

Third, are the associations between fine particulate air pollution and mortality due to regional or other spatial differences that are not adequately controlled for in the analysis? If there are unmeasured or inadequately modeled risk factors that are different across locations, then spatial clustering will occur. If this clustering is independent or random across metropolitan areas, then the spatial clustering can be modeled by adding a random-effects component to the Cox proportional hazards model as was done in our analysis. The clustering may not be independent or random across metropolitan areas due to inadequately measured or modeled

**Figure 2.** Nonparametric Smoothed Exposure Response Relationship

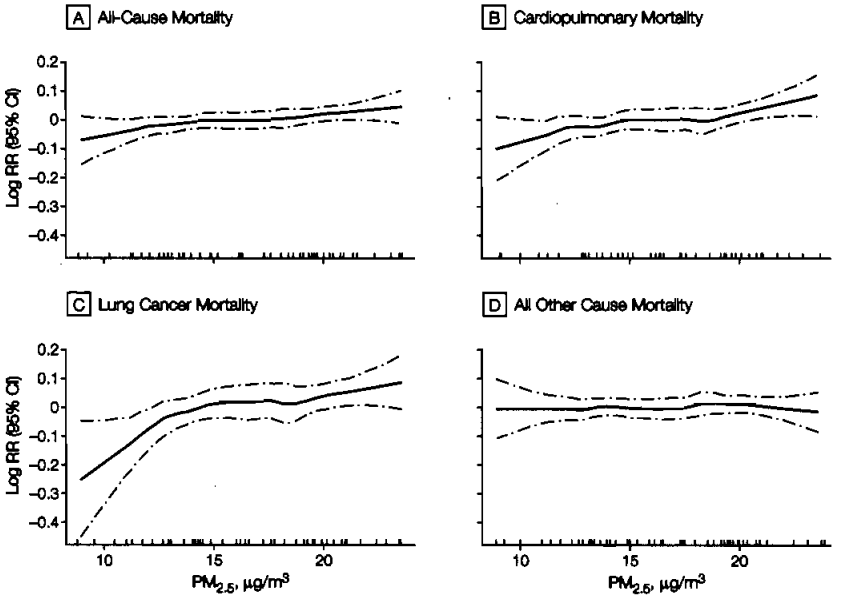


Vertical lines along x-axes indicate rug or frequency plot of mean fine particulate pollution; $PM_{2.5}$, mean fine particles measuring less than 2.5 µm in diameter; RR, relative risk; and CI, confidence interval.

**Figure 3.** Mortality Relative Risk (RR) Ratio Associated With 10-μg/m³ Differences of $PM_{2.5}$ Concentrations

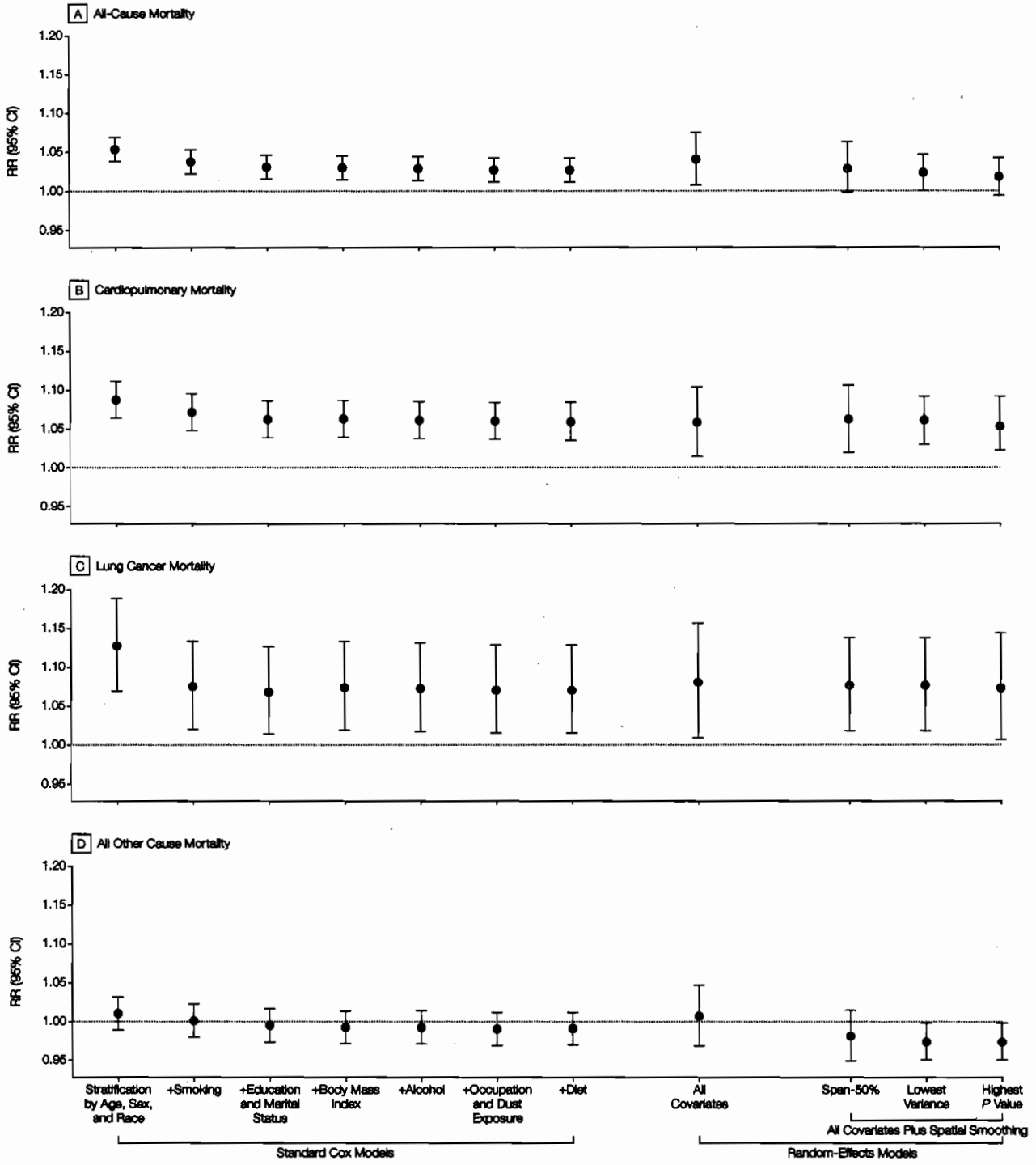


Data presented are for 1979-1983 for the different causes of death, with various levels of controlling for individual risk factors, and using alternative modeling approaches. The 3 models with spatial smoothing allow for increasingly aggressive fitting of the spatial structure. Plus sign indicates model included previous variables (ie, smoking included stratification by age, sex, and race); $PM_{2.5}$, mean fine particles measuring less than 2.5 μm in diameter; and CI, confidence interval.

risk factors (either individual or ecological). If these inadequately measured or modeled risk factors are also spatially correlated with air pollution, then biased pollution effects estimates may occur due to confounding. However, in this analysis, significant spatial autocorrelation was not observed after controlling for fine particulate air pollution and the various individual risk factors. Furthermore, to minimize any potential confounding bias, sensitivity analyses, which directly modeled spatial trends using nonparametric smoothing techniques, were conducted. A contribution of this analysis is that it included the incorporation of both random effects and nonparametric spatial smoothing components to the Cox proportional hazards model. Even after accounting for random effects across metropolitan areas and aggressively modeling a spatial structure that accounts for regional differences, the association between fine particulate air pollution and cardiopulmonary and lung cancer mortality persists.

Fourth, is mortality associated primarily with fine particulate air pollution or is mortality also associated with other measures of particulate air pollution, such as $PM_{10}$, total suspended particles, or with various gaseous pollutants? Elevated mortality risks were associated primarily with measures of fine particulate and sulfur oxide pollution. Coarse particles and gaseous pollutants, except for sulfur dioxide, were generally not significantly associated with elevated mortality risk.

Fifth, what is the shape of the concentration-response function? Within the range of pollution observed in this analysis, the concentration-response function appears to be monotonic and nearly linear. However, this does not preclude a leveling off (or even steepening) at much higher levels of air pollution.

Sixth, how large is the estimated mortality effect of exposure to fine particulate air pollution relative to other risk factors? A detailed description and interpretation of the many individual risk factors that are controlled for in the analysis goes well beyond the scope of

**Figure 4.** Adjusted Mortality Relative Risk (RR) Ratio Associated With 10-μg/m³ Differences of $PM_{2.5}$ Concentrations

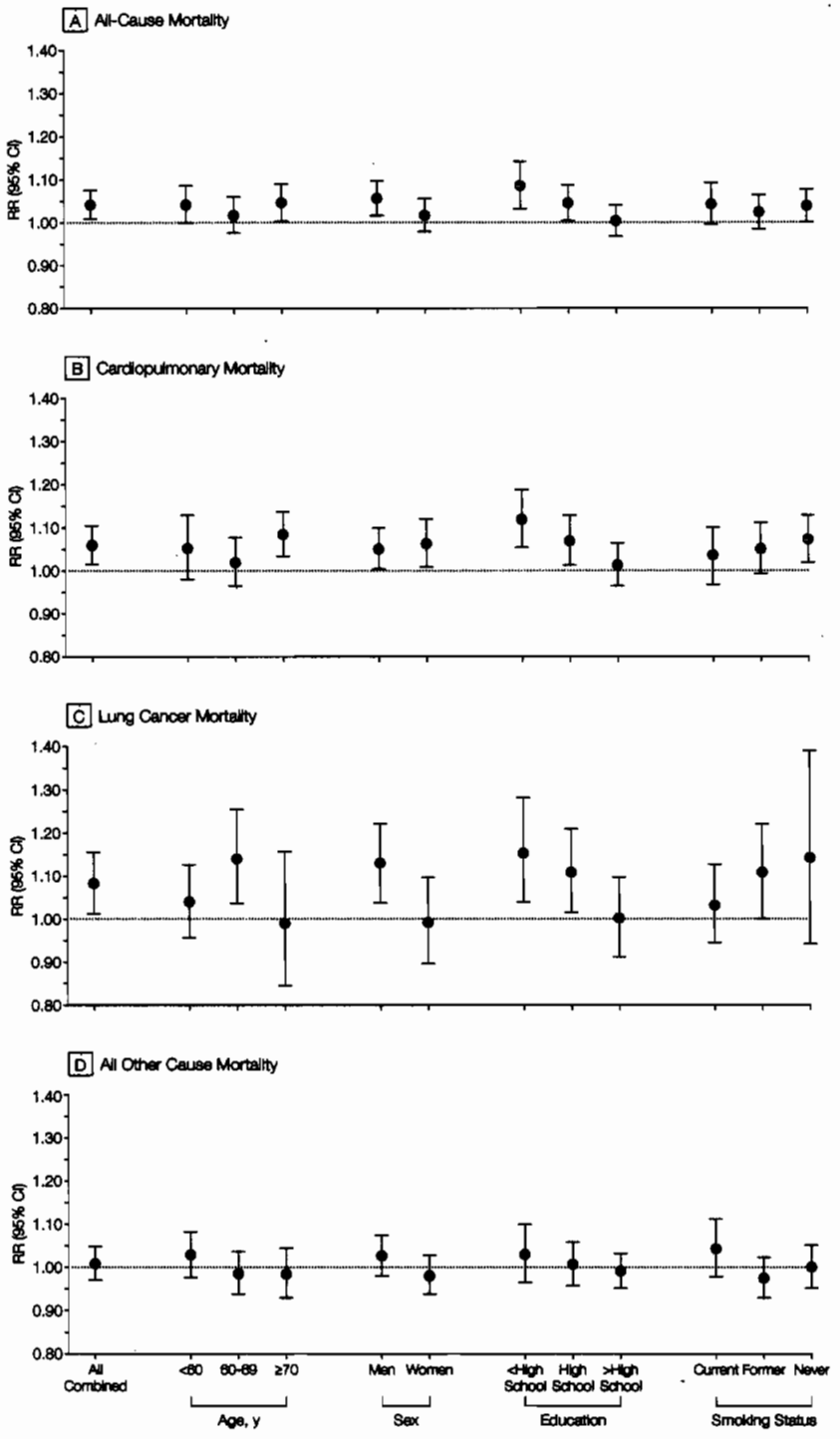


Data presented are for 1979-1983 for the different causes of death stratified by age, sex, education, and smoking status. $PM_{2.5}$ indicates mean fine particles measuring less than 2.5 μm in diameter; CI, confidence interval.

**Figure 5.** Adjusted Mortality Relative Risk (RR) Ratio Evaluated at Subject-Weighted Mean Concentrations

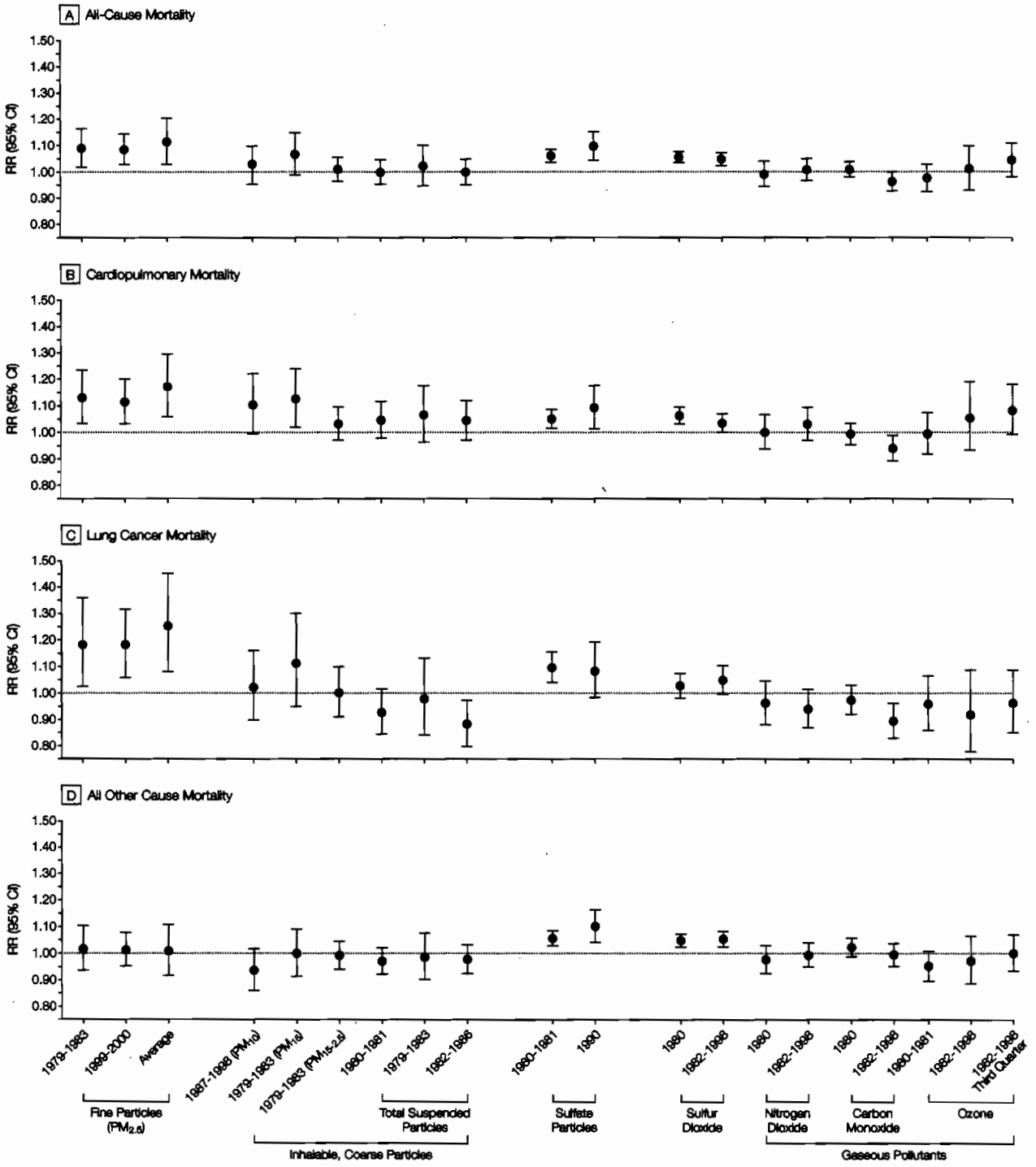


$PM_{2.5}$ indicates particles measuring less than 2.5 μm in diameter; $PM_{10}$, particles measuring less than 10 μm in diameter; $PM_{15}$, particles measuring less than 15 μm in diameter; $PM_{15-2.5}$, particles measuring between 2.5 and 15 μm in diameter; and CI, confidence interval.

this report. However, the mortality risk associated with cigarette smoking has been well documented using the CPS-II cohort.[16] The risk imposed by exposure to fine particulate air pollution is obviously much smaller than the risk of cigarette smoking. Another risk factor that has been well documented using the CPS-II cohort data is body mass as measured by BMI.[30] The Word Health Organization has categorized BMI values between 18.5-24.9 kg/m$^2$ as normal; 25-29.9 kg/m$^2$, grade 1 overweight; 30-39.9 kg/m$^2$, grade 2 overweight; and 40 kg/m$^2$ or higher, grade 3 overweight.[31] In the present analysis, BMI values and BMI values squared were included in the proportional hazards models. Consistent with previous ACS analysis,[30] BMI was significantly associated with mortality, optimal BMI was between approximately 23.5 and 24.9 kg/m$^2$, and the RR of mortality for different BMI values relative to the optimal were dependent on sex and smoking status. For example, the RRs associated with BMI values between 30.0 and 31.9 kg/m$^2$ (vs optimal) would be up to approximately 1.33 for never smokers. Based on these calculations, mortality risks associated with fine particulate air pollution at levels found in more polluted US metropolitan areas are less than those associated with substantial obesity (grade 3 overweight), but comparable with the estimated effect of being moderately overweight (grade 1 to 2).

In conclusion, the findings of this study provide the strongest evidence to date that long-term exposure to fine particulate air pollution common to many metropolitan areas is an important risk factor for cardiopulmonary mortality. In addition, the large cohort and extended follow-up have provided an unprecedented opportunity to evaluate associations between air pollution and lung cancer mortality. Elevated fine particulate air pollution exposures were associated with significant increases in lung cancer mortality. Although potential effects of other unaccounted for factors cannot be excluded with certainty, the associations between fine particulate air pollution and lung cancer mortality, as well as cardiopulmonary mortality, are observed even after controlling for cigarette smoking, BMI, diet, occupational exposure, other individual risk factors, and after controlling for regional and other spatial differences.

**Author Contributions:** *Study concept and design:* Pope, Burnett, Krewski, Thurston.
*Acquisition of data:* Thun, Calle, Krewski, Ito, Thurston.
*Analysis and interpretation of data:* Pope, Burnett, Krewski, Thurston.
*Drafting of the manuscript:* Pope, Burnett, Ito, Thurston.
*Critical revision of the manuscript for important intellectual content:* Pope, Thun, Calle, Krewski, Thurston.
*Statistical expertise:* Pope, Burnett, Krewski.
*Obtained funding:* Pope, Thun, Thurston.
*Administrative, technical, or material support:* Pope, Calle, Krewski, Ito, Thurston.
*Study supervision:* Pope, Krewski.
**Funding/Support:** The research for this article was supported largely by grant ES09560-01A1 from the National Institutes of Health/National Institute of Environmental Health Sciences (NIEHS). It was also supported in part by grant ES00260 from the New York University Center/NIEHS, grant R-827351 from the Environmental Protection Agency PM Health Effects Research Center, and funding from the R. Samuel McLaughlin Centre for Population Health Risk Assessment at the University of Ottawa.
**Acknowledgment:** We thank Morton Lippmann, PhD, for his help in developing the research grant application and various comments and suggestions and Yuanli Shi, MD, for computer programming and statistical analysis support.

**REFERENCES**

1. Firket J. The cause of the symptoms found in the Meuse Valley during the fog of December, 1930. *Bull Acad R Med Belgium.* 1931;11:683-741.
2. Ciocco A, Thompson DJ. A follow-up of Donora ten years after: methodology and findings. *Am J Public Health.* 1961;51:155-164.
3. Logan WPD, Glasg MD. Mortality in London fog incident, 1952. *Lancet.* 1953;1:336-338.
4. Pope CA III, Dockery DW. Epidemiology of particle effects. In: Holgate ST, Koren H, Maynard R, Samet J, eds. *Air Pollution and Health.* London, England: Academic Press; 1999:673-705.
5. Kaiser J. Showdown over clean air science. *Science.* 1997;277:466-469.
6. World Health Organization-European Region. *Update and Revision of the Air Quality Guidelines for Europe.* Copenhagen, Denmark: World Health Organization-European Region; 1995. Document EUR/ICP/EHAZ 9405/PB01.
7. CEPA/FPAC Working Group on Air Quality Objectives and Guidelines. *National Ambient Air Quality Objectives for Particulate Matter.* Ottawa, Ontario: Public Works and Government Services; 1998. Category No. H46-2/98-220.
8. Committee of the Environmental and Occupational Health Assembly of the American Thoracic Society. Health effects of outdoor air pollution. *Am J Respir Crit Care Med.* 1996;153:3-50.
9. Committee on the Medical Effects of Air Pollution. *Non-Biological Particles and Health.* London, England: United Kingdom Dept of Health; 1995.
10. Environmental Protection Agency. *Air Quality Criteria for Particulate Matter.* Washington, DC: Environmental Protection Agency; 1996. Document EPA/600/P-95/001cf.
11. Samet JM, Dominici F, Curriero FC, Coursac I, Zeger SL. Fine particulate air pollution and mortality in 20 US cities. *N Engl J Med.* 2000;343:1742-1749.
12. National Research Council. *Research Priorities for Airborne Particulate Matter, I: Immediate Priorities and a Long-Range Research Portfolio.* Washington, DC: National Academy Press; 1998.
13. National Research Council. *Research Priorities for Airborne Particulate Matter, III: Early Research Progress.* Washington, DC: National Academy Press; 2001.
14. *Whitman v American Trucking Associations Inc,* 532 US 457 (2001).
15. Dockery DW, Pope CA III, Xu X, et al. An association between air pollution and mortality in six US cities. *N Engl J Med.* 1993;329:1753-1759.
16. Pope CA III, Thun MJ, Namboodiri MM, et al. Particulate air pollution as a predictor of mortality in a prospective study of US adults. *Am J Respir Crit Care Med.* 1995;151:669-674.
17. Krewski D, Burnett RT, Goldberg MS, et al. *Reanalysis of the Harvard Six Cities Study and the American Cancer Society Study of Particulate Air Pollution and Mortality: Special Report.* Cambridge, Mass: Health Effects Institute; 2000.
18. Chao, A, Thun MJ, Jacobs E, Henley SJ, Rodriguez C, Calle EE. Cigarette smoking and colorectal cancer mortality in the Cancer Prevention Study II. *J Natl Cancer Inst.* 2000;92:1888-1896.
19. Calle EE, Terrell DD. Utility of the National Death Index for ascertainment of mortality among Cancer Prevention Study II participants. *Am J Epidemiol.* 1993; 137:235-241.
20. US Postal Service. *1989 National Five Digit Zip Code and Post Office Directory.* Washington, DC: National Information Data Center; 1989.
21. Fleming TR, Harrington DP. *Counting Processes and Survival Analysis.* New York, NY: John Wiley & Sons; 1991.
22. Burnett R, Ma R, Jerrett M, et al. The spatial association between community air pollution and mortality: a new method of analyzing correlated geographic cohort data. *Environ Health Perspect.* 2001; 109(suppl 3):375-380.
23. Easton DF, Peto J, Babiker GAG. Floating absolute risk: an alternative to relative risk in survival and case-control analysis avoiding an arbitrary reference group. *Stat Med.* 1991;10:1025-1035.
24. Burnett RT, Ross WH, Krewski D. Non-linear mixed regression models. *Environmetrics.* 1995;6:85-99.
25. Siemiatycki J, Nadon L, Lakhani R, Beegin D, Geerin M. Exposure assessment. In: Siemiatycki J, ed. *Risk Factors for Cancer in the Workplace.* Baton Rouge, La: CRC Press; 1991:45-114.
26. Cleveland WS, Devlin SJ. Robust locally weighted regression and smoothing scatterplots. *J Am Stat Assoc.* 1988;74:829-836.
27. Hastie T, Tibshirani R. *Generalized Additive Models.* London, England: Chapman & Hall; 1990.
28. *S-Plus 2000 Programmer's Guide.* Seattle, Wash: Math Soft; 2000.
29. Priestly MB. *Spectral Analysis and Time Series.* London, England: Academic Press; 1981.
30. Calle EE, Thun MJ, Petrelli JM, Rodriguez C, Heath CW Jr. Body-mass index and mortality in a prospective cohort of US adults. *N Engl J Med.* 1999;341:1097-1105.
31. Physical status: the use and interpretation of anthropometry: report of a WHO expert committee. *WHO Tech Rep Ser.* 1995;854:1-452.

# Reduction in Fine Particulate Air Pollution and Mortality

## Extended Follow-up of the Harvard Six Cities Study

Francine Laden, Joel Schwartz, Frank E. Speizer, and Douglas W. Dockery

Exposure, Epidemiology, and Risk Program, Department of Environmental Health, Harvard School of Public Health; and Channing Laboratory, Department of Medicine, Brigham and Women's Hospital and Harvard Medical School, Boston, Massachusetts

***Rationale:*** **A large body of epidemiologic literature has found an association of increased fine particulate air pollution ($PM_{2.5}$) with acute and chronic mortality. The effect of improvements in particle exposure is less clear.**

***Objectives:*** **Earlier analysis of the Harvard Six Cities adult cohort study showed an association between long-term ambient $PM_{2.5}$ and mortality between enrollment in the mid-1970s and follow-up until 1990. We extended mortality follow-up for 8 yr in a period of reduced air pollution concentrations.**

***Methods:*** **Annual city-specific $PM_{2.5}$ concentrations were measured between 1979 and 1988, and estimated for later years from publicly available data. Exposure was defined as (*1*) city-specific mean $PM_{2.5}$ during the two follow-up periods, (*2*) mean $PM_{2.5}$ in the first period and change between these periods, (*3*) overall mean $PM_{2.5}$ across the entire follow-up, and (*4*) year-specific mean $PM_{2.5}$. Mortality rate ratios were estimated with Cox proportional hazards regression controlling for individual risk factors.**

***Measurements and Main Results:*** **We found an increase in overall mortality associated with each 10 $\mu g/m^3$ increase in $PM_{2.5}$ modeled either as the overall mean (rate ratio [RR], 1.16; 95% confidence interval [CI], 1.07–1.26) or as exposure in the year of death (RR, 1.14; 95% CI, 1.06–1.22). $PM_{2.5}$ exposure was associated with lung cancer (RR, 1.27; 95% CI, 0.96–1.69) and cardiovascular deaths (RR, 1.28; 95% CI, 1.13–1.44). Improved overall mortality was associated with decreased mean $PM_{2.5}$ (10 $\mu g/m^3$) between periods (RR, 0.73; 95% CI, 0.57–0.95).**

***Conclusion:*** **Total, cardiovascular, and lung cancer mortality were each positively associated with ambient $PM_{2.5}$ concentrations. Reduced $PM_{2.5}$ concentrations were associated with reduced mortality risk.**

**Keywords:** air pollution; cohort studies; follow-up studies; mortality

An extensive epidemiologic literature has documented an association of fine particulate air pollution with mortality (1, 2). Most of this research consists of time-series studies of the effects of particle exposures experienced in the few days before death. The estimated effect of particulate air pollution has been shown to increase as longer exposure periods (up to 7 wk) are considered, indicating exposures in the month(s) before death may be important (3–6). Cohort studies have associated mortality with mean particulate air pollution concentrations over much longer periods. Three follow-up cohort studies in the United States (7–10) and a recent pilot study from Europe (11) evaluated the effects of long-term average ambient concentrations of fine particles and other air pollutants over many years. These cohort studies used annual or multiyear average pollution concentrations as the exposure index, but did not examine the time periods responsible for the observed association. Cohort studies with follow-up during periods of substantial change in air pollution can address this question. The linkage between improvements in air quality and improved health outcomes is of considerable public health interest.

A small number of studies have assessed the effect of reductions in air pollution on mortality. Mortality in Utah Valley decreased by 3% when average particulate air pollution ($PM_{10}$) concentrations decreased by 15 $\mu g/m^3$ as the result of a 13-mo strike at a local steel mill (12). Mortality in Dublin decreased by 8% after a 36-$\mu g/m^3$ decrease in average particulate air pollution (black smoke) due to a ban on coal sales (13). Restrictions on the sulfur content of fuel oil in Hong Kong resulted in a 45% average reduction in $SO_2$, and the average annual trend in deaths from all causes declined 2% and from respiratory causes declined 3.9% (14). In these studies, improvements in mortality were observed in the months after well-defined improvements in ambient air quality.

Dockery and colleagues (7) evaluated the effects of long-term pollution exposure on survival of adults participating in the Harvard Six Cities Study monitored for 14 to 16 yr during the 1970s and 1980s. Exposure to particulate matter smaller than 2.5 $\mu m$ in aerodynamic diameter ($PM_{2.5}$) was defined by the city-specific average during follow-up, ignoring the year-to-year fluctuations. The mortality rate ratio (RR) was 1.13 (95% confidence interval [CI], 1.04–1.73) for each 10-$\mu g/m^3$ increase in city-specific $PM_{2.5}$ concentrations. During follow-up, $PM_{2.5}$ concentrations dropped in all cities, although the rank ordering of cities was unchanged. Evaluation of time-varying $PM_{2.5}$ during this period showed slightly attenuated relative risk compared with estimates based on the average $PM_{2.5}$ over the entire period (15).

In this analysis, we extended the follow-up period through 1998. We evaluated the robustness of the previous findings with additional years of follow-up and examined the extent to which changes in $PM_{2.5}$ concentrations explain changes in mortality. Some of the results of this study have been previously reported in the form of an abstract (16, 17).

## METHODS

### Study Population and Follow-up

The study population consisted of 8,096 white participants residing in the following cities: Watertown, MA; Kingston and Harriman, TN; St. Louis, MO; Steubenville, OH; Portage, Wyocena, and Pardeeville, WI; and Topeka, KS. Participants were recruited between 1974 and 1977. The population and study design have been described previously (7),

*(Received in original form March 21, 2005; accepted in final form January 17, 2006)*

Supported by grants from the U.S. Environmental Protection Agency (EPA; R827353) and the National Institute of Environmental Health Sciences (ES00002).

This analysis has not been formally reviewed by EPA; the views expressed are solely those of the authors, and no official EPA endorsement should be inferred.

Correspondence and requests for reprints should be addressed to Francine Laden, Sc.D., Channing Laboratory, 181 Longwood Avenue, Boston MA 02115. E-mail: francine.laden@channing.harvard.edu

This article has an online supplement, which is accessible from this issue's table of contents at www.atsjournals.org

Am J Respir Crit Care Med Vol 173. pp 667–672, 2006
Originally Published in Press as DOI: 10.1164/rccm.200503-443OC on January 19, 2006
Internet address: www.atsjournals.org

and additional details are provided in the online supplement. Date and cause of death were determined by searching the National Death Index for calendar years 1979 to 1998. Deaths between 1974 and 1978 were identified from next-of-kin reports and Social Security records (7). Survival times were calculated as death date (or December 31, 1998, for surviving participants) minus enrollment date.

### Air Pollution Concentrations

Each participant's air pollution concentration was defined by city-specific mean concentrations of $PM_{2.5}$. During the original Six Cities follow-up (1979–1987), daily ambient $PM_{2.5}$ concentrations were measured at a centrally located air-monitoring station in each community (18). We estimated daily $PM_{2.5}$ concentrations after the shutdown of the Six Cities monitoring (1985–1998) using city-specific regression equations based on extinction coefficient (humidity-corrected visibility data from local airports) (19), routinely collected $PM_{10}$ concentrations (Environmental Protection Agency Aerometric Information Retrieval System [AIRS]) from representative monitors within 80 km, and indicators for season. (More details on the monitors selected and exposure metrics are provided in the online supplement) City-specific annual mean $PM_{2.5}$ was calculated as the average of the quarterly mean of the estimated seasonal values. The Pearson correlation ($r$) between the estimated and observed annual mean $PM_{2.5}$ from the Six Cities monitors during the years when both were available (1985–1987) was 0.93.

### Statistical Analysis

We estimated mortality rate ratios associated with $PM_{2.5}$ by Cox proportional hazards regression models (20), controlling for baseline individual risk factors and potential confounders. Time on study was measured by calendar date. Subjects were stratified by sex and 1-yr age groups, such that each sex/age group had its own baseline hazard. We controlled for current or former smoking, number of pack-years of smoking for former and current smokers separately, education, and body mass index (linear and squared terms). We first modeled exposure using period-specific (1974–1989 vs. 1990–1998) indicators for city. The end date of the original National Death Index search (1,989) was chosen as the cut-off. (Note that the Dockery and colleagues analysis [7] included several months of follow-up in 1990, which we have assigned to Period 2.) Portage, the city with the lowest $PM_{2.5}$ levels, was the reference. To adjust for temporal trends in mortality, we included an indicator for period. We then assessed the association of mortality with average city-specific $PM_{2.5}$ for the entire period of follow-up (pollution averaged from 1980–1998) and with the period-specific average $PM_{2.5}$. We tested for a difference in association between the two periods with an interaction term (period by $PM_{2.5}$) in the model. To evaluate the effect of change in mean $PM_{2.5}$ between the two periods, we estimated the associations of period-specific mortality by including both the mean $PM_{2.5}$ in Period 1 (1980–1985) and the change in mean $PM_{2.5}$ between Period 1 and Period 2 (Period 2 [1990–1998] minus Period 1) in the model simultaneously. Finally, we treated city-specific yearly mean $PM_{2.5}$ levels as a time-varying exposure variable to evaluate the effect of particle exposures in the year of death. All analyses were performed using SAS software (version 8; SAS Institute, Cary, NC).

## RESULTS

### Characteristics of the Dataset

The cohort has been described in detail elsewhere (7). In brief, the average age of participants at the beginning of the study was 50 yr (range, 25–74 yr) and 55% were female. Average body mass index was 25.8 kg/m$^2$ (standard deviation, 4.5). Current smoking on enrollment ranged from 33% in Topeka to 40% in Watertown, and former smoking ranged from 21% in Harriman to 25% in both Topeka and Watertown. Education varied between cities; 12% of participants in Topeka and 45% in St. Louis had less than a high school education.

There were 104,243 person-years of follow-up and 1,364 deaths between 1974 and 1989 (Period 1) and an additional 54,735 person-years of follow-up and 1,368 deaths between 1990 and 1998 (Period 2; Table 1). The overall death rate was 13.1 deaths per 1,000 person-years in Period 1 and 25.0 in Period 2, reflecting the aging of this cohort. As in previous analyses, crude mortality rates were highest in Steubenville and St. Louis (Table 1).

### Trends in $PM_{2.5}$ Concentrations

Annual mean $PM_{2.5}$ concentrations decreased during the study period in all cities (Figure 1) but most dramatically in the dirtiest cities. Fitting a straight line to the annual means, $PM_{2.5}$ declined on average 7 $\mu g/m^3$ per decade in Steubenville, 5 $\mu g/m^3$ in St. Louis, 3 $\mu g/m^3$ in Watertown, 2 $\mu g/m^3$ in Harriman, 1 $\mu g/m^3$ in Portage, and less than 1 $\mu g/m^3$ in Topeka.

### Association of $PM_{2.5}$ with Mortality

We calculated city-specific adjusted all-cause mortality rate ratios for Period 1, Period 2, and the complete period of follow-up compared with Portage (Table 2). City-specific rate ratios decreased with decreasing $PM_{2.5}$ (Figure 2). Similar results were found for cardiovascular mortality (*see* online supplement).

The effect of each 10-$\mu g/m^3$ increase in average annual $PM_{2.5}$ pollution was comparable in Period 1 (RR, 1.17; 95% CI, 1.08–1.26; p = 0.0001) and Period 2 (RR, 1.13; 95% CI, 1.01–1.27; p = 0.03, interaction p = 0.82). Controlling for exposure in Period 1, each 10-$\mu g/m^3$ reduction in Period 2 mean $PM_{2.5}$ was associated with a reduction in risk (RR, 0.73; 95% CI, 0.57–0.95; p = 0.019;

**TABLE 1. NUMBER OF PERSON-YEARS OF FOLLOW-UP AND TOTAL DEATHS IN SIX CITIES: PERIOD 1 (1974–1989 FOLLOW-UP) AND PERIOD 2 (1990–1998 FOLLOW-UP)**

| Characteristics | Portage | Topeka | Watertown | Harriman | St. Louis | Steubenville |
|---|---|---|---|---|---|---|
| No. participants | 1,630 | 1,238 | 1,332 | 1,258 | 1,292 | 1,346 |
| Period 1* (1,364 deaths; 104,243 person-yr) | | | | | | |
| Person-yr | 20,224 | 14,967 | 18,640 | 16,991 | 16,572 | 16,849 |
| No. deaths | 212 | 149 | 238 | 219 | 267 | 279 |
| Deaths/1,000 person-yr | 10.5 | 10.0 | 12.8 | 12.9 | 16.1 | 16.6 |
| Average $PM_{2.5}$ ($\mu g/m^3$) | 11.4 | 12.4 | 15.4 | 20.9 | 19.2 | 29.0 |
| Period 2 (1,368 deaths; 54,735 person-yr) | | | | | | |
| Person-yr | 11,658 | 9,062 | 8,979 | 8,363 | 8,172 | 8,501 |
| No. deaths | 264 | 184 | 194 | 229 | 251 | 246 |
| Deaths/1,000 person-yr | 22.6 | 20.3 | 21.6 | 27.4 | 30.7 | 28.9 |
| Average $PM_{2.5}$, $\mu g/m^3$ | 10.2 | 13.1 | 12.1 | 18.1 | 13.4 | 22.0 |

* Period 1 is restricted to 1,974 through 1989, whereas the original Dockery and colleagues (7) analysis included person-years of follow-up through June 1991 for a total of 111,076 person-years and 1,430 deaths. In Period 1, average $PM_{2.5}$ ($\mu g/m^3$) is the mean concentration in 1980–1985, the years when there are monitoring data for all cities (18). In Period 2, average $PM_{2.5}$ is the mean concentrations of the estimated $PM_{2.5}$ in 1990–1998.

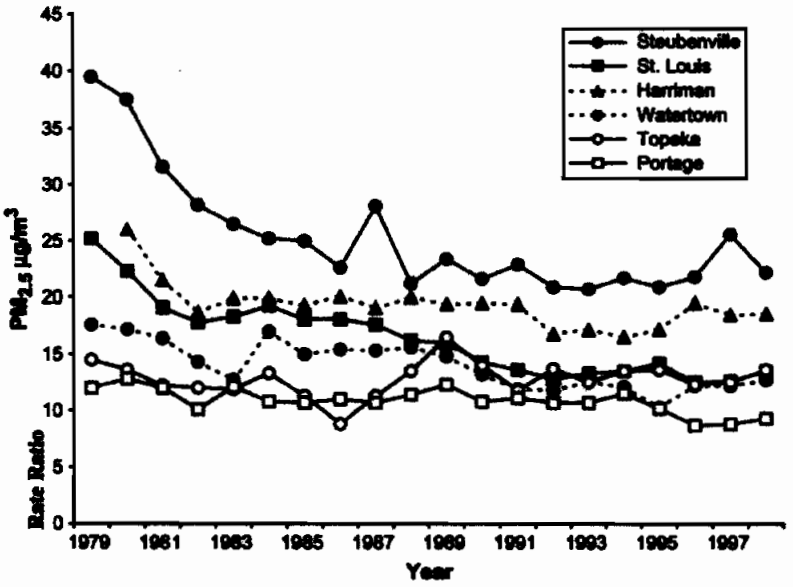


*Figure 1.* Annual average concentrations of $PM_{2.5}$ in the Harvard Six Cities Study. (Six Cities monitoring data for available years 1980–1988 and $PM_{2.5}$ estimated from Aerometric Information Retrieval System and extinction data for years where Six Cities data were not available.)

Table 3). We found an increased risk of total mortality associated with each 10-$\mu g/m^3$ increase in average $PM_{2.5}$ over the entire follow-up period (RR, 1.16; 95% CI, 1.07–1.26; p = 0.0004; Table 3). We found essentially the same association of total mortality with the annual mean $PM_{2.5}$ level in the year of death (RR, 1.14; 95% CI, 1.06–1.22; p = 0.0003). These results were not substantially changed in sensitivity analyses, removing one city at a time from the analysis (data not shown).

Cardiovascular mortality was positively associated with average $PM_{2.5}$ over the entire follow-up ($p < 0.0001$; Table 3). We found lung cancer mortality positively associated with average $PM_{2.5}$ (p = 0.10; Table 3). Respiratory mortality also was positively associated with average $PM_{2.5}$ (Table 3), but the association was not statistically significant (p = 0.63). There was no association (p = 0.71) with other causes of death (Table 3). There were stronger reductions in cardiovascular and respiratory mortality risk with each 10-$\mu g/m^3$ improvement in city-specific mean $PM_{2.5}$ in Period 2 compared with Period 1 (Table 3), but little evidence of reductions in lung cancer risk (Table 3).

## DISCUSSION

With approximately 50% more person-years of follow-up and twice the number of deaths compared with the original Six Cities chronic mortality air pollution analysis (7), we observed significant associations of fine particulate air pollution with mortality. More importantly, we were able to evaluate the effect of changing average ambient $PM_{2.5}$ concentrations since the original follow-up. Covariate adjusted mortality rates declined between 1974 and 1989 (Period 1) and 1990 and 1998 (Period 2), consistent with the general increase in adult life expectancy in the United States. However, the drop in the adjusted mortality rate was largest in the cities with the largest reductions in $PM_{2.5}$ after controlling for such a period effect. The proportional hazards rate ratio for a 10-$\mu g/m^3$ increase in $PM_{2.5}$ was comparable in both of these periods. However, we found a reduction in risk: 0.73 for each 10-$\mu g/m^3$ decrease in mean $PM_{2.5}$ between periods. This reduction was observed specifically for deaths due to cardiovascular and respiratory disease and not from lung cancer, a

**TABLE 2. ADJUSTED TOTAL MORTALITY RATE RATIOS AND 95% CONFIDENCE INTERVALS ESTIMATED FROM COX PROPORTIONAL HAZARDS MODEL FOR EACH FOLLOW-UP PERIOD (1974–1989 AND 1990–1998) AND THE COMPLETE FOLLOW-UP (1974–1998)**

| | Period 1 | Period 2 | Complete |
|---|---|---|---|
| Person-Yr of Follow-up | 104,243 | 54,735 | 158,978 |
| Deaths | 1,364 | 1,368 | 2,732 |
| | RR (95% CI) | RR (95% CI) | RR (95% CI) |
| City-specific model* | | | |
| Portage | 1.00 | | 1.00 |
| Topeka | 1.06 (0.86–1.31) | 1.01 (0.83–1.22) | 1.03 (0.89–1.19) |
| Watertown | 1.06 (0.87–1.28) | 0.82 (0.67–1.00) | 0.95 (0.83–1.08) |
| Harriman | 1.19 (0.98–1.44) | 1.10 (0.91–1.33) | 1.15 (1.01–1.32) |
| St. Louis | 1.15 (0.96–1.38) | 0.96 (0.80–1.15) | 1.05 (0.93–1.20) |
| Steubenville | 1.31 (1.10–1.57) | 1.06 (0.89–1.27) | 1.18 (1.04–1.34) |
| Period | 1.00 | 0.97 (0.70–1.35) | |

*Definition of abbreviations*: CI = confidence interval; RR = rate ratio.

Rate ratios have been adjusted for age in 1-yr categories, sex, current smoker, current pack-years of smoking, former smoker, former pack-years of smoking, less than high school education, and linear and quadratic terms for body mass index.

* City-specific rate ratios are all expressed in relation to Portage.

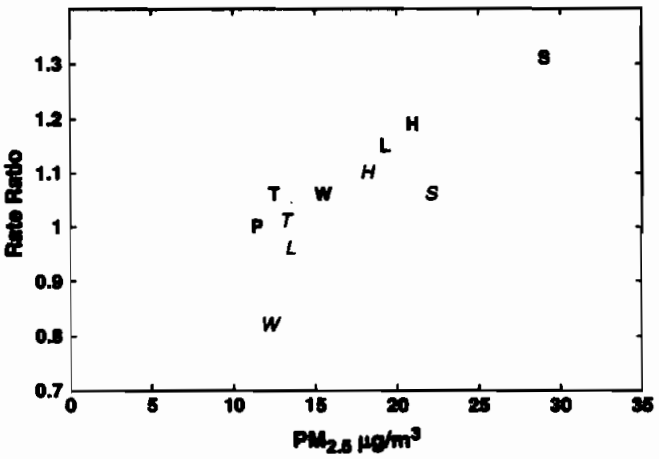


*Figure 2.* Estimated adjusted rate ratios for total mortality and $PM_{2.5}$ levels in the Six Cities Study by period. P denotes Portage, WI (reference for both periods); T = Topeka, KS; W = Watertown, MA; L = St. Louis, MO; H = Harriman, TN; S = Steubenville, OH. A term for Period 1 (1 if Period 2, 0 if Period 1) was included in the model. *Bold letters* represent Period 1 (1974–1989) and *italicized letters* represent Period 2 (1990–1998). In Period 1, $PM_{2.5}$ ($\mu g/m^3$) is defined as the mean concentration during 1980–1985, the years where there are monitoring data for all cities (18). In Period 2, $PM_{2.5}$ is defined as the mean concentrations of the estimated $PM_{2.5}$ in 1990–1998.

disease with a longer latency period and less reversibility. These findings suggest that the mortality effects of long-term air pollution may be at least partially reversible over periods of a decade.

We found equivalent, statistically significant increased risk in overall mortality associated with each 10-$\mu g/m^3$ increase in $PM_{2.5}$ modeled either as average over the entire follow-up (RR, 1.16; 95% CI, 1.07–1.26) or as average in the year of death (RR, 1.14; 95% CI, 1.06–1.22). These findings also suggest that mortality effects may be partially reversible, but over time periods possibly as short as a year.

Exposure to $PM_{2.5}$ was statistically significantly associated with deaths due to cardiovascular disease, and the association with lung cancer mortality was of borderline significance. The number of nonmalignant respiratory deaths was small (although comparable to numbers for lung cancer), but the $PM_{2.5}$-associated risk was positive, although weak.

Chronic exposure studies have observed increased mortality rates associated with PM. However, the evidence is limited mainly to the Harvard Six Cities Study and three other studies. The American Cancer Society Study, a cohort of 552,138 adults with 7 yr of follow-up, assessed risk for 151 U.S. metropolitan statistical areas (8). With an additional 9 yr of follow-up, statistically significant elevations in risk associated with $PM_{2.5}$ were observed for all-cause, lung cancer, and cardiopulmonary mortality (10). In analyses of cause-specific mortality, each 10-$\mu g/m^3$ increase in $PM_{2.5}$ was associated with 8 to 18% increases in cardiovascular mortality, but only weak associations were found with nonmalignant respiratory deaths (21). In the Adventist Health Study of Smog, a 15-yr follow-up of 6,338 nonsmoking Californians, Abbey and coworkers found mean $PM_{10}$ associated with increased lung cancer mortality in men and women, and nonsignificantly increased all-cause and cardiopulmonary mortality in men (9). A pilot prospective study of 4,466 participants monitored for 8 yr in the Netherlands concluded that long-term exposure to traffic-related particulate air pollution measured by black smoke was associated with increased all-cause mortality (11).

Although a large body of literature has shown associations between particulate air pollution and mortality, the relative contributions of acute and chronic exposures are not known. Effect estimates from prospective studies are substantially greater than those indicated by daily time-series studies (22). The majority of this difference may be explained by expanding the exposure period from days to months. Two independent studies have assessed the mortality effects over 40 d rather than 1 or 2 d after particle exposure. In both studies, the extended PM effects for periods of up to 6 wk were at least twice the short-term effects (3, 5). Schwartz showed in a time-series study in Boston that moving the time scale from days to months (i.e., 60 d) increased the estimated PM effect and captured approximately half the difference between the time-series and long-term cohort studies (4). He concluded that decades of exposure are not required to develop most of the risk increase seen in cohort studies. Our

**TABLE 3. ADJUSTED PROPORTIONAL HAZARD MORTALITY RATE RATIOS AND 95% CONFIDENCE INTERVALS FOR A 10-$\mu g/m^3$ INCREASE IN AVERAGE AMBIENT $PM_{2.5}$ OVER THE ENTIRE FOLLOW-UP (1974–1998) AND THE RATE RATIOS FOR AVERAGE $PM_{2.5}$ IN PERIOD 1 AND THE DECREASE IN LEVELS BETWEEN THE TWO PERIODS**

| | | RR (95% CI) | | |
|---|---|---|---|---|
| | | Model 1 | Model 2 | |
| | Cases | Entire Follow-Up Average $PM_{2.5}$† | Period 1 Average $PM_{2.5}$‡ | Decrease in Average $PM_{2.5}$‡ |
| Total mortality | 2,732 | 1.16 (1.07–1.26) | 1.18 (1.09–1.27) | 0.73 (0.57–0.95) |
| Cardiovascular* | 1,196 | 1.28 (1.13–1.44) | 1.28 (1.14–1.43) | 0.69 (0.46–1.01) |
| Respiratory* | 195 | 1.08 (0.79–1.49) | 1.21 (0.89–1.66) | 0.43 (0.16–1.13) |
| Lung cancer* | 226 | 1.27 (0.96–1.69) | 1.20 (0.91–1.58) | 1.06 (0.43–2.62) |
| Other | 1,115 | 1.02 (0.90–1.17) | 1.05 (0.93–1.19) | 0.85 (0.56–1.27) |

For definition of abbreviations, *see* Table 2.

Rate ratios have been adjusted for age in 1-yr categories, sex, current smoker, current pack-years of smoking, former smoker, former pack-years of smoking, less than high school education, and linear and quadratic terms for body mass index.

* Cardiovascular disease (International Classification of Disease, 9th edition [ICD-9] codes 400–440); nonmalignant respiratory disease (ICD-9 codes 485–496); lung cancer (ICD-9 code 162).

† Average $PM_{2.5}$ calculated as the average of Six Cities monitoring data for available years 1980–1988 and $PM_{2.5}$ estimated from Aerometric Information Retrieval System and extinction data for years where Six Cities data were not available.

‡ Average $PM_{2.5}$ in Period 1 calculated as the average from 1980–1985, the years where there are monitoring data for all cities, decrease in average $PM_{2.5}$ (average Period 2 (1990–1998) − average Period 1).

results show that PM-associated mortality decreased in the decade of the 1990s compared with the mid-1970s and 1980s, consistent with the decrease in ambient $PM_{2.5}$ concentrations. Furthermore, the similarity of effect for the annual air pollution metric compared with the mean over the study period (1980–1998) suggests that air pollution during the last year may be important. At least part of the $PM_{2.5}$-associated mortality may be reversible, suggesting ambient $PM_{2.5}$ is likely associated with exacerbation of existing disease. However, there also appears to be a second independent effect that could be described as development of chronic disease.

Our ability to assess the appropriate time scale is limited because, although $PM_{2.5}$ levels declined, the ranking of cities did not change substantially over most of the study period. However, the largest improvements in $PM_{2.5}$ concentrations were in cities with the highest initial concentrations. There was also some variation in city-specific annual mean $PM_{2.5}$ concentrations. We did not examine time periods shorter than 1 yr in this analysis.

The original Six Cities Study mortality analysis has undergone an extensive reanalysis performed by an independent group of researchers (23). The original data were validated, the original findings reproduced, and these estimates were found to be robust to alternative models and to inclusion of other posited city-specific confounders. Alternative metrics of $PM_{2.5}$ were not found to alter risk of all-cause mortality during the original period of follow-up (15).

Cardiovascular mortality rates have decreased in the United States over the course of this study (24). However, this improvement in cardiovascular mortality should affect all cities, and should not be larger in cities with the greatest improvement in $PM_{2.5}$ concentrations. Moreover, $PM_{2.5}$ concentrations fluctuated year to year, including increases as well as decreases from the preceding year. Yet, using $PM_{2.5}$ as a time-varying covariate did not noticeably change the association. Thus, long-term secular trends are unlikely to explain our results.

This analysis lacked continuous monitoring of $PM_{2.5}$ levels during the extended follow-up period. Six Cities monitoring of air pollutants ended in 1987 in most cities. The AIRS monitoring network began collecting $PM_{10}$ data in 1985. $PM_{2.5}$ measurements did not start until 1999, and even then did not include monitoring in all of the Six Cities or in the original monitoring sites. Therefore, Period 2 is completely dependent on estimated $PM_{2.5}$ levels. We estimated the levels and patterns of $PM_{2.5}$ during the missing years using city-specific regression of the original Six Cities $PM_{2.5}$ measurements against the relative humidity–adjusted extinction coefficients from nearby airports and routine $PM_{10}$ measurements from multiple nearby monitors. We assumed that the local change in $PM_{2.5}$ would follow the local $PM_{10}$ and extinction coefficient measurements, and that differences due to siting of the monitors and methodologies would have remained constant. Differences in measurement techniques and measurement locations preclude comparisons with current observations. Estimating the pattern of $PM_{2.5}$ over time using the actual measured $PM_{10}$ and extinction data has its limitations, but it is likely to be closer to reality than extrapolating levels beyond the available sampling data, as has been done previously (15).

Follow-up information on individual risk factors was available during the course of the first 12 yr of follow-up. Three follow-up questionnaires were administered to the participants. There was no updated information available on individual risk factors or residence during the extended period of follow-up. In the original study, baseline characteristics were used to control for confounding factors (7). Although these factors were significantly associated with mortality, they did not substantially confound the relationship with air pollution. In the reanalysis, Krewski and colleagues (23) evaluated the effect of updating smoking status and body mass index during the course of the original study. They restricted the study population to the 81.5% of the people who did not move from their original cities at any time during the study period. These alternative analyses did not change the conclusions about the association of air pollution and mortality. Therefore, we elected to use baseline characteristics in this analysis. We acknowledge that this modeling choice may lead to misclassification of confounders such as smoking status and body mass index, and that the associations of these factors and air pollution may have changed. For example, trends in smoking cessation are different in different parts of the country (25). Although these factors were significantly associated with mortality, they did not substantially confound the relationship with air pollution. In addition, censoring movers as defined in Krewski and colleagues' analysis (23) at the start of the continued follow-up or excluding all movers from the analysis did not change our results (data not presented). A limitation of this analysis is that individual level covariates were not available for this population in the second period of follow-up.

In this extended follow-up during a time of air pollution reductions, we had a unique opportunity to assess the effect of recent versus past exposures. City-specific average $PM_{2.5}$ levels were lower in the extended follow-up during the 1990s than in the first follow-up (1974–1989) and mortality risk ratios in this period also were lower. This suggests that the $PM_{2.5}$-associated mortality in this 25-yr follow-up was at least in part reversible.

***Conflict of Interest Statement***: None of the authors have a financial relationship with a commercial entity that has an interest in the subject of this manuscript.

***Acknowledgment***: The authors thank William Cormack Ramsey, Elizabeth Solomon, and Martha Fay for their work in tracking participants and Jaime Hart and Allan Heff for their help with manuscript preparation.

## References

1. Pope CA III, Dockery DW. Epidemiology of particle effects. In: Holgate ST, Samet JM, Koren HS, Maynard RL, editors. Air pollution and health. San Diego, CA: Academic Press; 1999. pp. 673–706.
2. U.S. Environmental Protection Agency. Air quality criteria for particulate matter. Washington, DC: U.S. Environmental Protection Agency, Office of Research and Development; 1996. Publication No. EPA/600/P-95/001cF.
3. Goodman PG, Dockery DW, Clancy L. Cause-specific mortality and the extended effects of particulate pollution and temperature exposure. *Environ Health Perspect* 2004;112:179–185.
4. Schwartz J. Harvesting and long term exposure effects in the relation between air pollution and mortality. *Am J Epidemiol* 2000;151:440–448.
5. Zanobetti A, Schwartz J, Samoli E, Gryparis A, Touloumi G, Atkinson R, Le Tertre A, Bobros J, Celko M, Goren A, *et al.* The temporal pattern of mortality responses to air pollution: a multicity assessment of mortality displacement. *Epidemiology* 2002;13:87–93.
6. Zeger SL, Dominici F, Samet J. Harvesting-resistant estimates of air pollution effects on mortality. *Epidemiology* 1999;10:171–175.
7. Dockery DW, Pope CA III, Xu X, Spengler JD, Ware JH, Fay ME, Ferris BG Jr, Speizer FE. An association between air pollution and mortality in six US cities. *N Engl J Med* 1993;329:1753–1759.
8. Pope CA III, Thun MJ, Namboodiri MM, Dockery DW, Evans JS, Speizer FE, Heath CW Jr. Particulate air pollution as a predictor of mortality in a prospective study of U.S. adults. *Am J Respir Crit Care Med* 1995;151:669–674.
9. Abbey DE, Nishino N, McDonnell WF, Burchette RJ, Knutsen SF, Lawrence Beeson W, Yang JX. Long-term inhalable particles and other air pollutants related to mortality in nonsmokers. *Am J Respir Crit Care Med* 1999;159:373–382.
10. Pope CA III, Burnett RT, Thun MJ, Calle EE, Krewski D, Ito K, Thurston GD. Lung cancer, cardiopulmonary mortality, and long-term exposure to fine particulate air pollution. *JAMA* 2002;287:1132–1141.
11. Hoek G, Brunekreef B, Goldbohm S, Fischer P, van den Brandt PA. Association between mortality and indicators of traffic-related air pollution in the Netherlands: a cohort study. *Lancet* 2002;360:1203–1209.

12. Pope CA III, Schwartz J, Ransom M. Daily mortality and $PM_{10}$ pollution in Utah Valley. *Arch Environ Health* 1992;42:211–217.
13. Clancy L, Goodman P, Sinclair H, Dockery DW. Effect of air-pollution control on death rates in Dublin, Ireland: an intervention study. *Lancet* 2002;360:1210–1214.
14. Hedley AJ, Wong CM, Thach TQ, Ma S, Lam TH, Anderson HR. Cardiorespiratory and all-cause mortality after restrictions on sulphur content of fuel in Hong Kong: an intervention study. *Lancet* 2002; 360:1646–1652.
15. Villeneuve PJ, Goldberg MS, Krewski D, Burnett RT, Chen Y. Fine particulate air pollution and all-cause mortality within the Harvard Six-Cities Study: variations in risk by period of exposure. *Ann Epidemiol* 2002;12:568–576.
16. Laden F, Schwartz J, Speizer FE, Dockery DW. Air pollution and mortality: a continued follow-up in the Harvard Six Cities Study. *Epidemiology* 2001;12:S81.
17. Laden F, Schwartz J, Speizer FE, Dockery DW. Continued follow-up of air pollution and mortality in the Harvard Six Cities Study. Health Effects Institute Annual Conference, Health Effects Institute, Washington, DC, 2001.
18. Schwartz J, Dockery DW, Neas LM. Is daily mortality associated specifically with fine particles? *J Air Waste Manage Assoc* 1996;46:927–939.
19. Abbey DE, Ostro BE, Fraser G, Vancuren T, Burchette RJ. Estimating fine particulates less than 2.5 microns in aerodynamic diameter (PM2.5) from airport visibility data in California. *J Expo Anal Environ Epidemiol* 1995;5:161–180.
20. Cox DR. Regression models and life-tables. *J Roy Stat Soc (B)* 1972; 34:187–220.
21. Pope CA III, Burnett RT, Thurston GD, Thun MJ, Calle EE, Krewski D, Godleski JJ. Cardiovascular mortality and long-term exposure to particulate air pollution: epidemiological evidence of general pathophysiological pathways of disease. *Circulation* 2004;109:71–77.
22. Kunzli N, Medina S, Kaiser R, Quenel P, Horak F Jr, Studnicka M. Assessment of deaths attributable to air pollution: should we use risk estimates based on time series or on cohort studies? *Am J Epidemiol* 2001;153:1050–1055.
23. Krewski D, Burnett RT, Goldberg MS, Hoover K, Siemiatycki J, Jerrett M, Abrahamowicz M, White WH. Reanalysis of the Harvard Six Cities Study and the American Cancer Society Study of particulate air pollution and mortality: a special report of the institute's Particle Epidemiology Reanalysis Project. Cambridge, MA: Health Effects Institute; 2000.
24. Davis DL, Dinse GE, Hoel DG. Decreasing cardiovascular disease and increasing cancer among whites in the United States from 1973 through 1987: good news and bad news. *JAMA* 1994;271:431–437.
25. National Center for Chronic Disease Prevention and Health Promotion [Internet]. STATE system http://apps.nccd.cdc.gov/statesystem/ [accessed March 1, 2005]. Centers for Disease Control and Prevention; 2004.

# IN-SITU ENGINE EMISSIONS TESTING AND COMPARISON FOR A HIGH SPEED FERRY AND COMPETING LAND TRANSIT VEHICLE, PHASE I: TASK 7.0: Final Report

**FY 2001, PROGRAM ELEMENT 1.16**
**SUBCONTRACT NO. DTMA91-97-H00007**


**Prepared For:** Center for Commercial Deployment
of Transportation Technologies (CCDoTT)
California State University, Long Beach
6300 State University Drive
Long Beach, CA 90815

**Prepared By:** Seaworthy Systems, Inc.
P.O. Box 965
Essex, CT 06426



This program has been funded by Center for Commercial Deployment of Transportation Technologies (CCDoTT) at California State University, Long Beach.

**JUNE, 2002**

## TABLE OF CONTENTS

## TABLE OF CONTENTS continued

## TABLE OF CONTENTS continued



## LIST OF ILLUSTRATIONS

## TABLE OF CONTENTS continued

## LIST OF TABLES

## EXECUTIVE SUMMARY

Phase I of the project for the In-Situ Engine Emissions Testing and Comparison for a High Speed Ferry and Competing Land Transit Vehicles comprises two aspects, divided into six tasks. The first aspect addresses the research and development of test methods and protocols for the comparison of emissions between the high-speed ferry and its competing land transit system, the diesel bus. The second aspect of Phase I is the review of current emissions reduction technologies that are applicable to the ferry.

The objective of the test program is to develop emissions rate factors for the same passenger-commute for the marine and land based vehicles of a pollutant expressed in grams/BHP-Hr and normalized for vehicle rider-ship (i.e. grams/passenger/day). The best available, laboratory-quality analyzers and test methods will be utilized in Phase II to measure emissions from the two sources to be tested. The same test methods, equipment and personnel will be used in both tests.

An extensive literature search was conducted that identified numerous protocols and standards for the measurement of emissions. Several references described emissions reduction technology and contained descriptions of testing methods either under consideration for use, or currently in use to demonstrate the effectiveness of a particular product. Industry experience and technical literature suggested that actual in-situ testing of an automobile will not be required for this study. A vast database of automobile emissions data is already available from the EPA. Therefore, the research focus is on the identification of test methods for the ferry and the diesel-powered bus.

There are two distinct issues relative to the development of test protocols for marine engines. The first is the need for a relatively simple and cost-effective test that can emerge as a standard for periodic emissions source testing. This low cost and easily implemented method would also serve the testing of various emissions reduction devices and alternative fuels. The second issue is the need for a detailed, laboratory-quality, field-adaptable protocol for the one-time testing of a diesel ferry in a particular service and a diesel bus in the same commuter service to create an absolute, scientifically defensible comparison. The technical literature offered ample information regarding cost-effective source test protocol. The literature also revealed a gap in the methods for conducting laboratory-quality field tests of passenger ferry engines and diesel passenger buses. Neither protocol exists for a satisfactory comparison.

This report concludes that well-established large-bore stationary diesel engine test methods are best suited for this analysis. This will be accomplished using extractive Fourier Transform Infrared Spectroscopy (FTIR) for testing of all targeted pollutants. The following pollutant species will be measured: acetaldehyde, acrolein, carbon 4+ straight-chain hydrocarbons, carbon dioxide, carbon monoxide, ethane, ethylene, formaldehyde and adelhyde compounds, methane, oxides of nitrogen (NOx), oxygen, particulate matter, sulfur dioxide, water vapor and any other FTIR-detected species. With FTIR, a single instrument will directly measure all targeted compounds and yield the highest quality data achievable utilizing any known test method. The FTIR analyzer will measure all targeted emissions simultaneously, in real-time, also enabling excellent measurement of engine transients.

The primary objective of obtaining precise real time in-situ data, comparing the exhaust emissions of competing auto, transit bus, and passenger ferry, remains unfinished. Until Phase II of the program element is completed, the actual emissions produced by competing transit modes, in particular buses and ferries, will remain undefined. The estimated time required for the in-situ testing portion of the Phase II effort is approximately 60 days. It is anticipated that another 60 days will be required for the proposed transit bus and ferry engine emissions test period to address all other administrative and contractual program requirements. This will permit some margin in the schedule in case of delays in obtaining test equipment or consumables, or to address any slippage due to the availability of the transit bus or ferry for testing. The total estimated cost for Phase II is $204, 680.

Passenger ferries for harbor service employ high-speed marine diesel engines in the range of 150 to 3000 brake horsepower (BHP). Regarding emissions reduction technologies for ferries, it appears that the most effective approach for sulfur oxide (SOx) reductions is the use of high quality low sulfur (100 ppm) distillate fuel. Further sulfur reductions (to 15 ppm) are anticipated to occur in 2006. Public health initiatives today in some cases assign greater harm to NOx and particulate matter (PM) than to other exhaust gases, such as CO, $CO_2$ and unburned hydrocarbons (HC). For commuter-type passenger ferry application, using high-speed marine diesel engines, it currently appears that the most cost-effective method of partial NOx reduction is the use water-fuel emulsions. Additionally for NOx and PM control, exhaust gas recirculation (EGR) is often effective and minimally intrusive for an engine retrofit. Some new engines can be purchased with EGR built into the design, and some older engine designs can be modified to employ this technique. Used independently, or together with water-fuel emulsions, NOx emissions can be expected to drop dramatically, though not as significantly as the 90 percent reduction demonstrated by the technology of selective catalytic reduction (SCR). Although SCR is the single most effective NOx eliminator, the drawbacks include its volume in the exhaust system, and significant capital and life cycle costs.

Particulate filters, although effective at reducing PM, can raise the exhaust gas backpressure, in some cases enough to compromise engine efficiency and fuel economy. An oxidizing catalyst that fits into the exhaust system as a relatively inexpensive muffler replacement effectively reduces CO, HC and PM emissions, which can increase when NOx-control equipment is installed.

# 1.0 INTRODUCTION

United States ports are faced with severe air quality problems that threaten to prevent future growth. Major California ports are already operating at or above the limits of acceptable air quality, so that planned projects, such as harbor dredging for the Port of Oakland, new ferry transit operations, floating and shore-based power-generating stations, and the planned San Francisco Airport runway extension are all being held in abeyance pending solutions to mitigate the harmful emissions that these proposals, if approved, are projected to generate. A definite and growing need therefore exists to better assess the sources of air pollution and provide innovative, pragmatic solutions to reduce or eliminate harmful emissions from those sources, in particular from mobile sources, such as vehicles and vessels.

This project, conducted by Seaworthy Systems, Inc., will directly support CCDoTT goals by helping to obtain the facts about emissions -- where virtually no reliable, published data on modern marine diesel-powered ferry systems exist. The completed analysis could likely show that fast ferries either already are or can readily be made to be less polluting than automobiles and public buses in congested urban/suburban areas and thus support the establishment of a U.S. fast ferry industry. This project will present the required data to enable viable comparisons of land versus marine transit emissions and their relative contributions to regional air quality. Whatever the findings, the information obtained will permit planners and managers of both civilian and military operations to focus on meaningful solutions to the problem of total air quality. Phase I of this effort comprises a complete literature review, a definition of scope, approach and methodology for in-situ (field) vehicle emissions testing. Phase I also includes development of specific pollutant test protocols and specification of required test equipment, facilities and support systems.

Seaworthy Systems, Inc., with the assistance of its subcontractor, Advanced Engine Technologies Corporation (AETC), continues with the preparatory work for the performance of in-situ testing to compare the emissions from high-speed passenger ferries to competing land-based vehicles. This unique analysis will develop emissions rate factors a passenger-commute aboard marine and land-based vehicles for various pollutants, expressed in grams/BHP-Hr and normalized for vehicle ridership (i.e. grams/passenger/day).

The Phase I portion of this program has been segmented into the following discrete tasks.

| | |
|---|---|
| Task 1.0 | Literature Search |
| Task 2.0 | Test Scope and Methodology Definition |
| Task 3.0 | Test Protocol Development |
| Task 4.0 | Test Equipment Specifications |
| Task 5.0 | Phase II Schedule and Cost Estimate |
| Task 6.0 | Emission Reduction Technology Evaluation |
| Task 7.0 | Final Report |

## 1.1 Objective

The objective of this project is to review and analyze exhaust emissions from parallel passenger commuter vehicles — the urban bus and the passenger ferry. The project further includes research and recommendations for the engine emission-reduction technologies that are best suited for incorporation in diesel engines and propulsion systems in passenger ferry applications.

## 1.2 Program Background

This program element comprises the definition, evaluation, and methods for the reduction of harmful emissions generated by three competing segments of the transportation sector — the largest single source of air pollution. Immediate and long-term program strategic objectives are to demonstrate how to optimize the air quality in ports by minimizing the regional sum of emissions generated by automobiles, transit buses, and passenger ferries. This optimization will foster progress for the agile port concept and in vessel and terminal design, improved public transit, increased port operational efficiency, and expanded cargo and passenger handling capabilities. Yet a lack of accurate data from mobile sources of emissions in ports damages programs that promise such benefits because of the public misperception that new development must always bring unacceptable hazards to health and the environment.

This report is part of the first portion of work (Phase I) to evaluate sources of the major mobile engine emissions in ports and to provide practical solutions to reduce exhaust emissions by diesel-powered ferry vessels. Phase I efforts an extensive technical literature search, a rational methodology for in-situ emissions testing, a list of required test instrumentation, test protocols, and estimates of cost and time to complete a projected Phase II program.

The Phase I research establishes that no credible emissions test results are available to conduct a fair comparison of diesel-powered transit buses and passenger ferry vessels. For various reasons, previous assessments of marine-propulsion emissions, in the absence of in-situ measurements, were consistently unreliable. Attempts to resolve emissions by source and quantity by a review of general literature or of vessel engine specifics (as published in Lloyd's Register) in combination with observed vessel traffic patterns have yielded inaccurate estimates. Consistently, such estimates are artificially high when compared to subsequent field tests. This overestimation has been noted in work by the southern California Port of Houston, and supported by tests conducted by the San Francisco Bay Area Water Transit Authority.

Phase I research also reveals deficiencies in the most recent efforts to gather emissions data from passenger ferries, by conducting field tests in Norfolk, Virginia and San Francisco, California in 2001 and 2002, respectively. These tests employed relatively inexpensive portable automotive test instrumentation. This equipment relied on bagging exhaust samples and transporting them to remote laboratories for analysis. Portable automotive test instrumentation and protocols are useful for comparing vector changes in quantities of emissions generated from a single engine type that undergoes various experimental modification, e.g. use of alternative fuels. However, such equipment is insufficient in both scope and accuracy for the comparison of one engine (as aboard a ferry) to another engine (as from a bus or auto). Tests designed to compare different transportation modes, with discrete operational profiles, atmospheric surroundings, and propulsion systems, require more sophisticated test instrumentation and more carefully planned test protocols. The utility-industry grade, state of the art, test instrumentation defined under Phase I for use in Phase II of this program element is of the highest scientific accuracy. When

combined with the engineering test protocols prepared under Phase I of this project, the final Phase II test results will be definitive, conclusive, and suitable for universal application.

# 2.0 LITERATURE SEARCH

## 2.1 Objective

The objective of this section is to review the available technical literature and identify laboratory-quality emission measurement methods and test protocols applicable for in-situ testing of exhaust emissions from marine diesel-cycle engines and diesel powered passenger buses. In addition, the goal is to identify methods for determination of emissions rate factors for automobiles serving the same commute. The results of the literature search will inform a test protocol for Phase II of this study.

## 2.2 Procedure

The technical literature search utilized the following methods:

1. Review of in-house test reports and technical papers from AETC.

2. Search of the worldwide web via the Internet.

3. Discussions with regulatory agencies including the California Air Resources Board (CARB), the Environmental Protection Agency (EPA) and the South Coast Air Quality Management District (SCAQMD).

4. Review of governmental and industry supported technical societies including the U.S. Maritime Administration (MARAD), the American Bureau of Shipping (ABS), CIMAC (the European technical society for internal combustion engines) and the European Commission (EC).

The information obtained from all sources was reviewed and numerous candidate protocols were reviewed for applicability.

## 2.3 Search Results

The search revealed numerous proposed protocols and test standards and found that a significant number of projects to develop protocols are currently underway. Several references for emissions reduction technologies described testing methods currently in use for product testing, or under consideration for use. A listing of reviewed sources, relevant to this program, follows.

**South Coast Air Quality Management District SCAQMD**
Rule 1631 Pilot Credit Generation Program for Marine Vessels
May 11, 2001
www.aqmd.gov/rules/html/r1631.html

**BAE Systems**
Guide to Emission Control Options
March 2000
MS3026
Don Memers, Glenn Walters

**ISO/TC 70/SC 8**
TC 70: Internal Combustion Engines
SC 8: Exhaust Emission Measurement
Aug 10, 1994

**AG Environmental Products LLC**
9804 Pflumm RD
Lenexa KS 66215
Product name: SoyGold
Description: Soydiesel used 2001-2002 on Blue and Gold Fleets in the San Francisco Bay area for emission reduction.

**SoyGold – Lubricity Study 12/27/00**
Product literature on the effect of the soydiesel alternative on diesel engines.

**SoyGold – Material Safety Data Sheet; MSDS**
Case number 67784-80-9

**INNOVATION 'Journal of the Association of Professional Engineers & Geoscientist of BC'**
Nov 2000 issue Page 12 "Continuous Water Injection"
Summary: Test results from ERMD (Emission Reduction & Means Division) 1998. Initial testing done by protocol on in-lab engines on a baseline to modification comparison.

**BioFuels DOE/GO-102001-1449**
September 2001
'Biodiesel Explanation and Emission Results'
'Biodiesel Fuel Properties'

**Dr. Anataoly D. Mezheritsky P.E.**
**"MA Turbo/Engine Design"**
'Development of new low emission technology for diesel engines' No date
Summary: Describes development of new low NOx emission technology tested on converted CAT 3406E/ Cummings NTC-350/ Wartsila 9R32D for EMRD. Lists test protocols used.

**J. Vollenweider, M. Geist and M. Schaub**
CIMAC 1995 Interlaken
'Residual Fuels in Emission Controlled Diesel Engines'
Subject: Background development and operational results.

**Blue and Gold Fleet LP**
October 2001
'Emission Reduction Demonstration Project'
Subject: Use of Biodiesel in Fleet. Test protocol and future testing.

**ABS Regulatory 'Air Pollution Prevention'**
www.eagle.org/regulatory/regupdate/mep39/air_pollution_prevention.htm
'New annex to MARPOL'
'Mandatory Code on NOx Reduction'

**BAE Systems- Guide to exhaust emission**
www.cimac.com
'Control Options'
Andy Write ABS Europe LTD

**CIMAC Program for May 8, 2001**
www.CIMAC.com
'Exhaust emissions- New Challenges in Emission Control"
A. Write ABS Europe LTD

**WTA Technical Advisory Committee**
"Clean Marine" Ad Hoc work group
November 16, 2001
'Protocol development'

**Emission Standards: USA**
Heavy-Duty Truck and Bus Engines
Diesel Net
November 13, 2001
www.dieselnet.com/standards/us/hd.html
'Emission Standards for New Engines'
'California Urban Bus Standards'
'Applicability and Test Cycles'
Summary: See Doc 2

**Emission Standards: USA**
Off-Road Engines
DieselNet
November 13, 2001
www.dieselnet.com/standards/us/offroad.html
'Harmonized with European Standards'
'Marine Applications'
'Emission Standards'

**Emission Standards: USA**
Marine Diesel Engines
DieselNet
November 13, 2001
www.dieselnet.com/standards/us/marine.html
'Marine Diesel Engines'
'MARPOL 73/78 Sept 27 1997'
'MARPOL Annex VI Limits'
'40CFRpart89'
'Emission Standards cat1/ cat2'
'Test Cycles- ISO8178 for cat 1'
'Test Cycles- ISO8178 for cat 2'
Summary: See Doc 2

**Emission Standards: USA**
Urban Bus Retrofit Program
DieselNet
November 13, 2001
www.dieselnet.com/standards/us/ubrr.html
'Urban Bus Retrofit Rebuild (UBRR) Program'
'40CFRpart85subO'

**Emission Standards: USA**
Occupational Health Regulations
DieselNet
November 13, 2001
www.dieselnet.com/standards/us/ohs.html
'Regulatory Authorities'
'Exposure Limits for Gasses'
'Exposure Limits for Particulates'

**Emission Standards: EU**
Heavy-Duty Truck and Buses
DieselNet
November 13, 2001
www.dieselnet.com/standards/eu/hd.html
'Euro I-V Standards 1992'
'Euro III Standard (Directive 1999/1996/EC)'
'Emission Standards'

**Emission Standards: EU**
Emission Test Cycles
DieselNet
November 13, 2001
www.dieselnet.com/standards/ecycles/ece_r49.html
'ECE R49 – 13 Mode Steady State Diesel Engine Test Cycle'

**Emission Standards: EU**
Emission Test Cycle; European Stationary Cycle (ESC)
DieselNet
November 13, 2001
www.dieselnet.com/standards/cycles/ESC/.html
'ESC replaces R49 protocol'

**Emission Standards: EU**
European Load Response
DieselNet
November 13, 2001
www.dieselnet.com/standards/cycles/elr.html
'Proposed smoke opacity measurement'

**Emission Standards: USA**
Heavy-Duty FTP Transient Cycle
DieselNet
November 13, 2001
www.dieselnet.com/standards/cycles/ftp_trans.html
'On-Road Engine test (40CFR86.1333)'
'New York/ Los Angeles Freeway Simulations'

**Emission Standards: USA**
Cars and Light-Duty Trucks
DieselNet
November 13, 2001
www.dieselnet.com/standards/us/light.html
'Emission Standards'
'Federal Standards'
'Tier I Standards'
'Tier II Standards'
'National LEV (Low Emission Vehicle) Program'
'National LEV II (Low Emission Vehicle) Program'
'California Standards'
'Measured by Federal Test Procedures FTP-75'

**Emission Standards: USA**
Non-Road Vehicles
DieselNet
November 13, 2001
www.dieselnet.com/standards/cycles/iso8178.html
'ISO 8178 Emission Test Cycles'
'Non-Road Steady State Test Cycles'
'Marine Test Cycles'

**Emission Standards: EU**
Light-Duty Vehicles
DieselNet
November 13, 2001
www.dieselnet.com/standards/cycle/ece.eudc.html
'Chassis Dynamometer specifications for Light-Duty Vehicles'

**Emission Standards: Sweden**
Environmental Zones Program
DieselNet
November 13, 2001
www.dieselnet.com/standards/se/zones.html
''City Zone Trucks and Buses July 1 1996'
'Emission enforcement'
'Emission Benefits'

**Emission Standards: EU**
Off-Road Diesel Engines
DieselNet
November 13, 2001
www.dieselnet.com/standards/eu/offroad.html
'Off-Road Diesel Engine 97/68/EC'

**Emission Standards: SE**
Off-Road Engine Program
DieselNet
November 13, 2001
www.dieselnet.com/standards/se/zones_off.html
'Emission requirements'
'Equipment Certification'

**Emission Standards: SE**
Environmental Zones Program (Buses and Trucks)
DieselNet
November 13, 2001
www.dieselnet.com/standards/se/zones.html
'Certification and Enforcement'
'Chassis Dynamometer on "Braunschwig City Driving Cycle"'

**Emission Standards: EU**
Off-Road Diesel Engines
DieselNet
November 13, 2001
www.dieselnet.com/standards/eu/offroad.html
'EU Emission Regulations for Off-road Diesels"

**Emission Standards: US**
Off-Road Engine Program
DieselNet
November 13, 2001
www.dieselnet.com/standards/us/offroad.html
'History Background'
'Emission Standards'
'Engine Useful Life'
'Environmental Benefit and Cost'
Summary: EPA is currently working on a Test Protocol for Off-Road Diesel Engines.

**Emission Standards: Germany**
Occupational Health Regulations
DieselNet
November 13, 2001
www.dieselnet.com/standards/de/ohs.html
'Exposure Limits'
'Diesel Engine Regulations'
'Future Directions; Fine Particles'

**Emission Standards: Japan**
On-Road Vehicles and Engines
DieselNet
November 13, 2001
www.dieselnet.com/standards/jp/onroad.html

**Emission Standards: Japan**
Japanese 10-15 Mode
DieselNet
November 13, 2001
www.dieselnet.com/standards/jp/jp_10-15mode.html
'Light Duty test cycle'

**Emission Standards: Japan**
Japanese 13 Mode
DieselNet
November 13, 2001
www.dieselnet.com/standards/jp/jp_13mode.html
'Heavy-Duty Engine Test Cycle'

**EPA - Office of Transportation and Air Quality**
Volunteer Diesel Retrofit Program
www.epa.gov/otaq/retrofit/retrotesting.htm
Air Pollution Control Technology Verification Center
October 2, 2001
Draft Generic verification protocol for retrofit catalyst, particulate filter and engine modification control technologies for highway and non-road use diesel engines.

**Fairplay Solutions**
October 2001
Issue No 61
Page 8 "Dual Fuel Marine Engines"

**MARAD**
**Emissions Monitoring Protocols for Commercial Ships**
James J. Corbett P.E. PhD
Allen Robinson, PhD.
Alex Farrell, PhD.
www.marad.dot.gov/MTS_RD/topics.html

**EPA**
**Test/QA procedures for verification of portable NO/NO2 emission analyzers**
December 4, 1998
www.epa.gov/etv/07/prot_no2.pdf

**MARPOL 73/78 Annex VI- Technical Code, International Maritime Organization. MP/CONF 3/35, 22 Oct 1997**

**MARPOL 73/78 Annex VI- International Maritime Organization, MP/CONF 3/34, 28 Oct 1997**

**R. Herrmann and G. Grosshans, "Exhaust Emissions of Ship Propulsion Engines" ASME Oct 1994**

**Research Project 396: Exhaust Gas Monitoring: Evaluation of Exhaust Gas Monitoring Equipment for Shipboard Use, Marine Information Note MIN 41 (M+F) Jan 1999**

**EPA**
EMC- CFR Promulgated Test Method
http://www.epa.gov/ttn/emc/promgate.html

## 2.4 Discussion

In consultation with AETC, and supported by industry experience and the results of this literature survey, we conclude that actual in-situ testing of an automobile will not be required for this study. This is due to the vast database of emissions data available from the EPA and other sources for automobile pollutant generation rates. Therefore, this review focused on the

identification of applicable test methods for the ferry, which could also apply to the test of the diesel-powered bus.

There are two distinct issues relative to the development of test protocols of marine engines. The first is the development of a relatively simple and cost-effective test that can be established as a broad-based standard for periodic emissions source testing. This low cost and easily implemented method would also apply to comparative testing of various emissions reduction devices and/or alternative fuels. The development and evaluation of such methods is currently underway by numerous groups as noted in the references.

The second issue, imperative to this study, is the generation of a detailed, laboratory-quality protocol applicable to the one-time testing of a diesel ferry in a particular service and a diesel bus in the same commuter service for the purpose of obtaining absolute, scientifically defensible data. The technical literature overwhelmingly offers information on the former, cost-effective source test protocol, while clearly demonstrating that results and/or the test methods utilized for conducting a laboratory quality field test of a marine ferry engine or diesel passenger bus are non-existent.

Therefore, we will move toward adapting well-established test methods for large-bore stationary diesel engines to the demands of this analysis. Based on a review of recent test work and emissions test protocol development performed by AETC for the New York State Department of Environmental Conservation and upon discussions with various agencies, this will primarily consist of the utilization of the extractive Fourier Transform Infrared Spectroscopy (FTIR) method for testing of all targeted pollutants.

Utilizing FTIR (EPA Method 320) a single instrument will directly measure all targeted compounds and will provide the highest quality data currently achievable utilizing any known test method. In addition, since the FTIR analyzer will measure all targeted compounds real-time, and the measurement of all compounds will occur simultaneously, excellent measurement of engine transients will be possible. We propose utilizing FTIR to measure the following compounds:

The following chemical species will be quantified:

- Acetaldehyde;
- Acrolein;
- Carbon4+ straight-chain hydrocarbons (aliphatic HCs, $C_4$ and larger);
- Carbon dioxide ($CO_2$);
- Carbon monoxide (CO);
- Ethane;
- Ethylene;
- Formaldehyde and aldehyde compounds;
- Methane;
- Oxides of Nitrogen ($NO_x$) (using NO + $NO_2$ on the FTIR);
- Oxygen (utilizing a paramagnetic analyzer);
- Particulate matter (utilizing EPA Method 5)

- Sulfur dioxide ($SO_2$);
- Water vapor ($H_2O$); and
- Any other FTIR-detected species.

The capability of the FTIR instrument to measure VOC's, methane and formaldehyde compounds in real-time with unsurpassed accuracy offers tremendous advantages over other indirect methods which would require the acquisition of an exhaust gas sample that is then sent (off-site) for laboratory analysis, typically utilizing "wet chemistry" methods.

As noted above, EPA Method 5 will be used for the measurement of particulate matter. EPA Method 5 is a mass-based particulate method, well established and universally accepted for stationary sources. The identical test equipment will be utilized for the in-situ test of the marine engines on the ferry as well as for measurement of the bus emissions while the bus is operated on a chassis dynamometer.

During the testing utilizing FTIR, we may recommend performing simultaneous testing with an inexpensive portable-type analyzer for the purposes of qualifying the portable instrument. Once qualified, the portable unit could be used for later portions of this analysis, which will evaluate various candidate emissions-reduction devices and/or alternative fuels.

# 3.0 TEST SCOPE AND METHODOLOGY DEFINITION

## 3.1 Objective

The objective of this section is to define in broad terms the scope and methodology to conduct transit bus and passenger ferry emissions testing and to capture required engine load and performance data.

## 3.2 Test Scope and Methodology

### *3.2.1 Engine Exhaust Emissions Measurements*

The imperative requirement of this research is the generation of a detailed, laboratory-quality protocol applicable to the one-time testing of a diesel engine powered ferry in a particular service and a diesel engine powered bus in the same commuter service for the purpose of obtaining absolute, scientifically defensible emissions data. Therefore, we will adapt well-established diesel engine test methods for use in this analysis. Utilizing Fourier Transform Infrared Spectroscopy Analysis, FTIR (EPA Method 320), a single instrument will directly measure all targeted compounds and will provide the highest quality data currently achievable utilizing any known test method. Moreover, since the FTIR analyzer will measure all targeted compounds in real-time, and the measurement of all compounds will occur simultaneously, excellent measurement of engine transients will be possible.

The following chemical species will be quantified:

- Acetaldehyde;
- Acrolein;
- Carbon4+ straight-chain hydrocarbons (aliphatic HCs, $C_4$ and larger);
- Carbon dioxide ($CO_2$);
- Carbon monoxide (CO);
- Ethane;
- Ethylene;
- Formaldehyde and aldehyde compounds;
- Methane;
- Oxides of Nitrogen ($NO_x$) (using NO + $NO_2$ on the FTIR);
- Oxygen (utilizing a paramagnetic analyzer);
- Particulate matter (utilizing EPA Method 5);
- Sulfur dioxide ($SO_2$);
- Water vapor ($H_2O$); and
- Any other FTIR-detected species.

To meet the objectives of this test program, it is essential to accurately capture engine power and speed (load) profiles for both the bus and the ferry. For the passenger ferry, this engine load data will be captured simultaneously with the exhaust emissions data. Regarding the transit bus, this data will be obtained in two-stages: (1) on-board testing to determine average daily engine load profile and passenger ridership profile and (2) chassis dynamometer testing with the engine load profile programmed into the dynamometer. A description of the engine parameters to be measured and the respective measurement methods follows.

### *3.2.2 Transit Bus Engine Performance Data Collection On-Board*

Based on review of the bus routing and routine, the test team will ride a representative bus for not less than three (3) days. During this time, in addition to recording the number of passengers, a log will be created noting times and activities of the bus.

In addition, a portable PC based data acquisition system (DAQ) will be used to continuously monitor the minimum parameters listed in Table 3.1. These parameters will then be used for programming the chassis dynamometer for the emissions test work.

**Table 3.1**
**Measured Parameters of the Transit Bus Test**

| Parameter | Measurement Method | Purpose |
|---|---|---|
| Fuel Flow | Engine control module | Input to emissions calculations. |
| Air manifold temperature | " " | To confirm engine operating condition on dynamometer. |
| Air manifold pressure | " " | " " |
| Jacket water temperature | " " | " " |
| Engine speed | " " | " " |
| Vehicle speed | " " | " " |
| Throttle position | Linear displacement transducer | " " |
| Ambient temperature | Thermometer | Input to emissions calculations. |
| Misc. engine operating data available from engine control module. | | Engine performance monitoring. |

As shown in Table 3.1, the majority of the data will be acquired through a serial-port (or similar) connection to the engine electronic control unit. Data not available from this source will be acquired from temporary, test-quality instrumentation, connected as analogue voltage inputs to the data acquisition computer.

Following the acquisition of the foregoing data, the test team will develop a time versus engine load and speed profile, relating the various engine operating conditions and the durations at which the engine operates at each load condition. In addition, the details of transients (i.e. acceleration /deceleration), observed during the onboard testing will be recorded.

*Dynamometer Testing*

Once the load profile is completely established, a test matrix will be generated for operation of the same bus on a chassis dynamometer. While field conditions are duplicated on the dynamometer, the engine performance data outlined in Table 3.1 will be captured in addition to, and simultaneously with, the emissions species outlined in Section 3.1 in real time. The data will be utilized to develop an accurate, scientifically defensible profile of emissions data for a fleet of buses.

*Data Reduction.*
For each of the steady-state conditions, not less than three (3) 30-minute test runs will be conducted on the dynamometer. For each of the transient conditions, each of the transient events will be tested not less than three (3) times. The three data sets of each type will be checked real-time to ensure that the data repeatability satisfies the criterion established in the test protocol. Tests yielding data unable to meet the repeatability standard as defined in the test protocol will be done again.

For the steady-state runs, the total mass emissions rates will be generated by multiplying the daily duration (hours) at the specific load condition by the emissions mass flow rates measured on the dynamometer (grams/hour). Similarly, for the transient data, the total mass of pollutants emitted during each transient (grams) will be multiplied by the number of transients of each type occurring each average day.

The total mass of the steady state and transient runs will then be summed to determine a total daily average mass emissions rate.

### *3.2.3 Passenger Ferry Engine Performance Data Collection*

Engine operating data will be recorded simultaneously with emissions data, while aboard the vessel as it performs its usual schedule. Testing will consist of not less than three (3) days, as equal to the testing of the transit bus.

In addition to the emissions test equipment, the portable DAQ, supplemented by manual data entry, will be used to continuously monitor the minimum parameters listed in Table 3.2. These measured parameters include engine combustion airflow, exhaust flow, fuel consumption, power output, etc., as required to develop a complete description of the engine's operational condition for developing mass emissions rates in transient and steady state periods.

**Table 3.2**
**Measured Parameters of the Passenger Ferry Test**

| Parameter | Measurement Method | Purpose |
|---|---|---|
| Fuel Flow (supply & return) | Test Meters connected to DAQ* | Input to emissions calculations. |
| Air manifold temperature | RTD Connected to DAQ | Engine performance monitoring. |
| Air manifold pressure | Pressure transducer connected to DAQ. | Engine performance monitoring and to support emission rates calculations. |
| Jacket water temperature | RTD Connected to DAQ | Engine performance monitoring. |
| Shaft speed | From shaft torque meter | Brake HP calculation. |
| Shaft Torque | From shaft torque meter. | Brake HP calculation. |
| Throttle position | Linear displacement transducer | Engine performance monitoring. |
| Ambient temperature | Thermometer | Input to emissions calculations. |
| Lube oil temperature | Local instrument | Engine performance monitoring. |
| Lube oil pressure | Local instrument | Engine performance monitoring |

*DAQ: Data Acquisition System.

Engine operating data, such as air manifold pressure, air manifold temperature, jacket water temperatures, etc., will be used to capture complete engine operating performance characteristics. These characteristics will be compared to data from different test runs at identical load points in order to validate the data in the final reported results.

In addition to obtaining passenger count from the operators' daily log, other parameters will be recorded to document the condition during each testing run:

1. Sea state.
2. Wind speed and direction.
3. Vessel heading and speed.
4. Vessel position or leg of route.
5. Vessel draft
6. Ambient conditions
7. Basic operating data from other engine as available from local instruments.

As the passenger ferry performs to actual field conditions, the emissions species data outlined in Section 3.1 will be captured simultaneously with engine performance data to develop an accurate, scientifically defensible profile of emissions data for this means of transportation.

### 3.3 Automobile Data Review

As discussed in our previous report, a test of an automobile will not be performed, as sufficient and widely accepted data is available from various regulatory bodies. In order to obtain a defensible comparison, the automobile emissions rates will be determined based on the general routing of the transit bus to determine the automobile daily load profile and average number of trip miles. Next, based on information from the Department of Motor Vehicles for the county to be studied, the average vehicle gross weight and age data will be obtained for that county. This data, together with Corporate Average Fuel Economy (CAFÉ) standards for these size and vintage of vehicles will be used to generate a per passenger daily mass emission rate for comparison with results from the transit bus and passenger ferry.

### 3.4 Discussion

During both the ferry and the bus tests, maximum effort will be extended to measure and record engine operating data for use in developing the emissions profile for the respective vehicles. The information is useful for data checks performed during the testing. Moreover, such data may also be used afterwards for comparison with data from the engine manufacturers to further validate the reduced test data.

# 4.0 TEST PROTOCOL DEVELOPMENT

## 4.1 Objective

The objective of this section is to develop protocols to determine emissions rate factors for the same passenger-commute for the marine and land based vehicles of a pollutant expressed in grams/BHP-Hr and normalized for vehicle rider-ship (i.e. grams/passenger/day).

## 4.2 Scope of Test Protocols

The scope of the test program is to develop emissions rate factors for the same passenger-commute for the marine and land based vehicles of a pollutant expressed in grams/BHP-Hr and normalized for vehicle rider-ship (i.e. grams/passenger/day). The best available, laboratory-quality analyzers and test methods will be utilized to obtain accurate measurements of the emissions from the two sources to be tested. In addition, the same test methods, equipment and personnel will be used in both tests.

The following chemical species will be quantified:

- Acetaldehyde;
- Acrolein;
- Carbon4+ straight-chain hydrocarbons (aliphatic HCs, $C_4$ and larger);
- Carbon dioxide ($CO_2$);
- Carbon monoxide (CO);
- Ethane;
- Ethylene;
- Formaldehyde and aldehyde compounds;
- Methane;
- Oxides of Nitrogen ($NO_x$) (using NO + $NO_2$ on the FTIR);
- Oxygen (utilizing a paramagnetic analyzer);
- Particulate matter (utilizing ISO Method 8178)
- Sulfur dioxide ($SO_2$);
- Water vapor ($H_2O$); and
- Any other FTIR-detected species.

Total hydrocarbons (THC) will be derived from the FTIR speciated hydrocarbon data. Moisture, $CO_2$, and $O_2$ will be reported in volume percent. Other gaseous emissions will be reported in parts per million by volume (ppmv), ppmv dry (ppmvd), ppmdv corrected to 15% oxygen, and pounds per hour (lb/hr). Particulate emissions will be calculated in pounds per million Btu (lb/MMBtu), lb/hr, and grains per dry standard cubic foot (gdscf). Test runs will be of a duration based on source route data. One-minute averages will be collected for the instrumental FTIR method test runs.

The following methods will be used to determine these parameters in conformance with 40 CFR 60, "Standards of Performance for New Stationary Sources".

**Table 4.1**
**Parameters and Test Methods**

| Parameter | Method |
|---|---|
| Traverse Point Locations | EPA Test Method 1 - *Sample and Velocity Traverses for Stationary Sources* |
| Gas Composition, Oxygen ($O_2$) | EPA Test Method 3A - *Determination of Oxygen and Carbon Dioxide from Stationary Sources (Instrumental Analyzer Procedures)* |
| Volumetric Flow Rate | EPA Method 19. *Actual fuel flow and intake airflow will be measured and summed as a data check for Method 19.* |
| Particulate | ISO Test Method 8178 - *Determination of Particulate Emissions* |
| Formaldehyde, Acetaldehyde, Acrolein, Water vapor ($H_2O$), Carbon monoxide (CO), Carbon dioxide ($CO_2$), Oxides of Nitrogen ($NO_x$) (using NO + $NO_2$ on the FTIR), Sulfur dioxide ($SO_2$), Methane, Ethane, Propane, C4+ straight-chain hydrocarbons, Ethylene | EPA Test Method 320 -*Measurement of Vapor Phase Organic and Inorganic Emissions by Extractive Fourier Transform Infrared (FTIR) Spectroscopy* |
| THC, TNMHC | THC & TNMHC will be derived from the FTIR speciated hydrocarbon data. |
| Fuel Flow Measurement | 40 CFR 92.107 "Fuel Flow Measurement" |
| Intake Air Flow | 40 CFR 92.108 "Intake Air and Cooling Air" |
| Torque (Ferry only) | ASME Power Test Code PTC-19.7 |

## 4.3 Testing Program and Description of Source

The testing of each source will be conducted utilizing identical emissions test techniques and with the same test team. A description of the test procedures for each follows.

### *4.3.1 Bus*

The candidate bus is a modern, passenger service bus operated by the Golden Gate Bridge Highway and Transportation District. The bus is powered by a four-stroke cycle, Detroit Diesel engine controlled by the DDEC Series IV electronic control system. The bus engine is fitted with Detroit Diesel's low-emission controls equipment.

The bus emissions test will be preceded by pre-test, on-board data logging during a period of not less than one-week. During the pre-testing, test personnel will ride the bus, monitoring and recording vehicle and engine parameters including load (HP), speed, torque, operating temperatures and logging rider-ship. Monitoring will be performed using a laptop computer connected to the on-board Detroit Diesel Electronic Control (DDEC) system and operating the DDEC companion software program.

Based on the duty-cycle data gathered during the pre-test, the test team will operate the bus on a chassis dynamometer to duplicate the actual bus performance, including transients, while conducting the emissions testing. The test procedure will be as follows:

- Bus on Dynamometer.
- Discuss procedure with test team and driver.
- Review safety measures with all participants.
- Connect computer to DDEC system & establish communications.
- Install intake air mass flow meter.
- Install fuel oil supply / return metering system.
- Connect fuel flow and air flow transducers to data acquisition system.
- Mobile emissions laboratory set-up and calibrate.
- Begin Trial Test runs
- Commence Test Program
  - Steady-state data
    - 10-minute averages
    - Repeat each condition three-times and average data.
  - Transient Conditions
    - For each transient repeat three-times and average the data.
- Post Test Calibration.
- Uninstall test equipment.
- Bus returns to service.

### *4.3.2 Ferry*

The Seaworthy team will perform all testing of the passenger ferry, M/V Mendocino, a new high-speed, multi-hull (catamaran), passenger vessel. The ferry is powered by four (4) identical Cummins KTA-50, sixteen-cylinder marine diesel engines which each drive a water-jet via a ZF Marine reduction gear. The engines are fitted with the engine manufacturer's electronic governing system.

All testing will be performed during normal service between Larkspur and San Francisco over a period of approximately three-days. Test equipment will be installed during the evenings or to coordinate with planned vessel maintenance activities to minimize impact on ferry operations or schedule.

The test procedure will be as follows:

- Discuss procedure with test team and crew.
- Review safety measures with all participants.
- Connect computer to engine control module & establish communications using the Cummins' "INSITE" software program.
- Install intake-air mass flow meter.
- Install fuel oil supply / return metering system.
- Install shaft torque meter.

- Connect fuel flow, torque meter and air flow transducers to data acquisition system.
- Mobile emissions laboratory set-up outside engine room and calibrate.
- Begin Trial Test runs / check equipment.
- Commence Test Program
  - Determine voyage average mass emissions rates (Dock to Dock)
  - Confirm Steady-state data
    - 10-minute averages.
    - Observe each condition three-times and average data.
  - Transient Conditions
    - For each transient observe three-times and average the data.
- Post Test Calibration.
- Uninstall test equipment.
- Ferry returns to service

### *4.3.3 Schedule of Activities*

Testing on-site for each source will commence following the completion of pretest engine equipment checks. A list of activities by days is shown below.

**Table 4.2**
**Test Agenda**

| DAY | ACTIVITY | LAB AT-SITE |
|---|---|---|
| 1 | INSTRUMENT SET-UP - BUS | NO |
| 2 | EMISSIONS MOBILE LAB SET-UP | YES |
| 3 | EQUIPMENT SET-UP, CALIBRATION AND TRIAL RUNS | YES |
| 4 | EMISSIONS TESTING | YES |
| 5 | EMISSIONS TESTING, POST-TEST CALIBRATION | YES |
| 6 | DEMOBILIZATION | YES |
| 7 | INSTRUMENT SET-UP –FERRY | NO |
| 8 | INSTRUMENT SET-UP | NO |
| 9 | EMISSIONS MOBILE LAB SET-UP | YES |
| 10 | EQUIPMENT SET-UP, CALIBRATION AND TRIAL RUNS | YES |
| 11 | EMISSIONS TESTING | YES |
| 12 | EMISSIONS TESTING, POST-TEST CALIBRATION | YES |
| 13 | DEMOBILIZATION | YES |

## 4.4 Determination of Flue Gas Parameters

### *4.4.1 Stratification Check (Ferry Only)*

Prior to testing of the ferry engine, the FTIR operator may be directed to determine if stratification of the exhaust stream is present. Stratification is a variation in measured analyte

concentration as a function of the sample probe traverse position within the stack. Stratification is usually found in situations where two or more source streams are combined in a laminar (i.e., poorly mixed) manner ahead of the measurement point. If there is only one source stream, then it may indicate a leak of ambient air into the stack upstream of the measurement point with poor mixing. It is possible to observe stratification in a leak-free multi-cylinder internal combustion engine exhaust, if individual cylinder exhaust streams are (1) different in composition; and (2) exhibit laminar flow characteristics. Based on current experience, however, stratification is extremely rare in internal combustion engine exhaust streams.

The procedure to measure stratification is straightforward. A set of five 1-minute data points are measured by the FTIR at each of three (or greater) traverse points across the stack cross section. The number of traverse points depends on EPA Method 1 criteria (Appendix B), and will be determined once the stack diameter is known. A statistical comparison, analysis of variance (ANOVA), between the three (or greater) data sets for a selected analyte (e.g., formaldehyde) will be performed. ANOVA will reveal if there is a statistically significant difference between data sets. If the ANOVA test shows significant differences, then the percent difference between the lowest and highest value data sets is computed. If a statistically significant difference of greater than 5 percent between the lowest and highest points is found, then stack traversing using EPA Method 1 points must be conducted during sampling to obtain a representative sample. If a difference of less that 5 percent is found between traverse points, then subsequent sampling will be carried out with the probe tip located at the estimated centroid of the stack cross section.

An insignificant ANOVA result indicates no stratification is detected, and subsequent sampling is carried out with the probe tip at the estimated centroid of the stack cross section.

### *4.4.2 Volumetric Flow Rate*

Exhaust flow rates for the engines will be determined by direct measurement of the inlet air and net fuel oil flows to cross-check EPA Method 19. Calculated average F-Factor values will be used in determining the exhaust gas flow rate based on individual fuel heat input rates and F-Factors.

### *4.4.3 Oxygen Concentration*

Oxygen concentrations in the flue gas during each test run will be determined in accordance with procedures outlined in EPA Test Method 3A - *Determination of Oxygen and Carbon Dioxide Concentrations in Emissions from Stationary Sources. (Instrumental Analyzer Procedure).* (Other relevant references are contained in Appendices B, C and D.)

Samples will be collected from a single point in the stack and transported to the mobile laboratory using a heat-traced sampling system. Further information about the sampling system is given in Section 6 of this test protocol.

### *4.4.4 Determination of Stack Gas Moisture Content*

Stack gas moisture will be determined using EPA Test Method 320 (Appendix F), which is described in Section 6 of this test protocol. EPA Test Method 320 has been validated for moisture in gas-fired engines. This data is presented in a report published by the Gas Research Institute entitled, *Fourier Transform Infrared (FTIR) Method Validation at a Natural Gas-Fired Internal Combustion Engine*, GRI Document No. GRI-95/0271, December 1995.

## 4.5 Particulate Matter Emissions Testing Using ISO Method 8178

The test team will utilize a partial dilution tunnel-type sampling system from either Sierra Instruments or from AVL. The equipment provider will be selected once a test schedule has been established and will be based on equipment and operator availability. A number of different test methods and equipment types for the particulate sampling portions of this test program were investigated before deciding on the method described in this section. Background information and a topical discussion follow.

### *4.5.1 Background*

Due to unique historical circumstances, the EPA has never published emissions test methods for stationary (or marine) Internal Combustion (IC) engines similar to 40CFR60 Method 20 for gas turbines. In the absence of such a rule, testers have typically utilized one of two separate sets of emissions testing methods, automotive/transport testing specifically for IC engines or generic stationary methods. A brief summary of each follows.

*Automotive/Transport 40CFR86/89*

Historically, the automotive/transport methods always included various load cycles and/or transient tests. Data Acquisition Systems (DAQ) and analyzers of the time lacked sufficient transient response, so samples were simply collected in bags at regular intervals to achieve a simple robust averaging method. This necessitated a cool sample to keep from damaging the (typically plastic) bag, so it became standard practice to dilute the full exhaust sample with fresh air to achieve a temperature of ~125°F or less. The dilution had many beneficial side effects:

- Prevented water condensation, eliminating the need for water knockouts.
- Permitted the use of atmospheric analyzers.

Once particulates were added to the testing, the dilution and cooling process caused aerosols and vapors to solidify - just as they would in the atmosphere. Consequently only a filter was needed to catch the particulates (or said another way, the particulates were defined as what could be caught with a filter).

*Stationary Sources 40CFR60*

Stationary source test methods presume the source operates at steady state, or that the rate of change is sufficiently slow that direct on-line sampling suffices. In addition, the large volume of exhaust flow precludes full dilution of the exhaust stream. Consequently, a small fractional portion of the exhaust is collected, and kept hot until it reaches a conditioning station where particulates are removed and water rapidly dropped out and removed. Sampling is then conducted generally cold and dry.

To accommodate particulates, EPA Method 5 requires the use of a separate manually traversed sampling probe to directly collect hot sample gas. The hot gas immediately passes through both a filter for particulates and canisters to condense the liquids, which have not yet solidified. At this time there is not a good correlation between Method 5 and the automotive dilution method.

*Hybrid Approach*
With the advent of high-speed data acquisition systems, many large engine testers have begun directly collecting a fractional sample and passing that through the analyzers, either hot and wet or cold and dry. This is particularly attractive where the tremendous volume of the exhaust precludes dilution.

However, to obtain data that better correlates with dilution tunnel measurements, several researchers have developed "partial dilution" methods specifically for particulates. These include Sierra Instruments in the USA and AVL in Europe. These methods extract a precisely measured isokinetic fraction of the exhaust flow and then dilute it similar to a full dilution tunnel. Depending on the specifics of the method, it would appear to more or less correlate with full dilution data, though this requires further investigation.

Rather interestingly, 40CFR94, the new test method for marine diesels, uses 40CFR92 (locomotive) test methods. This method permits partial dilution for particulate measurement, offering few specifics. Again much more information is needed.

In developing methods for the current protocol AETC recommends using 40CFR60 methods for gaseous components in conjunction with a good partial dilution sampling method for particulates.

### *4.5.2 Principle of Operation*
Referring to Figure 4.1 on the following page, the dilution tunnel operates by drawing a known volume of exhaust from the stack and into the dilution tunnel where it is diluted with a known quantity of clean air. The fresh air keeps the exhaust gases cool and at the same times prevents moisture from condensing out of the exhaust stream. Some of the diluted air/exhaust mixture is then passed through a filter medium, which captures the particulate matter.

Filters are weighed before and after testing and the particulate matter concentrations in the exhaust system are then derived from the difference in the before and after weights. Appendices B and D of this protocol contain detailed descriptions of the sampling operation and the accuracies of the method.

### *4.5.3 Sampling Equipment*
Detailed descriptions, certifications test reports and operating instruction manuals appear for the two partial dilution particulate sampling systems evaluated by AETC appear in AETC Report 4005.01.04, deliverable No. 4, "Emissions Test Equipment".

**Figure 4.1**
**Partial Dilution Sampling System**

EXAMPLE OF PARTICULATE DILUTION TUNNEL

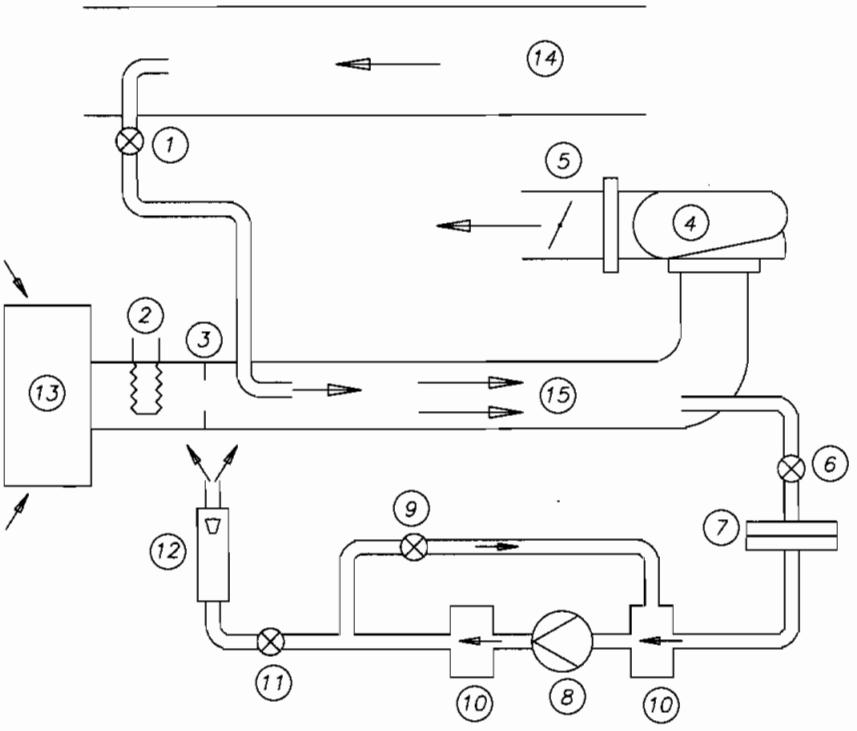


LEGEND

1. Transfer tube gate valve
2. Heater (aptianal)
3. Restrictar (adjustable)
4. Extractor pump or fan
5. Throttle
6. Sample tube gate valve
7. Filter halder
8. Sample pump
9. Back pressure control valve
10. Damping volumes (optional)
11. Control valve
12. Sample flow meter
13. Dilution air filter
14. Exhaust duct
15. Dilution tunnel

## 4.6 Fourier Transform Infrared (FTIR) Spectroscopy Analysis

### *4.6.1 Introduction*

The extractive FTIR measurement method is based on continuous extraction of sample gas from the stack, transporting the sample to the FTIR spectrometer and performing real-time spectral measurement of the sample gas. The sample gas spectra are analyzed in real time for target analytes, archived, and re-analyzed, if necessary, at a later date for other target analytes.

Our proposed FTIR subcontractor, Spectral Insights (SI), has conducted over 75 compliance tests using FTIR on natural gas-fired engines, using EPA Method 320 or equivalent. Each of these tests was completed successfully. In approximately 50 of the tests, corresponding EPA reference methods for THC, $NO_x$, $CO_2$, and CO were conducted simultaneously. The agreement between the methods was very good, except in cases where high levels of $NO_2$ were present. This was found to be due to low converter efficiency in chemiluminescent $NO_x$ analyzers. It was also determined at low $NO_x$ levels, the chemiluminescent analyzer is subject to fluorescence quenching due to $CO_2$. FTIR is not subject to these known problems. The U.S. EPA has accepted all SI-collected FTIR data submitted to them without question, including $NO_x$ and CO data. (For further information on EPA's position on the use of FTIR for $NO_x$, CO, and other species, please contact Ms. Rima Dishakjian at (919) 541-0443, Mr. Ken Durkee at (919) 541-5425, or Mr. Mike Toney at (919) 541-5247).

The proposed method will follow all of the procedures described in EPA Test Method 320. SI performed (as Radian Corporation) the successful EPA Method 301 FTIR validation test funded by the Gas Research Institute (GRI) in 1994. The validation was accepted by EPA, and EPA stated in a letter to GRI that FTIR can be used at any "gas-fired source". These data are reported in a document published by the Gas Research Institute entitled, *Topical Report: Fourier Transform Infrared (FTIR) Method Validation at a Natural Gas-Fired Internal Combustion Engine*, GRI Document No. GRI-95/0271, December 1995.

SI has conducted EPA Method 301 validation studies for the following compounds:

- Acetaldehyde;
- Acrolein;
- Carbon dioxide ($CO_2$);
- Carbon monoxide (CO);
- Formaldehyde;
- Oxides of Nitrogen ($NO_x$) (using NO + $NO_2$ on the FTIR); and
- Water vapor ($H_2O$).

SI has successfully used FTIR to determine THC and TNMHC data from engines. These components of engine exhaust are primarily methane ($CH_4$), ethane, ethylene, and formaldehyde. Because FTIR can measure these species separately, it is straightforward to measure THC and TNMHC using the FTIR system by adding the concentration of the appropriate species, either un-weighted, or carbon-weighted. Because the usual detector used in Method 25A analysis is a flame ionization detector (FID), the measurement of THC can be biased with the varying relative responses for each hydrocarbon. However, because THC in the engine exhaust is primarily

methane, the differences between THC by FID and FTIR are typically negligible. TNMHC determination has historically been difficult using M25A, due to the high levels of methane expected to be present in the effluent gas and the difficulty of selectively removing methane. A recent EPA-sponsored test of Internal Combustion (IC) engine exhaust measurements at Colorado State University using a "TNMHC" analyzer showed the difficulties with attempts to remove high (1000 ppm) levels of methane.

### *4.6.2 Summary of FTIR Method*

FTIR measurement is based on the absorbance of infrared energy by gas phase compounds. Most molecules absorb infrared energy at characteristic frequencies based on the molecular vibrational and/or rotational motion within the molecule. The absorption characteristics of a particular compound can be used to identify and quantitate the concentration of that compound. The concentration of a single target compound is related to its absorbance according to Beer's Law:

$$A(\nu) = a(\nu)bc$$

Where:

| | | |
|---|---|---|
| $A(\nu)$ | = | absorbance at wavelength □, |
| $a(\nu)$ | = | absorption coefficient at wavelength □, |
| $b$ | = | path-length, and |
| $c$ | = | concentration. |

If more than one compound absorbs light at a given wavelength, then the total absorbance is found from a linear combination of Beer's Law for each compound.

Where:

$$A_{total}(\nu) = b\sum_{i=1}^{N} a_i(\nu)c_i$$

| | | |
|---|---|---|
| $A_{total}$ | = | total absorbance at wavelength $\nu_i$, |
| $a_i(\nu)$ | = | absorption coefficient for compound I at wavelength v, |
| $c_i$ | = | concentration of compound I, |
| N | = | total number of absorbing compounds, and |
| $b$ | = | path-length. |

Compounds with very sharp spectral features, such as CO, can exhibit nonlinear analyzer response, requiring correction algorithms to accurately calculate concentrations. Correction algorithms are generated by measuring the spectrum of the compound at several different concentrations and fitting the resulting data to an appropriate correction curve.

Quantitation of each target compound is based on the application of a reference spectrum that is specific to that compound and is measured at a known concentration, temperature, and pressure. For the target compounds, quantitation is performed by selecting characteristic absorbance regions that have minimal interferences from other compounds present in the gas stream.

The classical least squares (CLS) method is applied to fit the reference spectra to the sample spectrum, with the resulting scaling factors used to calculate concentrations. The CLS method finds the set of concentrations that minimizes the residuals in the analysis region and provides a confidence interval for each concentration calculated. The confidence interval is used as a diagnostic to determine how well the CLS method fit was accomplished. It is used to assess instrument performance and to alert the user to review the data for the presence of new or elevated concentrations of interferants in the sample.

### *4.6.3 Analytes*

The analytes that will be measured by this method and their CAS numbers are shown below.

**Table 4.3**
**Target Analytes**

| Compound | Chemical Abstract Number |
|---|---|
| Acetaldehyde | 75-07-0 |
| Acrolein | 107-02-8 |
| C4+ straight-chain hydrocarbons | NA |
| Carbon dioxide ($CO_2$) | 124-38-9 |
| Carbon monoxide (CO) | 630-08-0 |
| Ethane | 74-84-0 |
| Ethylene | 74-85-1 |
| Formaldehyde | 50-00-0 |
| Methane | 74-82-8 |
| Nitrogen dioxide ($NO_2$) | 10102-44-0 |
| Nitric oxide (NO) | 10102-43-9 |
| Propane | 74-98-6 |
| Sulfur dioxide ($SO_2$) | 7446-09-5 |
| Water vapor ($H_2O$) | 7732-18-5 |

### *4.6.4 Applicability*

This method applies to the analysis of vapor phase organic or inorganic compounds that absorb energy in the mid-infrared spectral region, about 400 to 4000 $cm^{-1}$ (25 to 2.5 um). This method is used to determine compound-specific concentrations in a multi-component vapor phase sample that is contained in a closed-path gas cell. Spectra of samples are collected using double beam infrared absorption spectroscopy. A computer program is used to analyze spectra and report compound concentrations.

### *4.6.5 Method Range and Sensitivity*

Range and sensitivity of the method are functions of the following factors:

- Measurement cell path-length;
- Absorption coefficient of each target compound at the selected analytical frequency region;
- Spectral resolution;

- Interferometer sampling time;
- Number of individual interferograms used to produce each time-averaged spectrum;
- Detector sensitivity and response time;
- Compounds comprising the sample matrix; and
- Biases due to the sample collection and/or analysis system.

Measurement cell path-length is the primary determinant of the range and sensitivity of the method. Appropriate path-length of the measurement cell will be determined by considering the following:

- The lowest expected concentration or the desired target detection limit of each target compound; and
- The expected concentration of any potential interfering compound.

### *4.6.6 Performance Specifications*

Prior to the performance of the work, the performance specifications shown below will be verified with the FTIR instrumental configuration anticipated for this program.

**Table 4.4**
**FTIR Method Performance Specifications [a]**

| Compound | Detection Limit |
|---|---|
| Acetaldehyde | 1.0 ppmv |
| Acrolein | 1.0 ppmv |
| C4+ straight-chain hydrocarbons[b] | 0.1 ppmv |
| Carbon dioxide ($CO_2$) | <0.04% |
| Carbon monoxide (CO) | 0.1 ppmv |
| Ethane | <1 ppmv |
| Ethylene | 0.1 ppmv |
| Formaldehyde | 0.2 ppmv |
| Methane | <5 ppmv |
| Oxides of Nitrogen ($NO_x$) | <5 ppmv |
| Propane | <1 ppmv |
| Sulfur dioxide ($SO_2$) | <5 ppmv |
| Water vapor ($H_2O$) | <0.1% |

[a] Precision (% RSD) and Accuracy (% bias) equal to ±10% and are defined at concentrations 10 times greater than the analyte detection limit.
[b] Reported as hexane equivalents.

### *4.6.7 FTIR Sampling Equipment*

The sampling and measurement system consists of the following components:

- Heated probe;
- Heated filter;
- Heat-traced Teflon® sample line;
- Teflon® coated, heated-head sample pump;
- FTIR spectrometer; and
- QA/QC apparatus.

The following Figure 5.1 illustrates the FTIR sampling and measurement system. In operation at any source, the sample is continuously extracted from the stack through the heated probe. Sample gas is then sent into a heated filter assembly, which will remove any particulate matter from the sample stream to protect the remainder of the sampling and analysis system. The probe liner and filter body are made of glass, and the filter element is polytetrafluoroethylene. In addition to providing an inert surface, the glass filter holder allows the operator to observe the filter loading during sampling operations. The probe and filter are contained in a heated box, which is mounted on the stack and maintained at a temperature of 250 °F.

After passing through the filter assembly, the sample gas is transported to the FTIR spectrometer by a primary heat-traced PTFE sample line maintained at 250 °F driven by a heated- PTFE head sample pump maintained at approximately 204° C (400° F). The sampling flow rate through the probe, filter, and sampling line is a nominal 20 standard LPM. Sample gas then enters an atmospheric pressure heated PTFE distribution manifold where it is sent to the FTIR spectrometer via a slipstream flowing at 9 LPM. Another slipstream from this manifold supplies sample to the oxygen analyzer for EPA Test Method 3A analyses. Excess sample gas not used by instruments is vented to atmosphere.

FTIR spectrometer sample gas is taken from the distribution manifold by a secondary heated PTFE head sample pump maintained at approximately 204° C (400° F) and directed into the FTIR sample cell maintained at 185° C (365° F) for real-time analysis. The cell is made of nickel-plated aluminum, with gold-plated glass substrate mirrors and potassium chloride windows. Exhaust gas from the cell is vented to the atmosphere.

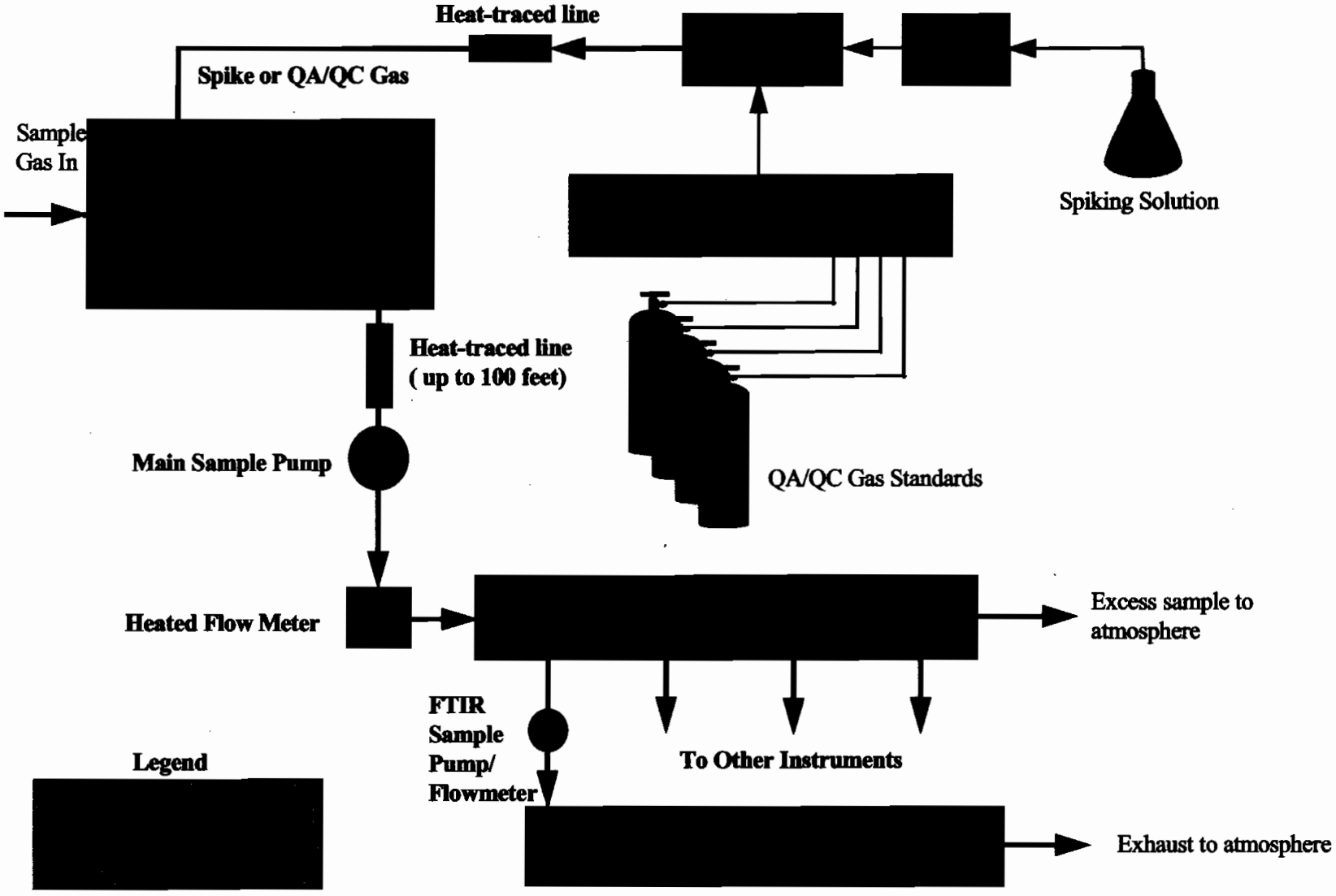


**Figure 4.2**
**FTIR Sampling and Measurement System**

### *4.6.8 Preparation for Sampling*

Before commencement of daily sampling operations, the following tasks will be carried out:

- System leak check;
- Measurement of FTIR background spectrum;
- Instrumental QC; and
- Sampling and measurement system QC spike run.

Detailed descriptions of these tasks are presented in the paragraphs below.

The heated sampling lines, probes, and heated filter will be positioned at the inlet and outlet locations. All heated components will be brought to operating temperature, and a leak check of both inlet and outlet sampling systems is performed. The leak check will be performed by plugging the end of the probe and watching the main sample flow meter to see that the value goes to zero.

A background spectrum is measured using zero air or zero nitrogen through the cell. Next the QC gases are measured by flushing the cell and they must agree to within a percentage of target value. The QC gases used for this program include (with acceptance criteria):

- Carbon monoxide (CO) used for frequency calibration. Carbon monoxide is directly injected into the sample cell to measure photometric accuracy, validity of the non-linear correction algorithm and serve as a frequency (i.e., wavelength) calibration. Acceptable limits for CO standard analysis are ±6 percent of certified concentration; and
- Methane/nitric oxide/carbon dioxide mixture, used for overall system performance check (calibration transfer standard) (acceptance limits are ±6% of the certified concentration).

These two mixtures are typically combined into one mixture. The gas standards are also known as calibration transfer standards, as described in EPA Test Method 320.

The sampling and measurement system spike test will be used to perform validation and directly challenge the complete system and provide information on system accuracy and bias. Dynamic analyte spiking involves injecting a known concentration of spike analyte at the probe exit and looking for an appropriate instrument response. Formaldehyde will be used as a surrogate for all target analytes. Formaldehyde is selected as the surrogate due to its potential difficulties in sampling. While this procedure can be performed for $NO_x$ and CO, experience has shown that the direct instrumental challenges are sufficient for those species. While it is certainly possible to perform spikes for $NO_x$ and CO, this would add to the cost of the program by obtaining an additional gas standard containing $NO_x$, CO and a sulfur hexafluoride tracer (to determine dilution) as well as approximately 30-45 minutes per day extra to perform the spikes before and after the day's testing. The standard must contain 10 times the usual concentration of the target species because the spike gas will be diluted by at least a factor of 10, according to EPA Method 320.

This test is conducted to satisfy the requirements set in EPA Test Method 320. Section 6, Equipment and Supplies, of Method 320 gives a description of the dynamic spiking apparatus. FTIR has been validated for the compounds listed in Section 6.1 of this test protocol.

The FTIR spiking procedure used will be the following:

- Measure native stack gas for a 3 minute period (i.e., 3-1 minute samples);
- Start spike gas flow into sample stream, upstream of the heated filter;
- Let system equilibrate for at least 2 minutes;
- Measure spiked sample stream for 3 minutes (i.e., 3 - 1 minute samples); and
- Turn off spike gas flow.

The above procedure will produce 3 spiked/unspiked sample pairs. Spike recovery and relative standard deviations for 3 spiked/unspiked sample pairs will be computed from the procedure given in Sections 8.6.2 and 9 of EPA Method 320. The recovery must be 70-130% for the system to be considered acceptable for testing.

The spiked/unspiked pairs will not be recorded simultaneously, because only one FTIR system will be available for this test program. This procedure should produce acceptable results because previous experience indicates that this type of source is very stable for a given operating condition.

### *4.6.9 Sampling and Analysis*

FTIR sampling will be performed simultaneously with EPA Test Method 3A and ISO Method 8178 (particulates) during the testing. The start and stop times of the PM method will be coordinated with the FTIR operator, so that FTIR data files can be coordinated with method 8178 start and stop times. FTIR sampling will be accomplished using a heated transfer line.

Typical FTIR operating conditions are shown below. These parameters provide the detection limits given previously in section 5.6. Some of these parameters are sample matrix dependent.

**Table 4.5**
**Typical FTIR Operating Parameters**

| Parameter | Value |
|---|---|
| Spectral Range ($cm^{-1}$) | 400 - 4000 |
| Spectral Resolution ($cm^{-1}$) | 0.5 (or better) |
| Optical Cell Path length (m) | 3.4 (variable -- 1-10) |
| Optical Cell Temperature (°C) | 185 |
| Sample Flow Rate (liters/minute) | 9 (3.0 optical cell volumes/minute) |
| Integration Time (minutes) | 1 (Average of 43 spectra) |

Sample flow rate will be determined by the data averaging interval and FTIR spectrometer sample cell volume. A minimum of 3 sample cell volumes of gas must flow through the system to provide a representative sample during a single integration period. Typically, a 1 minute

averaging period with a 3 liter volume sample cell gives a minimum flow rate of 9 LPM. Typically a flow rate of 20 standard LPM is used to accommodate the FTIR and EPA Test Method 3A instrumentation on-site, and to minimize sample residence time in the sampling system.

The temperature of all sampling system components will be at a minimum of 250 °F to prevent condensation of water vapor or other analytes in the sampling system. Actual sampling system operating temperatures will be determined before start of testing. The FTIR sample cell temperature will be maintained at 365 °F (185 °C) to ensure that condensation of high-boiling point analytes on the cell optics is minimized.

FTIR sample cell pressure will be monitored in real-time in order to calculate analyte concentration in parts-per-million. The cell is normally operated near atmospheric pressure with the cell pressure continuously monitored.

Stack gas temperature will also be monitored to provide information on potential sample analyte condensation in the sampling system. If the stack gas temperature is higher than the lowest sampling system component temperature, then an assessment by the spectroscopist or field team leader must be made whether any analytes of interest may condense within the sampling system, resulting in measurement bias.

Sampling probe location will be determined by the requirements set in EPA Method 1 in terms of duct diameters upstream and downstream of disturbances. Sampling and analysis procedures are straightforward for a single-source measurement. Once QA/QC procedures have been completed at the beginning of a test day, the sample will be allowed to flow continuously through the FTIR spectrometer cell and the software will be instructed to start spectral data collection. The spectrometer collects one interferogram per second and averages a number of interferograms to form a time-integrated interferogram. Typical averaging times range from 1 to 5 minutes. The interferogram is converted into a spectrum and analyzed for the target analytes. After spectral analysis, the spectrum is stored on the computer and later permanently archived. Spectral data collection is stopped after a pre-determined time, corresponding to a "run". Typical runs will be 1 hour long, giving 60 1_minute averaged points for each target analyte. At the end of the test day, the end-of-day QA/QC procedures are conducted.

Correction of all target analyte (except water) concentrations to a dry basis will be made using the following equation:

$$\text{Dry} = \frac{\text{Wet}}{1-(\text{H20}/100)}$$

Where:

Dry = Corrected dry concentration of the target analyte;
Wet = Measured concentration of the target analyte on a wet basis, at a specific point in time;
$H_2O$ = Corresponding measured concentration of $H_2O$ (in percent).

Before any testing is started at a given site, an initial "snapshot" of the stack gas is taken with the FTIR measurement and analysis system to determine the true sample matrix. If any target

analytes are present at significantly higher levels than expected, adjustments will be made to the cell path length and/or the spectral analysis regions used for quantitative analysis. These adjustments will minimize interferences due to unexpectedly high levels of detected analytes.

FTIR method performance is gauged from the results of the QA/QC procedures given in Section 9, Quality Control, of EPA Test Method 320. Acceptable spiking tests will meet acceptance criteria of 70 to 130 percent recovery. The acceptable instrument diagnostic and system response check accuracy will be within ± 6 percent of target. Acceptable system response check precision will be 6 percent RSD.

Quantitative analysis is performed by a mathematical method called multi-variate least squares (commonly known as Classical Least Squares or CLS). CLS constructs an optimized linear combination (or 'fit') of the reference spectra to duplicate the sample spectrum, utilizing the Beer-Lambert Law. The Beer-Lambert Law states that the absorbance of a particular spectral feature due to a single analyte is proportional to its concentration. This relationship is the basis of FTIR quantitative analysis. The coefficients of each compound in the linear fit yield the concentration of that compound. If it is found that the quantitative analysis of a given compound responds non-linearly to concentration, a calibration curve is developed by measuring a series of reference spectra with differing optical depths (concentration times path length) and using them in the linear fit. Low molecular weight species such as water vapor and carbon monoxide require non-linear correction, possibly even at levels as low as 100 ppm-meters (concentration times path length). Analytes greater than 50-60 amu molecular weight usually do not require non-linear corrections. An experienced spectroscopist can determine whether non-linear corrections are necessary for an analyte in a given source-testing scenario.

The SI validated spectral database includes the compounds shown below. These spectra were validated in the laboratory at a cell temperature of 185° C against certified gaseous standards. Any compounds identified in the stack gas and not included in the SI database can be quantified if necessary after subsequent laboratory reference spectrum generation.

**Table 4.6**
**Available Reference Compound FTIR Spectra [a]**

| | | |
|---|---|---|
| 1-butene | chlorobenzene | methylene chloride |
| 1,3-butadiene | *cis*_2_butene | *n*_butanol |
| 2-methylpropane | cyclohexane | *n*_butane |
| 2-propanol | cyclopentane | *n*_pentane |
| 2-methoxyethanol | cyclopropane | nitric oxide |
| 2-methyl-2-propanol | ethane | nitrogen dioxide |
| 2-methylbutane | ethylbenzene | nitrous oxide |
| 4-vinylcyclohexane | ethylene | *o*_cresol |

| | | |
|---|---|---|
| Acetaldehyde | formaldehyde | *o*_xylene |
| acetic acid | hexanes | *p*_cresol |
| acetone | hydrogen fluoride | *p*_xylene |
| Acetylene | hydrogen chloride | phenol |
| acrolein | isobutylene | propane |
| ammonia | *m*_xylene | propylene |
| benzene | *m*_cresol | styrene |
| carbon monoxide | methane | sulfur dioxide |
| carbon dioxide | methanol | toluene |
| carbonyl sulfide | methyl ethyl ketone | *Trans*-2-butene |
| | | water vapor |

[a] Spectra were collected at a cell temperature of 185° C.

### *4.6.10 FTIR Analytical Uncertainty and Detection Limits*

FTIR analytical uncertainty for each analyte will be reported in real-time by the FTIR quantitative analysis software. After each run, the estimated detection limits for each analyte of interest can be computed. These real-time calculations exceed the requirements set in Method 320, since they are actual values in the presence of the real sample matrix, not estimates as computed in the method.

### *4.6.11 FTIR Method Data Review Procedures*

The following procedure will be conducted to review and validate the FTIR data.

*Post-test Data Review procedure (on-site)*

1. Examine the concentration vs. time series plot for each compound of interest, and identify regions with the following characteristics:
   - sudden change in concentration;
   - unrealistic concentration values;
   - significant changes in 95 percent confidence intervals reported by software; and
   - sudden increase of noise in data.
2. Select representative spectra from the time periods indicated from Step 1.
3. Subtract from each representative spectrum chosen in Step 2 a spectrum, which was taken immediately prior in time to the indicated time region.
4. Manually quantitate (including any non-linear corrections) for the species in question and compare the result to the difference in software-computed concentrations for respective spectra.

5. If concentration values in Step 4 do not agree to within 5 percent, determine whether the difference is due to a recoverable or non-recoverable error.

6(i). If the error is non-recoverable, the spectra in the indicated time region are declared invalid.

6(ii). If the error is recoverable, and time permits, determine possible source(s) of error and attempt to correct. If time is critical, proceed with measurement. If correction is achieved, conduct QA/QC checks before continuing.

7. Determine the peak-to-peak scatter or the root mean square (RMS) noise-equivalent-absorbance (NEA) for the representative spectra.

8. If the NEA exceeds the limits required for acceptable detection limits, the spectra in the time region are declared invalid (due to non-recoverable error).

9. Data found invalid are subject to re-measurement.

*Final Data Review (off-site)*

The procedures for final data review include those given above; however, if a non-recoverable error is found during this phase, the data are considered invalid. In addition, the following procedures will be carried out by the spectroscopist to perform a final data validation:

1. If any recoverable data errors are detected from the procedure, determine the cause and perform any necessary corrections.
2. For analytes which were not detected or detected at low levels:
   i. Estimate detection limits from validated data;
   ii. Check for measurement bias.

### *4.6.12 FTIR QA/QC Procedures*

The FTIR QA/QC apparatus will be used to perform two functions:

- Dynamic analyte spiking; and
- Instrumental performance checks.

Dynamic analyte spiking is used for quality control/quality assurance of the complete sampling and analysis system. Dynamic spiking is continuous spiking of the sample gas to provide information on system response, sample matrix effects, and potential sampling system biases. Spiking is accomplished by either:

- Direct introduction of a certified gas standard; or
- Volatilization of a spiking solution.

Certified gas standards are preferred due to simplicity of use, but many target analytes cannot be obtained as certified gas standards, and must be spiked using standards generated by volatilized solutions.

Gaseous spiking is carried out by metering the spike gas into the sample stream at a known rate. Spike levels are calculated from mass balance principles. When certified gas standards are used, a dilution tracer, such as sulfur hexafluoride, is used to directly measure the fraction of spike gas spiked into the sample. This technique can be used instead of mass balance calculations.

FTIR method performance is gauged from the results of the QA/QC. EPA Test Method 320 instructs the user to determine the percent spike recovery of 3 pairs of spiked/unspiked samples. EPA Test Method 320 acceptance criterion is 70 to 130 percent recovery for the three pairs of samples. The acceptable instrument diagnostic and system response check accuracy will be within ± 6 percent of target. Acceptable system response check precision will be 6 percent RSD.

## 4.7 Sampling Locations

Sample locations were selected based on obtaining the most representative samples by meeting the requirements of EPA Method 1, *Sample and Velocity Traverses for Stationary Sources*. As indicated in Section 4.0, a stratification check at the ferry engine sampling location will be performed prior to commencement of testing to confirm the suitability of the sample location. The small diameter of the bus exhaust system precludes this test for the bus.

### *4.7.1 Bus*

Downstream of the turbocharger a special collar / stack extension section will be installed to accommodate both the particulate and FTIR (heated) sampling probes.

### *4.7.2 Ferry*

In engine room, five (5) pipe diameters downstream of the turbocharger outlet.

## 4.8 Site Requirements

Sample ports will be designed, fabricated and installed during pre-test set-up and prior to the mobilization of the emissions laboratory. The facilities will provide either 240 volts at 40 amperes (single phase) or 480 volts at 20 amperes (single or three-phase) power at each engine location.

The mobile laboratory will be located adjacent to the bus and in the case of the ferry will be set-up near the entrance to the engine room on the main deck so that no more than 100 feet of heat-traced sample line will be required for the FTIR sampling train.

It will also be necessary for the bus and ferry operating personnel to assist with starting, stopping and normal operation of the engines as required during the test program.

## 4.9 Quality Assurance Program

The quality assurance effort to be implemented as part of this test program will incorporate both quality assurance and quality control. Quality control (QC) is a system of routine technical activities implemented by the project team personnel to measure and control the quality of the data as it is collected and manipulated. QC activities include technical reviews, accuracy checks, and the use of standard procedures for data collection, analysis, and reporting. Quality assurance includes those activities that provide an independent assessment of a project or project tasks, including quality control functions. The Quality Assurance Coordinator assigned to this project will be responsible for coordinating the development and execution of QA/QC activities in all phases of the project and will supervise and check data collected from the Method 8178 equipment as well.

The Seaworthy project team will conduct all QA/QC procedures specified in the EPA test methods.

## 4.10 Safety

### *4.10.1 Responsibilities*

This section of the field test plan describes the general health and safety requirements for field work. Test personnel will also abide by all safety measures administered by the facility.

#### *4.10.1.1 On-Site*

The person responsible for implementing and ensuring compliance with the health and safety requirements during the on-site testing is the FTIR Project Manager. All supervisors are responsible for ensuring that assigned employees and their subcontractors under their direction comply with the requirements. All employees and subcontractors on-site are responsible for complying with the requirements and those of the host facility. Each Test Team member reads and signs a copy of the safety plan prior to arrival on-site.

#### *4.10.1.2 Authorities*

The Project Manager and Test Team Leaders will have the authority to upgrade the requirements of this plan if, in either's judgment, such adjustments are necessary and will complete the following Project Health and Safety Sign-Off Sheet prior to the initiation of the testing program.

The designated representative at the test facility (ferry or dynamometer operator) also has the authority to impose additional constraints or to waive particular facility Health and Safety restrictions.

# Project Health and Safety Sign-Off Sheet

**Project Number/Title:** _____

**Location:** _____

**CHECK ONE**

☝ **NO PROJECT SPECIFIC HEALTH AND SAFETY PLAN REQUIRED**

**RATIONALE:** _____
_____
_____
_____

**Project Manager:** _____ **Date:** _____
**Health and Safety Officer:** _____ **Date:** _____

☝ **PROJECT SPECIFIC HEALTH AND SAFETY PLAN REQUIRED**

**CERTIFICATION:** Spectral Insights and its subcontractors will conduct the activities specified in the contract and/or work assignment in accordance with the approved Health and Safety Plan unless instructed otherwise by the authorized Health and Safety Officer.

I certify that I have read, understood, and if applicable, approved the Health and Safety requirements in the Health and Safety plan cited above.

**Project Manager:** _____ **Date:** _____
**Health and Safety Officer:** _____ **Date:** _____
**Project Team Members:**

_____ **Date:** _____
_____ **Date:** _____
_____ **Date:** _____
_____ **Date:** _____
_____ **Date:** _____
_____ **Date:** _____
_____ **Date:** _____

**Project Manager:** Distribute completed, signed copies of this form to:
Project File

**Figure 4.3**
**Project Health and Safety Sign-off Sheet**

### *4.10.2 Site Entry*

At the start of each day of sampling, the on-site team leader or his designee informs the plant contact of the test crew arrival.

### *4.10.3 Hazard Analysis*

#### *4.10.3.1 Physical Hazards*

The physical hazards expected to be encountered in performing the sampling tasks are discussed below.

Falls

If test personnel are required to work on sampling platforms during the sample collection phase of this project, the platforms and their access ladders present fall hazards. All platforms will have handrails and safety harnesses will be used as necessary.

Heat

Source sampling tasks involve collecting samples from hot flue gases. The ducts covering these gases and the probes used to sample them present the hazard of thermal burns. It is expected that the stack gas temperature will exceed 500°F. Working in elevated ambient temperatures has the potential for causing heat stress. Regular work breaks will be enforced as the ambient working conditions dictate. Ambient temperatures are expected to not exceed 95°F during the daytime.

Electrical

The use of electrical equipment, particularly portable equipment and extension cords, often poses electrical shock hazards. Furthermore, work at heights may require working in close proximity to power lines.

Noise

The potential for overexposure to noise will exist at locations near the engines.

Fire

Flammable reagents are the primary fire hazard. The facility may also have areas where ignition sources are prohibited.

#### *4.10.3.2 Chemical Hazards*

In addition to the analytes expected in the flue gas, several chemicals are used for QA/QC purposes. The table below contains a list of the known chemical hazards.

**Table 4.7**
**Chemical Hazards**

| Exposure Location | Chemical |
|---|---|
| Sample Collection | Acetone |
| | Carbon dioxide |
| | Carbon monoxide |

| Exposure Location | Chemical |
|---|---|
| | Formaldehyde |
| | Methane |
| | Nitric oxide |
| | Total mass particulate |

The Material Safety Data Sheets (MSDS) for chemicals kept at the test location are listed below:

- Acetone;
- Carbon dioxide;
- Carbon monoxide;
- Methane;
- Nitric oxide;
- Nitrogen, compressed; and
- Nitrogen, liquefied.

Ambient air monitors are maintained in the mobile laboratory to monitor the following:

- PPM levels of $SO_2$ and NO;
- Percent $O_2$;
- PPM levels of CO; and
- Percent lower explosive limit (LEL).

### *4.10.4 Hazard Abatement*

This section describes the general requirements for hazard abatement.

#### *4.10.4.1 Physical Hazard Abatement*

Fall Prevention

Inspection of the scaffolding and platforms is required before any are used. If the sampling platforms are unstable or structural defects are detected, measures must be taken to correct the problem prior to platform loading. When accessing elevations, no more than one person is to climb access ladders at a time.

Burn/Heat Stress Prevention

Hot sampling probes are handled only by persons wearing heat-insulating gloves. Personnel monitor each other for signs of heat stress: profuse perspiration, cool or pale skin, dizziness, or nausea. Affected individuals should rest in a cool area and sip cool water or electrolytes. If symptoms of heat stroke, such as hot, dry skin or unconsciousness appear, obtain medical attention immediately.

Electrical Shock Prevention
Field crewmembers should be constantly aware of the position of power lines and cords relative to themselves and their electrical equipment in use to prevent electric shock. All equipment that is not required to operate overnight is left unplugged. The use of power strips with multiple outlets is limited to strips with internal circuit breakers. All cord connections are secured so there is no direct stress on joints or terminal screws. All electrical sampling equipment is properly grounded to reduce electrical hazards. The cord connections are manually disconnected from the power source prior to any work that allows direct access to potentially energized parts.

Noise Exposure Control
Test personnel wear hearing protection when working in areas that are either designated as requiring protection or in areas where they must raise their voices to converse with someone no more than three feet away. Earplugs are provided to all sampling personnel.

Fire Prevention
In areas where flammable materials are stored or in use, no ignition sources, including smoking, are permitted. Personnel will follow the facility's safety requirements to prevent fires in other areas.

Dust
In areas where process dust might cause eye and/or respiratory problems, all sampling personnel will wear dust masks and sealed goggles, as necessary.

4.10.4.2 Chemical Hazard Abatement

Personal Protective Equipment
All on-site test team personnel will, at a minimum, wear:

Hardhat;
Safety glasses;
Safety shoes or boots; and
Work clothing (long-sleeved shirts), if required.

Beyond the personal protective equipment routinely required as listed above, the personnel on the following tasks will wear additional gear as specified below.

Source Samplers
Under general sampling conditions, there is an opportunity for exposure to contaminants transported in the flue gases. Therefore, during set-up, breakdown, or under any other conditions where exposure may result, personnel wear full-face respirators with organic vapor/HEPA filter cartridges.

Work Practices
Compressed gases will be used during the sampling and analysis phase of this program. No protective equipment is required, but care will be exercised when handling, shipping, connecting and disconnecting gas lines to the cylinders.

# 5.0 TEST EQUIPMENT SPECIFICATIONS

## 5.1 Objective

The objective of this section is to identify and describe the principal test equipment for use in the Phase II program and justifies decisions to use particular devices with regard to accuracy and robustness.

## 5.2 Equipment

### *5.2.1 Gaseous Emissions Measurement*

Measurement of oxygen will be made using a paramagnetic analyzer as described below. All other gaseous exhaust emissions constituents will be measured using an FTIR analyzer as configured by Spectral Insights.

#### *5.2.1.1 Oxygen Analyzer*

The oxygen analyzer will be a California Analytical Model 100P, which measures the paramagnetic susceptibility of the sample gas by means of a magneto-dynamic type measuring cell. The measuring cell consists of a dumbbell of diamagnetic material, which is temperature controlled electronically at 50° C. The higher the oxygen concentration, the greater the dumbbell is deflected from its rest position. This deflection is detected by an optical system connected to an amplifier. Surrounding the dumbbell is a coil of wire. A current is passed through this coil to return the dumbbell to its original position. The current applied is linearly proportional to the percent oxygen concentration in the sample gas. This concentration is displayed on a digital panel meter.

The 100P is a rack-mounted paramagnetic analyzer that provides two types of analog outputs: (1) Current (0-20 or 4-20 mA) or (2) Voltage (0-1 or 0-10 volts). The 100P requires a conditioned sample. Sample conditioning is achieved with a gas chiller (Apex Instruments).

The analyzer 4-20 mA output is fed to a 16-bit ADC system (Strawberry Tree) for storage and display. Data is collected every 2 seconds and averaged for typically 1 minute. Digital filtering algorithms (by Spectral Insights) are used to process data.

**Table 5.1**
**$O_2$ Analyzer Specifications**

| | |
|---|---|
| Concentration Ranges | 0-5, 0-10, 0-25 percent |
| Response Time (90 percent) | 2 seconds |
| Linearity | Better than 1 percent |

#### *5.2.1.2 FTIR Analyzer*

The Spectrometer to be utilized is a Thermo-Nicolet model Nexus 670. This is Thermo-Nicolet's research-grade, fully upgradeable FTIR spectrometer. The instrument is fitted with a 1 to 10 meter optical path length heated cell made by Infrared Analysis (Model 4-10) with custom

coupling optics by Spectral Insights. This cell allows the FTIR spectrometer to measure gas samples with sub-ppm sensitivity for many species.

Data collection is controlled by custom software (by Spectral Insights) that interfaces with the Thermo Nicolet OMNIC software. The custom software contains digital signal processing algorithms, which enable lower detection limits for some species.

**Table 5.2**
**FTIR Specifications**

| | |
|---|---|
| Spectral Range | 400 to 4000 wave numbers |
| Resolution | 0.5 wave number |
| Data collection rate | 1 spectrum per 1.2 seconds |
| Gas Cell Optical path length | 3.2 meters |
| Number of Compounds Measured | 10 or more, depending on application |
| Noise Equivalent Absorbance | $1 \times 10^{-5}$ (5 minute average) @ 2000 $cm^{-1}$ |

### *5.2.2 Particulate Sampling*

Two different types of partial dilution tunnel, particulate sampling systems were evaluated. The first was the SPC model 472 Smart Sampler manufactured by AVL. The second was the BG-2 system as manufactured by Sierra Instruments based on dilution tunnel technology licensed from the Caterpillar Engine Company. (See Appendices A, B, C, and D.)

Both systems offer (relative) portability and high accuracy. Final decision regarding which system to use will be based on pricing and availability at the time of testing.

#### *5.2.2.1 AVL SPC 472 Smart Sampler*

The AVL system offers excellent accuracy and the company has demonstrated extensive application experience with shipboard particulates testing in Europe. This model represents the third generation in the product's development, indicating a mature device. Meetings with representatives from AVL to discuss the current project at the March 2002 Society of Automotive Engineers conference confirmed the suitability for their device for the bus and ferry testing.

The complete system includes sample probe, dilution tunnel, filters, pumps, flow meters and a data acquisition system for real-time data logging.

#### *5.2.2.2 Sierra Instruments Model BG-2*

Sierra Instruments Inc. combined their expertise in the manufacture of precision flow meters with Caterpillar's micro-dilution tunnel design to create the BG-1/2 family of micro-dilution tunnel test devices. Similar to the AVL Smart Sampler, the BG-2 is a complete, modular engine test station including sampling equipment, the dilution pumps, flow meters, controls and a data acquisition program written in National Instruments Labview software. (Refer to Appendices E and F.)

### *5.2.3 Air Flow*

Due to the relatively small engine sizes concerned in the test program, and based on the requirement to obtain best possible accuracy, it was decided to utilize direct measurement of the inlet air flow in order to determine exhaust flow rate and ultimately mass emissions rates.

Based on a survey of the technical literature, including other marine engine test work performed by the USCG and MARAD, AETC selected the model 780S-EIA, Engine Inlet Airflow meter manufactured by Sierra Instruments was selected for this task (Appendices G and H).

This device is a direct indicating mass flow meter incorporated into an airflow conditioning body. The flow conditioner allows the meter to function accurately even in short runs of piping. Since it is a direct (thermal method) flow device, pressure and temperature corrections are not necessary.

For testing, the output signal from the transmitter will be connected to the data acquisition computer.

### *5.2.4 Fuel Flow*

Fuel flow will be measured on the supply and return lines of each test engine utilizing precision, positive displacement meters manufactured by KRAL (Appendix N). Net fuel consumption (pounds) will be summed with the inlet air mass flow to determine exhaust flow. The wide range flows coupled with excellent accuracy will permit the use of the same meter pair for both the ferry engine and the bus engine.

The meters will be the KRAL Volumeter model OMG in conjunction with KRAL's BEM 4U flow management and totalizing unit.

### *5.2.5 Shaft Torque*

Shaft torque will be measured on the Ferry to monitor engine power output. A reusable / removable strain gage collar system will be utilized. An analogue voltage output from the torque measuring signal conditioning unit will be brought into the data acquisition system. The system selected is the Wireless Data Corporation model 1625 (Appendix O). Due to the use of strain gages attached to parallel bars, the accuracy of the system exceeds that of shunt calibrated strain gages mounted directly to the drive shaft.

The system can also be moved to different shafts in order to compare the horsepower developed by each of the four different propulsion engines on the ferry.

### *5.2.6 Engine Communications*

Communication with the engines will be necessary for both tests, however, in the case of the bus, obtaining the duty cycle information will be of paramount importance to the representativeness of the emissions data.

Both engine types utilize an electronic governor and engine control module which can communicate, via a serial port or USB connection, to a laptop computer operating companion software.

*5.2.6.1 Detroit Diesel DDEC*

Of the two products, the DDEC system and software is vastly more capable, benefiting from years of development and use by the engine manufacturer. The DDEC system will be to obtain accurate duty cycle load profiles for the bus while riding the bus for approximately one-week of commuting.

The software permits monitoring and logging of all engine parameters for which a sensor is installed including all non-emissions engine parameters needed for the testing.

DDEC technical literature, including a list of diagnostic fault codes provides a clear summary of the amount and type of data available with the system and is presented in Appendices K and L.

*5.2.6.2 Cummins INSITE*

The Cummins software, "INSITE" is much simpler than that offered by Detroit Diesel, however, it will provide the basic engine data required including torque, fuel pump pressure and engine speed. (Refer to Appendix N.)

# 6.0 PHASE II SCHEDULE AND COST ESTIMATE

## 6.1 Objective

The objective of this section is to assess the effort required to plan, prepare, conduct and complete all activities necessary to accomplish comprehensive engine and exhaust emission pollutant characterization testing for a the passenger ferry and transit bus.

## 6.2 Summary of Phase II Scope of Work

The effort required to plan, prepare, conduct and complete all activities necessary to accomplish comprehensive engine and exhaust emission pollutant characterization testing for a transit ferry and bus is summarized below on a task-by-task basis.

**Task IA - Pre-Test Design and Preparatory Work:** This task will consist of the detailed design work that must be completed prior to mobilization of the test team. This effort includes such activities as design and fabrication of sampling ports, determination of inlet air system modifications required for the installation of combustion airflow metering equipment, design and fabrication of brackets and piping modifications for fuel oil supply and return meters, etc.

**Task IB - Automotive Emissions Data Survey:** Work on this task includes the review and analysis of existing emissions data for the purpose of developing comparable parameters for automobiles in the same commute service as the bus and ferry.

**Task II - Bus Pre-Test Data Collection:** To develop a representative transit bus passenger load profile, a Seaworthy project team technician will ride the bus for one week, equipped with a laptop computer connected to the on-board engine control system. At completion of the week of data collection, the technician and an engineer will review the data and determine the final load profile to be utilized for bus emissions factor computation.

**Task III - Emissions Testing of Bus:** This task will address controlled emissions test of the bus engine while in operation on the chassis dynamometer.

**Task IV - Ferry Pre-Test Set-up:** All work necessary for preparing the ferry for the emissions testing, including the installation of the fuel oil and air flow meters, installation of the shaft torque meter and installation of sampling probe penetrations into the exhaust system will be completed as part of this task. In addition, all required test equipment will be brought aboard. Test equipment checkout and initial calibration will also be performed at this time.

**Task V - Emissions Testing of Ferry:** Emissions testing of the ferry engine will consist of obtaining specific emissions data for a typical round trip. Up to three (3) emissions reduction methodologies will also be tested, including alternative diesel fuels (bio-diesel and/or fuel water emulsions).

**Task VI - Summary Report:** After thoroughly and precisely reducing and analyzing all collected emissions and related data to engineering units, the Seaworthy team will prepare a detailed summary report. Appendices of the report will include all raw data and instrumentation calibration information. The report will describe the test methods utilized, present an analysis of

the errors (if any) for all measurements taken, discuss the test results and make recommendations for future follow-on test work, if necessary. In addition, the efficacy of any emissions reduction methodologies tested aboard the ferry will also be addressed.

### 6.3 Phase II Schedule

For the in-situ testing portion of the Phase II effort, as shown in Figure 3-1, the total elapsed time is approximately 60 days. It is anticipated that an additional 60 days will be added to the proposed transit bus and ferry engine emissions test period to address all the other administrative and contractual program requirements; to provide some margin in the schedule in case of unforeseen delays in obtaining test equipment or consumables; and to address any slippage in the availability of the transit bus or ferry for testing.

### 6.4 Phase II Cost Estimate

Table 4.1 presents a categorized breakdown of anticipated costs to accomplish the in-situ transit bus and ferry engine emissions testing work scope outlined previously.

**Table 6.1**
**Phase II Cost Estimate**

| | |
|---|---|
| 1. Labor (SSI, AETC, Spectral Insights) | $ 127,710 |
| 2. Test Equipment (F.O. meters, torsion meter, air flow meters, dynamometer and dilution tunnel, rental, etc.) | $ 29,770 |
| 3. Other Project Related Costs (fuel oil, laboratory materials, travel/equipment, transportation, etc.) | $ 47,200 |
| **Total:** | $204,680 |

It should also be noted that the above, more precise Phase II cost estimate is approximately 12% higher than the original estimate submitted with our Phase II proposal to CCDoTT in November 2001. This difference is due to increases in fuel and laboratory materials and related consumable costs that more than offset the lower total labor cost shown above when compared to our initial labor cost estimate as proposed in November 2001. The costs shown above are also based on the assumption that all testing will be completed during the first quarter of Fiscal Year 2003.

## 6.5 Inventory of Harmful Emissions and Regulations

Each category of harmful exhaust emissions represents unique threats to health and the environment. However, one of the problematic issues in restoring air quality is that proven methods of reducing one harmful component of engine exhaust can often increase the emission of another. As one example, tests conducted to date on biodiesel fuel indicate that it reduces harmful particulate emissions, but increases equally damaging emissions of NOx. The inventory of harmful diesel engine exhaust emissions to be reduced and the threat(s) each imposes can be briefly described in roughly descending order of importance as follows:

1. *Oxides of Nitrogen (NOx)* have local, regional, and global effects. They cause climate change, atmospheric acidification, increased ground level ozone (and consequent respiratory diseases), and formation of toxic compounds. In addition, NOx compounds have been identified as precursors to toxic particulate. The California Air Resources Board estimates that heavy duty mobile engine sources generate 40 percent of NOx emissions statewide, chiefly from trucks, aircraft, locomotives, and marine vessels.
2. *Particulates, or Particulate Matter (PM)* have local effects. They are characterized as solid particles primarily less than 2.5 microns in diameter. PM contributes to smog, reduces atmospheric visibility and is a pulmonary carcinogenic. When inhaled and lodged in the lung, PM can cause cancer. Particulate also collects on and discolors buildings, monuments, bridges, and other structures.
3. *Oxides of Sulfur (SOx)* have both local and regional effects. They cause atmospheric acidification and form toxic compounds, which precipitate out into lakes, streams and reservoirs as acid rain.
4. *Carbon Dioxide* ($CO_2$) has a global effect. It is a leading greenhouse gas, believed to contribute to trends of global warming.
5. *Hydrocarbons (HC)* have local and regional effects. They contribute to ground level ozone and consequent respiratory disease.
6. *Carbon Monoxide (CO)* has a local effect. It is toxic to breathe.

Until the 1980's, engine manufacturers concentrated development efforts on continuously improving fuel economy, reliability, power-to-weight ratio, durability, life cycle economy, and overall performance. Little attention was paid to exhaust emissions because they were not a legally recognized problem. Although emissions were largely ignored during this period of advancement in engine thermal efficiency, reduced emissions was a fortunate, but unintended consequence. The improved fuel economy that diesel engines would achieve has brought a significantly beneficial change to global air quality. Because diesels burn the least fuel per unit of power output, diesel engine exhaust contains much lower quantities of toxic and global warming CO and $CO_2$ per unit of power output than any other type of internal combustion engine. In short, because of fundamental differences in fuel consumption, a modern automotive spark ignition engine or gas turbine will tend to burn more fuel and emit from 10 to 30 percent more CO and $CO_2$ than a comparable diesel engine developing the same power.

As scientific knowledge of air quality problems increased, the need to legally regulate engine emissions became apparent. The nationwide fleet of automotive (spark ignition) engines was

quickly recognized to have the most numerous point sources of air pollution. These engines were the first to face regulation, fuel (gasoline) reformulation, and design improvements to reduce harmful emissions. Exhaust catalysts became standard equipment and computer-controlled fuel injection systems superceded the mechanical carburetor, enabling substantial improvements in automotive exhaust emissions. The reformulation of gasoline and steady retirement of older automobiles, combined with the required exhaust gas catalytic converter caused a significant improvement in vehicular emissions by the end of the twentieth century.

The second most numerous category of mobile equipment to be regulated was the diesel-powered highway vehicle. The first effort in the U.S. to improve and reduce highway diesel engine emissions was the introduction of low-sulfur highway diesel fuel in 1993. Subsequent engine design improvements such as electronic fuel injection and exhaust gas recirculation began to appear on new highway vehicle engines, further improving the emissions profile. A major stumbling block on the road to capital improvements of the nation's trucking fleet has been the inherent robustness of diesel-powered trucks and buses on the roadways. Truck and bus drive trains are significantly costlier than automobiles and are designed for decades of reliable service. The greater durability and cost of these engines makes for slow retirement of generations of vehicles, which are pollution sources. The automobile fleet, on the other hand, with its short life span is quickly updated and replaced with more efficient, cleaner-burning engines. Nevertheless, new highway diesel engines have been developed and are now available with emission characteristics that are 40 percent less polluting than earlier models.

The most recent category of mobile source emissions to be regulated is the off-road diesel engine. These comprise the diverse inventory of railroad locomotive, mining, earth moving, heavy construction equipment, marine container terminal equipment, general seaport cargo handling equipment, and ship engines. Engines in these categories, while comparatively few in number and often subject to lower duty cycles than their highway counterparts, are now the focus of increased regulatory scrutiny. The timing and scope of anticipated international regulations on marine engine emissions is still being debated. The Montreal Protocol of 1987, amended in London in 1990, and the Kyoto Protocol of 1997 have largely framed the debate. International Maritime Organization (IMO) MARPOL (marine pollution) regulations are effectively motivating engine manufacturers and U. S. government regulatory agencies towards lower engine emissions. MARPOL 73/78 Annex VI Marine Diesel Engine Requirements sets worldwide limits on engine NOx and SOx emissions.

U.S. federal and state agencies are simultaneously focusing more on the adverse impacts to air quality by marine diesel engines and are working to improve emission standards. In 1998, the U.S. Environmental Protection Agency proposed a set of emission standards for all diesel engines rated from 50 to 750 horsepower. In 1999 the E.P.A. published NOx, HC, CO, and PM emission standards for commercial marine engines rated greater than 50 horsepower. These standards are scheduled to be effective in 2004, 2005, and 2007, depending on engine cylinder displacement. Engine manufacturers expect to meet these standards with new production designs. Meanwhile, the inventory of existing marine engines with more harmful emissions characteristics continues to constitute a serious air quality problem. The two pollutants believed to require the most rapid reduction are NOx and PM.

# 7.0 EMISSION REDUCTION TECHNOLOGY EVALUATION

## 7.1 Objective

The objective of this section is to review and analyze engine emission-reduction technologies that are best suited for incorporation in diesel engines and systems for use in passenger ferry applications.

## 7.2 Scope of Engines and Fuels Addressed

### *7.2.1 Recreational Boating*

With few exceptions, recreational watercraft are powered either by diesel- or gasoline-powered (spark ignition) engines. While prominent in recreational boating, gasoline fueled engines are virtually nonexistent within industrial marine applications. To date, excepting two-cycle outboard motors and engines on personal watercraft, recreational marine engines have been subjected to virtually no significant emission regulations. No recreational boating engines are included in the scope of this program element.

### *7.2.2 Deep Sea Vessels*

Diesel engines are the vastly dominant source of propulsion and auxiliary power aboard large oceangoing ships. The rare exceptions to this rule comprise either nuclear or oil/coal-fired Rankine steam-cycle plants, and gas turbine plants, or one of the above in the case of a liquefied natural gas (LNG) tanker, burning cargo boil-off for fuel. This program element does not address the emissions of any large seagoing ships. Deep-sea ships almost invariably operate on a variety of high-viscosity, heavy residual-fuel oils, which are outside the scope of this analysis.

### *7.2.3 Inland Waterway and Harbor Craft*

The remaining classes of vessels are diesel-powered inland waterway and harbor craft. This class of vessels operates on a much more restricted, typically more refined, range of fuels. This report addresses emissions from the passenger ferry, one segment among the inland waterway and harbor craft class of vessels. Power outputs for the typical high-speed diesel engines utilized in main propulsion and auxiliary engine applications in these vessels range from 150 to 3,000 brake horsepower (BHP). Passenger ferry engines have been designed to operate on distillate liquid fuel termed marine gas oil (MGO), the marine equivalent of standard California highway diesel fuel known as Number 2 diesel oil.

The standard California highway diesel oil is low-sulfur diesel fuel. MGO was once differentiated from low-sulfur highway diesel fuel by statutory limits that maintained a lower sulfur threshold for highway diesel fuel than for MGO. Low-sulfur highway diesel fuel was set apart from dirtier (MGO) fuels by use of a red-colored dye additive. Eventually, for economic and logistical reasons, MGO was folded into the much larger highway fuels market. Consequently, there is no difference between the fuels today, and MGO, too, is low-sulfur and dyed red. The diesel-powered ferry engines analyzed for this program will burn low-sulfur highway diesel fuel, the same as the bus engines burn, because that is the actual fuel used by each of these transit operations.

## 7.3 Marine Diesel Engine Emission Reduction Alternatives

A broad range of alternatives exists to reduce harmful marine engine emissions. Environmental advocates have endorsed most of these options at one time or another. The challenge posed by many technologies is that they are either too costly or are inconsistent with the safety, regulatory, and operational requirements of practical operating vessels. Many green concepts themselves are obstacles to plausible implementation such as solar-powered storage batteries, stored kinetic energy flywheels, the inconsistency of wind-power, the high cost, and the massive size-to-power ratios that many alternative prime movers offer, even in their best configurations. Many alternative, and presumably cleaner-burning marine fuels that have been promoted for ferry use, such as biodiesel and compressed or liquid natural gas, are likewise problematic for their high costs, safety, logistics, and other operating issues (such as the refitting of fueling, storage and engine systems for natural gas fuel). Some alternative fuel problems will be resolved in the future. In the near term, cost and technical obstacles are preventing a broader switch to alternative fuels in existing vessels.

The forecast for other advanced engineering concepts, in particular fuel cells, is likewise beyond immediate reach. The current and ten-year anticipated levels of development in fuel cell technology and comparably advanced energy sources (such as nuclear power) preclude their near term application to all but a few experimental vessels as restricted by fundamental laws of economics, physics, chemistry, and thermodynamics.

There are, however, practical alternative solutions available to reduce marine diesel engine emissions in the near term. These can be categorized under three general categories: feasible alternative fuels, replacement of older engines, and engine system modifications. A primary benefit of any practical cleaner-burning fuel is that its impact is immediate and universal, regardless of engine type or age. Whether or not engine replacement or modification may be economically practical, a successful fuel change is capable of delivering the most wide-ranging benefits and therefore should be considered a primary step to achieve lower diesel engine exhaust emissions.

### *7.3.1 Low Sulfur Fuels*

One of the first breakthroughs in diesel engine emission reductions was the U.S. introduction of the low-sulfur highway diesel fuel in 1993. Prior to this reformulation, the sulfur content of No. 2 diesel oil was approximately 5,000 parts per million (ppm) or roughly 0.5 percent. Low sulfur highway diesel fuel limits sulfur content to 2 percent of this number, or a maximum of 100 ppm. The use of low sulfur highway fuel, as mandated by Clean Air statutes, led to significant benefits for regional air quality, described below.

(1.) Engine emissions of acid rain-causing SOx were reduced 98 percent. SOx emissions occur commensurately with sulfur content of the fuel oil.

(2.) A less-noticed achievement was the small increases in engine performance per unit of fuel consumed. The drop in sulfur content increased the mole fraction of hydrocarbons in the fuel, which account for the superior properties of flame propagation and heat content in fuel oils. The total energy released from combustion of low sulfur fuel is therefore slightly greater than with pre-1993 No. 2 diesel fuel.

(3.) Engine wear dropped as much as 50 percent. Cleaner, sulfur-free combustion yielded lower engine wear and subsequent repair and maintenance costs. Much of the wear improvement is attributed to the absence of acidity that sulfur is known to form in the engine lubricating oil.

(4.) Another direct result of the cleaner combustion process was a small but measurable decline in toxic exhaust particulate matter (PM).

These improvements to air and equipment came with a temporary cost. The initial price of low-sulfur highway diesel fuel was approximately 5 percent greater than its higher-sulfur alternative. Once the oil refiners recouped their investment for the low-sulfur conversion, and as production and distribution of the new fuel matured, the early cost premium quickly disappeared. A second notable problem occurred with some of the older engines, as they sustained compatibility problems with some of the older-type rubber gaskets and seals. This problem, though predictable and readily corrected, is useful for future iterations of fuel reformulation. Engine owners and operators must first contact the original equipment manufacturer to verify that all propulsion components are will function with new fuel or other emissions-control devices. By 2006, industry is likely to use even lower sulfur fuel – 15 ppm vice today's "low sulfur" fuel of 100 ppm – as required by pending EPA regulations.

### *7.3.2 Emulsified Diesel Fuels*

Consideration of water emulsions in diesel fuel should first stipulate a low or ultra-low sulfur diesel fuel for the benefits discussed above.

The emissions improvement achieved by properly engineered fuel-water emulsification is universal and immediate, regardless of engine age or make. The primary benefit of water-fuel emulsions in diesel engines is a well-documented reduction in NOx emissions. NOx can roughly be lowered one percent for each percent (by weight) of water content in the fuel, up to a practical limit of 25 to 30 percent, depending on engine design and service profile. In cases of the largest-bore marine diesel engines, emulsions with up to 50 percent water content have been successfully used. This reduction is achieved by lowering the peak combustion temperature in the engine cylinders. NOx production is a cubic function of combustion temperature. Better fuel atomization and more complete combustion serve to offset any reduced thermal efficiency resulting from the quenching effect of water during the combustion process. The net impact on engine power development and fuel economy is minimal.

It is important to recognize that water contains no energy and, to the extent that water displaces fuel in the emulsion, the total volumetric flow of an emulsion will exceed the flow of unblended (pure) diesel fuel required to produce the same power. This means that it may be necessary to resize (enlarge) engine fuel system components, in particular injector port size, and water-storage tanks, to handle the increased volume of the emulsified fuel blend.

Vessel owners and operators have been reluctant to implement emulsified fuels because most engine manufacturers have been unwilling to extend warranties to cover engine operation on emulsified fuels. In large part, OEMs have felt no compulsion to include emulsions-operation under engine warranty when the propulsion market has overwhelmingly abided pure, unblended diesel fuel and its attendant higher emissions as acceptable. The engine warranty limitation has

been a simple matter of practical self-interest for OEMs. The pure-diesel-only paradigm must be overcome if emulsified fuel systems are ever going to take their deserved place in engine emissions-reduction technology. The gradual growth in successful land-based emulsified fuel applications indicates that emulsions are finally trending toward greater industrial acceptance and use.

There are two fundamental approaches to utilizing water-fuel emulsions, described below.

*7.3.2.1 Onboard Emulsification Systems*

This approach requires design and installation of a suitably sized fresh water storage tank, a piping system, an electric motor-driven fuel blender/agitator, an emulsifying surfactant chemical for use in low sulfur diesel fuels with water, and a control system to regulate fresh water flow into the blend. The blending control system must achieve minimum NOx emissions under variable operating conditions. Considerations for this system must address the initial capital investment, ongoing (but minimal) system energy consumption, system maintenance and repair costs (also very small), and availability of fresh water supply when refueling.

There are several advantages to onboard emulsification systems vice the loading of pre-blended emulsion fuels. Advantages of onboard blending include a vessel life-cycle savings in fuel costs, freedom from complications which might arise with the stability of pre-blended fuels during long-term storage, such as during vessel inactivation; roughly 25 percent higher fuel quantities per delivery, greater options for selecting fuel vendors, and the ability to blend fuel emulsions tailored for individual engine applications.

*7.3.2.2 Preblended Emulsified Fuels*

As the name implies this approach utilizes direct delivery of emulsified fuel to the vessel by tank truck. The blending is accomplished at a remote facility and the water-fuel emulsion is simply pumped into the vessel's fuel storage tanks for use. The Lubrizol Corporation, for example, has developed a proprietary blend of emulsified fuel called PuriNOx. PuriNOx contains a patented stabilizing additive to maintain the emulsion over prolonged periods of time.

There are several advantages of pre-blended fuel emulsions. The vessel owner/operator has no initial capital investment, nor an extra onboard (fuel) system to operate, maintain and repair, nor a need to acquire and store volumes of fresh water.

The disadvantages are slightly higher life-cycle costs for fuel, the potential for instability of the emulsion during extended storage periods, less flexibility in selecting the ratio of the fuel-water blend, restricted sources of fuel vendors, and roughly a 25 percent reduction in the volume of fuel (due to its displacement by water). The displacement issue equates to larger fuel tanks or more frequent refueling events.

### *7.3.3 Summary*

Operators of diesel-powered vessels can lower their fleet exhaust NOx emissions by as much as 25 to 30 percent for smaller-bore diesel engines and as much as 50 percent for the largest-bore diesel engines, by employing water-fuel emulsion technology. The first priority for bringing proven fuel-water emulsion technology to broader commercial application is to overcome the

existing proprietary, often parochial, resistance by many engine manufacturers to the acceptance of this innovation. Manufacturers' acceptance of emulsions is the critical step toward commercial application, which in many cases awaits the extension of warranties to cover engines using this technology.

The selection of onboard emulsion blending or bunkering with pre-emulsified fuel depends on several factors. In the case of pre-blended emulsion fuels, principal considerations include the availability of multiple suppliers of emulsion fuels for price competition; whether more frequent refueling is acceptable, or if the vessel's fuel tanks may be expanded to accommodate a greater volume of less energy-dense emulsion fuel to maintain the same range as operation on pure diesel oil. In the case of onboard blending of emulsion fuels, principal considerations include whether there is such limited availability of pre-blended fuel vendors that prices remain artificially high, whether the capital cost of the water and surfactant tanks and blending systems is manageable, and whether there is space enough aboard the vessel to outfit it with that equipment. A simple list of pros and cons for each method, with respect to a particular vessel and operating location, would point to the better option.

### 7.4 Engine Replacement for Reduced Emissions

Diesel engine designs have evolved substantially since the 1980s to attain significantly cleaner exhaust emissions. Older marine engines, particularly two-cycle models, cannot approach the 40 percent lower NOx emissions typically achieved by modern four-cycle engines equipped with electronic fuel injection systems. Other notable design improvements to the diesel engine, such as exhaust gas recirculation, are continually added to new generations of engines. Each successive generation of engines, complete with new develops in emissions control, achieves lower levels of harmful NOx, HC, and PM emissions.

It follows that every owner/operator of a vessel with a technically obsolete propulsion engine, from an emissions standpoint, should consider the option of replacing that engine with the newest equivalent low-emissions model. The basic obstacle to this solution is the inherently high cost of replacing a durable marine diesel engine. The vast majority of older units are too reliable, economical, and serviceable to be discarded lightly. Vessel life cycle economics bear heavily on the engine replacement decision and are seldom favorable without substantive public assistance. A variety of government incentive programs exist to reduce the financial burden on vessel owners and operators wishing to develop cleaner fleets. The State of California's Carl Moyer Memorial Program is an example of a program that has effectively promoted the replacement of environmentally obsolete engines with cleaner, modern substitutes. The Carl Moyer Memorial Program received $114,000,000 in appropriations between 1998 and 2002 and has facilitated enormous near-term emissions benefits that California must achieve in order to meet impending federal air quality deadlines. Shrewd vessel owner/operators will investigate the availability of incentive programs that apply to them by contacting the relevant air quality agencies to get the specifics of how to participate in such programs. In many cases, plans to lay up a vessel for extensive repairs, re-powering, or other life-extending modifications will coincide nicely with an emissions-reducing engine replacement program.

## 7.5 Engine System Modifications for Reduced Emissions

There are several proven propulsion plant modifications for reducing harmful engine exhaust emissions. These modifications can include humidification of the engine intake air, altered fuel injection and valve timing, ceramic coatings on valves and piston crowns, or post-combustion treatment of exhaust gases. Some of these approaches are readily applicable to marine installations and others, for unique reasons, are not. The available options span a measurable range of cost-effectiveness. Merits of each technique should be evaluated on a case by case basis. The emphasis on near term and future marine air-quality problems will be placed on NOx and PM. emissions. In the sections that follow, the four most promising retrofit options for limiting NOx and PM will be described and their merits and drawbacks assessed.

### *7.5.1 Selective Catalytic Reduction (SCR)*

The maximum reductions in NOx emissions effected to date have employed selective catalytic reduction technology. An engine exhaust system fitted with an SCR module will typically reduce NOx emissions by 75 to 90 percent, depending on engine design and service profile. This is far in excess of what can be achieved with simple water-fuel emulsions. In addition, SCR applications on diesel engines have demonstrated up to an 80 percent reduction in unburned hydrocarbons (HC) and a 20 to 50 percent reduction in particulate (PM). The Europeans have proactively and fairly successfully applied SCR technology to diesel engines. In the United States, the application of SCR is now gaining momentum.

SCR modules require minimum exhaust gas temperatures that are generally not achieved at loads less than 30 percent of an engine's rated capacity. SCR is therefore effective in reducing emissions only at sustained engine loads in excess of 30 percent. SCR applications in the marine industry have been very rare to date. Impediments to broader acceptance of SCR in marine transportation are outlined below.

- Sulfur content in fuel is incompatible with SCR. The previous dominance of (high sulfur) marine gas oil and heavy (residual) fuel oil as standard marine engine fuels prohibited use of this technology. The specification and exclusive use of low sulfur and ultra low sulfur distillate fuels will overcome this industry impediment.
- The acquisition cost of marine SCR equipment remains high. At present, each new SCR installation is virtually custom designed and built to suit a specific application. There is no "mass production" of SCR equipment for heavy-duty diesel engines. As a result, economies of scale have not emerged in marine or industrial SCR purchases to date. SCR installation costs on smaller highway truck and bus engines have ranged from $10,000 to $50,000 per unit. Larger marine engines will face significantly higher costs. A recent (February, 2002) cost estimate for a European SCR/particulate filter installation on a 7,000 horsepower diesel ferry was $500,000. At least one vendor, RJM Corporation, has progressed in the situation by offering pre-engineered designs that employ standardized components suitable for engines from 100 to 3,000 horsepower.
- The close confines of typical marine engine room spaces, particularly aboard workboats and high-speed passenger ferry vessels, generally do not allow the space required for SCR modules and urea storage tanks.

- The additional weight of an SCR installation can also present a significant problem for finely tuned high-speed passenger vessel designs. With an SCR module aboard, the passenger capacity (payload) may be diminished to maintain vessel displacement tonnage and service speed.
- SCR requires continuous injection of a reagent into the exhaust gas flow. The optimum choice for this application is urea, which is a naturally occurring non-hazardous material. Nevertheless, the need to continuously supply any reagent requires addition of a storage tank and a delivery piping system, and some degree of operator-attention to ensure that flow is maintained and that ample supplies of reagent are on hand. The cost of the reagent itself may be modest (5 to 8 kilograms are used per megawatt-hour) remains a consideration.

Despite some significant obstacles, SCR technology still embodies the maximum opportunity for practical reductions in NOx, HC, and, to a lesser extent, PM emissions from existing marine diesel engines. The capital expense of SCR can be entirely absorbed by the vessel owner or shared by a variety of government-sponsored air quality-improvement incentive programs. If a vessel can accommodate the space and weight penalties of SCR equipment, then this technology merits serious consideration.

### *7.5.2 Exhaust Gas Recirculation (EGR)*

Exhaust gas recirculation (EGR) is a development in diesel engine control technology which obtains significant NOx reductions. The recirculation of exhaust gas reduces peak temperatures in the combustion chamber (engine cylinders) by slowing the reaction rates and absorbing some of the heat generated from combustion. While NOx is reduced, PM and fuel consumption can increase, especially at high loads, because available oxygen for combustion is reduced and burn times are consequently lengthened. Reducing the flow of recirculated exhaust gas or by cooling the exhaust gas, and reducing its specific volume, can enable better combustion and mitigate these penalties at high load.

In the case of large slow-speed marine diesel engine, EGR in conjunction with direct water-injection (a variant of the emulsion technology), a 70 percent reduction in NOx was achieved. Without EGR, only a 50 percent NOx reduction was achieved. Also with some large, slow-speed marine diesel engines, the exhaust was recirculated simply by decreasing the efficiency of the scavenging process and trapping additional exhaust in the cylinder. This internal EGR eliminates the need for external hardware such as piping and valves, reducing cost and complexity. Second, by capturing the exhaust gas in the cylinder and not recirculating it into the intake system, deposits and wear are eliminated from the intake manifold and turbocharger that might otherwise be caused by EGR. The cost of retrofitting an EGR system to the average truck or bus engine is estimated to be $13,000 to $15,000. The cost is expected to be higher for a larger marine diesel engine.

### *7.5.3 Particulate Filters*

This particular option could achieve only near-term practicality in a minority of marine engine applications, specifically on low powered vessels. The sole reason that particulate filters are worthy of discussion is that they are the most effective established means to reduce PM emissions by much as 90 percent. As mentioned above, the use of low and ultra-low sulfur

diesel fuels, water-fuel emulsions, modern low-emission engine designs, and SCR all have beneficial impacts on particulate emissions. The sum of these initiatives, while not directly additive, would probably enable a cumulative reduction of PM emissions by roughly 20 to 55 percent, depending on engine model, age, and operating profile. By contrast, the particulate filters cut PM emissions 90 percent, regardless of engine model, age, and operating profile. It is therefore anticipated that more government incentives will promote the installation of particulate filters, as attention focuses on the carcinogenic effects of PM.

Until now, particulate filters have primarily been demonstrated in thousands of European stationary, mining, and highway vehicle applications. Typical vehicular PM filter costs are in the range of $7,500 each. A marine unit, even for a small ferry vessel, would likely be considerably more expensive. Periodic maintenance (filter regeneration/cleaning) requirements would also add financial burdens to the vessel owner. For large, high-speed vessels, these practical and economic issues would likely preclude particulate filters from consideration until less troublesome filter technology were demonstrated. The list of other prerequisites and problems for particulate filters generally follows the pattern already established for emissions reducing options discussed above.

- Low sulfur fuel is required.
- Vessel engine room space and weight limitations may preclude consideration.
- Particulate filters will increase backpressure on engine exhaust flow. Excessive backpressure compromises fuel economy and, therefore increases emissions of carbon-based greenhouse gases.

In summary, it is clear that the benefits of particulate filters have been well established, but that too many penalties come with this technology, as it exists today, for widespread acceptance by the marine industry. The optimum installation would undoubtedly be on a new vessel designed from the beginning to incorporate both SCR and a particulate filter. Nevertheless if, as expected, future air quality regulations impose stringent restrictions on particulate emissions, some form of particulate filter could have to be considered.

### *7.5.4 Diesel Oxidation Catalyst*

The diesel oxidation catalyst is a stainless steel canister with a honeycomb structured catalyst support, fixed into the exhaust stream. The platinum or palladium metal catalyst coatings inside convert exhaust gas pollutants to less harmful gases by a process of chemical oxidation. The catalyst is most effective at converting carbon monoxide (CO) and unburned hydrocarbons (HC) into $CO_2$ and $H_2O$ vapor. The level of PM reduction is influenced by the content of liquid HC particles in the particulate, which varies with engine design and fuel type. In many cases the HC is reduced from the PM by as much as 90 percent by the catalyst.

Although the oxidation catalyst by itself has not demonstrated great effectiveness at reducing NOx emissions, it is very useful with other NOx-control methods. Because the combustion characteristics are altered by NOx-control methods such as EGR and water-fuel emulsions, the improvement in NOx emissions is typically offset by higher PM, CO and HC emissions. Standard NOx-control techniques that boost these other emissions will benefit from an oxidation catalyst in the exhaust stream. Together, a NOx-control system with an oxidation catalyst can

effectively reduce NOx, PM, CO, HC and smoke emissions. One such system, approved under the EPA's urban bus rebuild/retrofit program uses an oxidation catalyst with proprietary engine controls for NOx control, yields 40 percent lower NOx very low PM emissions to below 0.1 g/bhp-hr. The history of the 20,000 catalysts installed on urban buses in Europe and the U.S. has proven to be virtually maintenance free. In mining and other non-road materials-handling activities, nearly 250,000 units have been installed over the past 30 years, demonstrating significant reductions in CO, HC and PM emissions. Many oxidation catalysts are designed to simply replace an existing muffler in the exhaust system. The cost for truck and bus engines has ranged from $475 to $1750, depending on engine size and installation.

## 7.6 Conclusions and Recommendations

The primary objective of this program element, to obtain precise real time in-situ data comparing the exhaust emissions of competing auto, transit bus, and passenger ferry, remains unfinished. Until Phase II of the program element is completed, the actual emissions produced by competing transit modes, in particular buses and ferries, will remain undefined. As a consequence, attempts to improve regional air quality, to upgrade port facilities and infrastructure, and to increase the speed, efficiency, and cost effectiveness of port operations would likely be delayed by public opposition based on the perception that such objectives would degrade regional air quality.

As discussed in sections 4.0, 5.0 and 6.0, there are a variety of methods for reducing harmful exhaust emissions from marine diesel engines. The best, most sweeping method is the improvement of fuel quality, which has been incrementally accomplished through the reduction of the sulfur content in the fuel. Further sulfur reductions are anticipated in the near future. Public health initiatives today place the higher priorities on the reduction of NOx and PM above the other exhaust gases, such as CO, $CO_2$ and HC. The most cost-effective method of NOx reduction is the proven technology of water-fuel emulsions. Depending on the criteria discussed in section 4.3, such as fuel suppliers available and space on board for fresh water and blending equipment, a decision would have to be made on a case-by-case basis whether to purchase pre-blended emulsions from ashore, or whether to install water, fuel and surfactant blending equipment on board the vessel.

In addition to water-fuel emulsions, the technology of exhaust gas recirculation (EGR), is proven effective and minimally intrusive for an engine retrofit. New engines can be purchased with EGR built into the design, and old engines can be modified to employ this technique. Used independently, or together with water-fuel emulsions, NOx emissions can be expected to drop dramatically, though not as significantly as the 90 percent reduction demonstrated by the SCR technology. SCR has several drawbacks, however. The catalyst requires much volume in the exhaust system. There is the lifetime capital cost of the urea reagent that is consumed in the catalyzing process. And the retrofit is expensive for its materials and custom fabrication, from vessel to vessel.

Particulate filters, although effective, pose the obstacle of raising the exhaust gas backpressure high enough that engine efficiency and fuel economy is compromised. The oxidizing catalyst, on the other hand, drops into the exhaust system as a relatively inexpensive muffler replacement. The oxidizing catalyst effectively reduces CO, HC and PM emissions, which are precisely what increase with supplementary NOx-reduction equipment. The best combination of emissions

reduction equipment, therefore, would employ: either EGR, water-fuel emulsion, or both, to reduce NOx and an oxidizing catalyst to reduce the other harmful emissions of CO, HC and PM.

The operator's financial cost for lowering emissions is undoubtedly greater than if emissions were ignored altogether. Various federal and state environmental agencies, aware of this business consideration, offer financial incentives in tax relief and grants for transportation operators who would make capital improvements to their fleets to improve exhaust emissions and regional air quality.

# 8.0 BIBLIOGRAPHY


Barry, C, Duffy, B., and Kamen, P., The Society of Naval Architects and Marine Engineers (SNAME) *Ferries For The San Francisco Bay Area; New Paradigms From New Technologies,* (to be presented at the California Joint Sections Meeting, May 31, 2002).

California Environmental Protection Agency, Air Resources Board, *The Carl Moyer Program Annual Status Report,* (March 26, 2002).

International Maritime Organization (IMO), *International Convention for the Prevention of Pollution from Ships (MARPOL 73/78).*

Manufacturers of Emissions Controls Association, *Retrofitting Emission Controls On Diesel-Powered Vehicles,* (March 2002).

San Francisco Bay Area Water Transit Authority, The, *New Technologies and Alternative Fuels,* (May 2, 2002).

Skjolsvik, K.O., *Emissions From Ships (The 4th Stanley Gray lecture)*, Transactions, Institute of Marine Engineers, Vol 112, part 3/4 pp 95-102, (2000).

Sweeney, J. et al, The Society of Naval Architects and Marine Engineers (SNAME), *Ferry Transit Systems for the Twenty First Century,* (January 10, 2000).

United States Environmental Protection Agency (EPA) 40 CFR Part 94, [AMS-FRL- ], RIN 2064-AJ98, *Control of Emissions of Air Pollution from New Marine Compression-Ignition Engines at or Above 30 Liters per Cylinder (Proposed),*(2002).

UNFCCC, *Kyoto Protocol to the United Nations Framework Convention on Climate Change,* (1998).

# APPENDIX A

# DESCRIPTION OF THE FTIR TEST METHOD

# APPENDIX A

## FOURIER TRANSFORM INFRARED (FTIR) SPECTROSCOPY ANALYSES

### I. Introduction

The extractive FTIR measurement method is based on continuous extraction of sample gas from the stack, transporting the sample to the FTIR spectrometer and performing real-time spectral measurement of the sample gas. The sample gas spectra are analyzed in real time for target analytes, archived, and re-analyzed, if necessary, at a later date for other target analytes.

Spectral Insights (SI) has conducted over 75 compliance tests using FTIR on natural gas-fired and diesel engines, using EPA Method 320 or equivalent. Each of these tests was completed successfully. In approximately 50 of the tests, corresponding EPA reference methods for THC, NOx, $CO_2$, and CO were conducted simultaneously. The agreement between the methods was very good, except in cases where high levels of $NO_2$ were present. This was found to be due to low converter efficiency in typical chemiluminescent $NO_x$ analyzers. It was also determined at low $NO_x$ levels, the chemiluminescent analyzer is subject to fluorescence quenching due to $CO_2$. FTIR is not subject to these known problems. We believe that SI possesses the greatest amount of knowledge and experience regarding the use of FTIR spectroscopy on engine (as well as other source) emissions measurements.

The U.S. EPA has accepted all SI-collected FTIR data submitted to it without question, including $NO_x$ and CO data. For further information on EPA's position on the use of FTIR for $NO_x$, CO, and other species, please call either Ms. Rima Dishakjian at (919) 541-0443, Mr. Ken Durkee at (919) 541-5425, or Mr. Mike Toney at (919) 541-5247, all at EPA.

The proposed method will follow all of the procedures described in EPA Test Method 320. SI performed (as Radian Corporation) the successful EPA Method 301 FTIR validation test funded by the Gas Research Institute (GRI) in 1994. The EPA accepted the validation, as stated in an EPA letter to GRI that FTIR can be used at any "gas-fired source". These data are reported in a document published by the Gas Research Institute entitled, *Topical Report: Fourier Transform Infrared (FTIR) Method Validation at a Natural Gas-Fired Internal Combustion Engine*, GRI Document No. GRI-95/0271, December 1995.

SI has successfully used FTIR to determine THC and TNMHC data from engines. Engine exhaust primarily contains methane ($CH_4$), ethane, ethylene, and formaldehyde. Because FTIR can measure these species separately, it is straightforward to measure THC and TNMHC using the FTIR system by adding the concentration of the appropriate species, either unweighted, or carbon-weighted. Because the usual detector used in Method 25A analysis is a flame ionization detector (FID), the measurement of THC can be biased with the varying relative responses for each hydrocarbon. However, because the engine exhaust is primarily methane, the differences between THC by FID and FTIR are typically negligible. TNMHC determination has historically been difficult using M25A, due to the high levels of methane expected to be present in the effluent gas and the difficulty of selectively removing methane. A recent EPA-sponsored test of IC engine exhaust measurements at Colorado State University using a "TNMHC" analyzer showed the difficulties with attempts to remove high (1000 ppm) levels of methane.

## II. Summary of FTIR Method

FTIR measurement is based on the absorbance of infrared energy by gas phase compounds. Most molecules absorb infrared energy at characteristic frequencies based on the molecular vibrational and/or rotational motion within the molecule. The absorption characteristics of a particular compound can be used to identify and quantitate the concentration of that compound. The concentration of a single target compound is related to its absorbance according to Beer's Law:

$$A(\nu) = a(\nu)bc$$

Where:

| | | |
|---|---|---|
| $A(\nu)$ | = | absorbance at wavelength v, |
| $a(\nu)$ | = | absorption coefficient at wavelength v, |
| $b$ | = | path length, and |
| $c$ | = | concentration. |

If more than one compound absorbs light at a given wavelength, then the total absorbance is found from a linear combination of Beer's Law for each compound:

$$A_{total}(\nu) = b\sum_{i=1}^{N} a_i(\nu)c_i$$

Where:

| | | |
|---|---|---|
| $A_{total}$ | = | total absorbance at wavelength $\nu_i$, |
| $a_i(\nu)$ | = | absorption coefficient for compound I at wavelength v, |
| $c_i$ | = | concentration of compound I, |
| N | = | total number of absorbing compounds, and |
| $b$ | = | path length. |

Compounds with very sharp spectral features, such as CO, can exhibit nonlinear analyzer response, requiring correction algorithms to accurately calculate concentrations. Correction algorithms are generated by measuring the spectrum of the compound at several different concentrations and fitting the resulting data to an appropriate correction curve.

Quantitation of each target compound is based on the application of a reference spectrum that is specific to that compound and is measured at a known concentration, temperature, and pressure. For the target compounds, quantitation is performed by selecting characteristic absorbance regions that have minimal interferences from other compounds present in the gas stream.

The classical least squares (CLS) method is applied to fit the reference spectra to the sample spectrum, with the resulting scaling factors used to calculate concentrations. The CLS method finds the set of concentrations that minimizes the residuals in the analysis region and provides a confidence interval for each concentration calculated. The confidence interval is used as a

diagnostic to determine how well the CLS method fit was accomplished. It is used to assess instrument performance and to alert the user to review the data for the presence of new or elevated concentrations of interferants in the sample.

# APPENDIX B

# EPA TEST METHOD 1 — SAMPLE AND VELOCITY TRAVERSES FOR STATIONARY SOURCES.

## APPENDIX C

**SILVIS, WILLIAM M., MAREK, GERALD, KREFT, NORBERT, "DIESEL PARTICULATE MEASUREMENT WITH PARTIAL FLOW SAMPLING SYSTEMS: A NEW PROBE AND TUNNEL DESIGN THAT CORRELATES WITH FULL FLOW THROTTLES," SAE PAPER NO.2002-01-0054, PRESENTED MARCH, 2002.**

# APPENDIX D

# EPA TEST METHOD 3A — DETERMINATION OF OXYGEN AND CARBON DIOXIDE FROM STATIONARY SOURCES (INSTRUMENT ANALYZER PROCEDURE).

**APPENDIX E**

**EXHAUST EMISSIONS MEASUREMENT, RECOMMENDATIONS FOR RECIPROCATING ENGINES AND GAS TURBINES. APPENDIX 7: PARTICULATE SAMPLING AND MEASUREMENT, INTERNATIONAL COUNCIL ON COMBUSTION ENGINES (CIMAC), APRIL, 1991.**

# APPENDIX F

# EPA TEST METHOD 320 — MEASUREMENT OF VAPOR PHASE ORGANIC AND INORGANIC EMISSIONS BY EXTRACTIVE FOURIER TRANSFORM INFRARED (FTIR) SPECTROSCOPY SOURCES.

# APPENDIX G

# AVL MODEL SPC 472 SMART SAMPLER — BROCHURE.

## APPENDIX H

## AVL MODEL SPC 472 SMART SAMPLER — CUT SHEET FROM WEB SITE.

**APPENDIX I**

**MAGAZINE ARTICLE FROM MECHANICAL ENGINEERING, "A FLEXIBLE SAMPLER FOR DIESEL EXHAUST," FEATURING SIERRA INSTRUMENTS.**

# APPENDIX J

## SIERRA INSTRUMENTS, MODEL BG MICRO-DILUTION TEST STAND — BROCHURE.

# APPENDIX K

## SIERRA INSTRUMENTS, MODEL BG-1 MICRO-DILUTION TEST STAND — OPERATING INSTRUCTIONS.

## APPENDIX L

## MODEL BG-1 CERTIFICATE OF CONFORMITY FROM TUV HANNOVER.

## APPENDIX M

## MODEL 780S THERMAL MASS FLOW METER — PRODUCT BULLETIN.

# APPENDIX N

## KRAL VOLUNTEER FUEL METERING SYSTEM — CUT SHEET FROM WEB SITE.

# APPENDIX O

## WIRELESS DATA CORPORATION, MODEL 1625 TORQUE SENSOR ASSEMBLY — PRODUCT BULLETIN.

**APPENDIX P**

**DDEC IV SYSTEM PRODUCT DATA — CUT SHEET FROM WEB SITE.**

# APPENDIX Q

# DDEC REPORTS — USER MANUAL

# Gasmet™ In-Situ 5.0

## In-Situ Multicomponent FTIR Gas Analyser

GASMET FTIR In-Situ SERIES includes industrial multicomponent gas analysers for continuous monitoring applications. The GASMET In-Situ 5.0 incorporates a Fourier Transform Infrared spectrometer, a sample cell which is directly inserted into the sample gas flow, and signal processing electronics. The analyser is fully equipped for fixed installations and it offers versatility and high performance for a wide range of applications.

Standard In-Situ 5.0 analyzer includes analog outputs 4-20 mA for measuring data and relay contacts for alarms. As an option the In-Situ analyser can be equipped with an external computer unit. In this case the In-Situ employs the same Calcmet user interface as an extractive GASMET CEMS.

The sample must be non-condensing and the upper limit for sample temperature is 250 °C. Sample cell absorption path length is 5.0 meters. Insertion depth of the sample probe is 590 mm and the flange diameter is 240 mm.

| General parameters | |
|---|---|
| **Measuring principle:** | Fourier Transform Infrared, FTIR |
| **Performance:** | simultaneous analysis of up to 50 gas compounds |
| **Response time, $T_{90}$:** | typically < 120 s, depending on the gas flow and measurement time |
| **Operating temperature:** | -30 – 40 °C non condensing |
| **Storage temperature:** | -30 – 60 °C, non condensing |
| **Power supply:** | 100-115 or 230 V / 50 -60 Hz |
| **Power consumption:** | 500 W max. |
| **Instrument air:** | Dew point –20 °C, oil free |
| **Max. air consumption:** | 120 l/min for vortex cooling (cont.) |
| | 100 l/min for zero calibration/purge |
| | (15 minutes at 24 hour intervals) |

| Spectrometer | |
|---|---|
| **Resolution:** | 8 $cm^{-1}$ |
| **Scan frequency:** | 10 scans / s |
| **Detector:** | Peltier cooled MCT |
| **Source:** | SiC, 1550 K |
| **Beamsplitter:** | ZnSe |
| **Window material:** | ZnSe |
| **Wavenumber range:** | 900 - 4 200 $cm^{-1}$ |

**Gasmet Technologies Oy** | Pultittie 8 A, FI-00880 Helsinki, Finland

TEL: +358 9 759 00 400
FAX: +358 9 759 00 450
EMAIL: contact@gasmet.fi

WEB: www.gasmet.fi
VAT NO: FI19526395

## Sample Cell

| | |
|---|---|
| **Structure:** | Multi-pass, fixed path length 5.0 m |
| **Probe body material:** | AISI 316 steel |
| **Mirror material:** | Rhodium coated aluminium |
| **Mirror coating:** | Reflective gold coating |
| **Gaskets:** | Viton® O-rings |
| **Window material:** | $BaF_2$ |
| **Insertion depth** | 589 mm |
| **Mounting flange** | 240 mm diameter |

## Measuring parameters

| | |
|---|---|
| **Zero point calibration:** | 24 hours, calibration with instrument air |
| **Zero point drift:** | < 2 % of measuring range per zero point calibration interval |
| **Sensitivity drift:** | none |
| **Linearity deviation:** | < 2 % of measuring range |
| **Temperature drifts:** | < 2 % of measuring range per 10 K temperature change |
| **Pressure influence:** | 1 % change of measuring value for 1 % sample pressure change. Sample pressure changes are measured and compensated |

## Sample Gas Conditions

| | |
|---|---|
| **Gas temperature:** | Up to 250 °C, non condensing |

## Electrical Connectors

| | |
|---|---|
| **A/D Converter:** | Dynamic range 95 dB |
| **Signal Processor:** | 2 32-bit floating point DSP's 120 MFLOPS |
| **Digital Interface:** | Bayonet locking 10-pole circular connector (MIL-C-5015) for serial and relay output. |
| **Measuring data:** | 4-20 mA, max 8-channel |
| **Alarm Relays:** | Function, alarm, service relays |
| **Power connection:** | Terminal connectors for L + N + PE wires |

## Optional Computer Unit

Analyzer is connected to an external computer via serial cable. The external computer controls the GASMET In-Situ analyzer

| | |
|---|---|
| **Minimum Configuration:** | 512 MB Memory, > 40 GB hard disk, > 2.4 GHz Intel Pentium IV Processor, Modem, Network card |
| **Operating system:** | Windows Xp operating system |
| **Software included:** | Calcmet for Windows |
| **Watchdog support:** | Included |
| **Relay contacts (status):** | Function Fault<br>Service required<br>Sampling Alarm |
| **Relay contacts (valves):** | Sample gas<br>Zero gas<br>Span gas 1 |
| **Mouse:** | Included |
| **Keyboard:** | Not included |

| | |
|---|---|
| **Display:** | TFT display |
| **Digital Interface** | RS-232 cable to analyzer, max 10m |
| **Remote control:** | Built-in modem/network card and PC Anywhere support |

## Options

Adapters for flanges larger than 240 mm

RS-422/485 interface instead of RS-232 for longer distance, max 1 km.

## Enclosure

| | |
|---|---|
| **Material:** | Aluminium / Steel / Polyethylethylketone (PEEK) |
| **Dimensions (mm):** | 1018 x 390 x 250 |
| **Weight:** | 30 kg |
| **CE - Label:** | According to EMI guideline 89/336/EC |

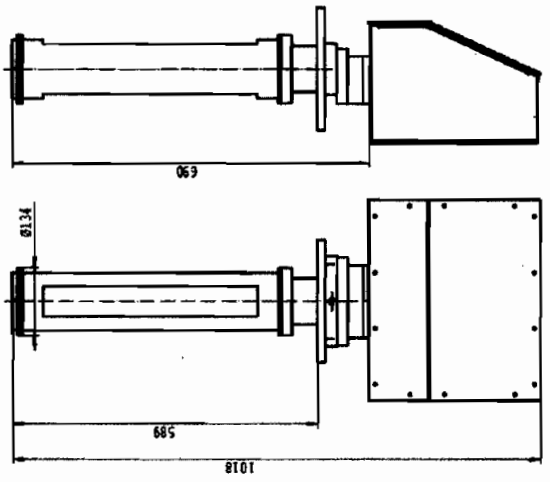


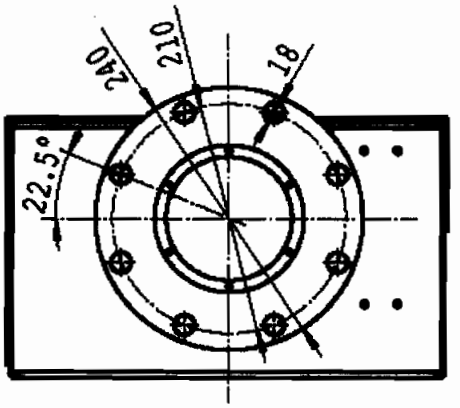


**Gasmet Technologies Oy** | Puistotie 8 A, FI-00880 Helsinki, Finland | TEL: +358 9 759 00 400, FAX: +358 9 759 00 450, EMAIL: contact@gasmet.fi | WEB: www.gasmet.fi, VAT NO: FI19526395

GE
Energy

technical
overview

# Extractive FTIR Air Emissions Testing

Following the 1970 Clean Air Act, impinger-based, manual air emissions tests were called into service. Technology later brought us single-component instrument monitors, capable of identifying compounds such as $SO_2$, $NO_X$, and CO.

Increasingly stringent air pollution regulations continue to spur development in emissions measurement technology, as requirements call for more sensitive detection across a growing list of pollutants. Timely data delivery is a critical issue, too. It is no longer practical to manually gather and send samples out for analysis, and wait sometimes weeks to see if a facility is in compliance.

Extractive Fourier Transform Infrared (FTIR) technology, available from GE Energy, represents the latest generation of emissions testing, with numerous advantages over traditional methods, including:

- Real-time, on-site data
- Multi-component measurements
- High sensitivity/low detection limits
- Fully archived data

## Robust Infrared Measurement

Extractive FTIR measurements are performed using an analyzer that detects gas phase molecules by infrared absorbance spectroscopy. The analyzer components include the infrared light source, the interferometer, transfer optics, a heated multipass gas cell, and an infrared detector. The analyzer is coupled to a heated, extractive sampling system, allowing sampled stack gases to flow through the gas cell.

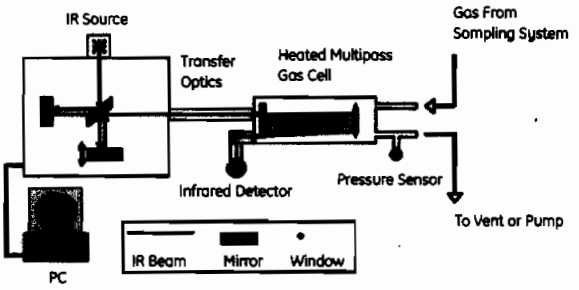


The analyzer collects a complete infrared spectrum (a measurement of the infrared light absorbed by molecules in the gas cell) with each sweep of the moving mirror in the interferometer. In a typical measurement, data is collected on a one-minute basis, with multiple sweeps "co-added" to improve signal-to-noise. The FTIR software immediately analyzes the spectrum and concentrations are reported on-screen.

## Real-Time, On-Site Data

FTIR simultaneously measures multiple analytes in a complex gas matrix, detecting virtually all gas-phase species, including multiple Clean Air Act Hazardous Air Pollutants (HAPs), criteria pollutants, diluents, and Volatile Organic Compounds (VOCs). Measurements are made on a continuous basis and reported in real time.

The most important advantage of real-time FTIR data is that it demonstrates whether or not a facility is meeting emissions requirements *while the test is being conducted.* This is particularly beneficial when working to optimize pollution control equipment or while modifying process variables. The effect on emissions is known, and process can be adjusted, prior to compliance testing. This not only saves time, versus off-site lab analysis, but saves considerably in retesting fees as well.

## Multi-Component Measurements

FTIR detects gaseous compounds by their absorbance of infrared radiation. All gases—with the limited exception of homonuclear diatomic compounds such as nitrogen ($N_2$) and oxygen ($O_2$)—absorb in the infrared spectral region and can, in principle, be detected. While detection limits vary by compound, the majority of gaseous compounds can be detected at the parts-per-million (ppm) level, with a large number detectable at parts-per-billion (ppb) concentrations.

Up to 30 compounds can be detected simultaneously in an FTIR measurement. Examples of the compounds detected by FTIR include:

- Acid gases (HCl, HF, HCN)
- Inorganics (CO, $SO_2$, $NH_3$)
- Nitrogen Oxides (NO, $NO_2$, $N_2O$)
- Diluents ($H_2O$, $CO_2$)
- Greenhouse gases (CFCs, $N_2O$, $CO_2$)
- All Volatile Organic Compounds (VOCs)
  - Aromatics (benzene)
  - Aldehydes (formaldehyde)
  - Aliphatics (methane)
  - Alcohols (ethanol)
  - Ketones (acetone)
  - Amines (triethylamine)
  - Acetates (ethyl acetate)
  - Acids (formic acid)
- Over 100 Clean Air Act HAPs

## Parts-Per-Billion to Percent Level Sensitivity

While FTIR can measure a broad range of compounds at ppm/ppb concentrations, the detection range extends to high percent levels. Indeed, an FTIR measurement can simultaneously detect compounds present at very low and high concentrations. For example, FTIR can quantify emissions from a gas-fired combustion process with water and carbon dioxide present at concentrations over 10%, while at the same time detecting CO, $SO_2$, NO, $NO_2$, and $NH_3$ at less than 10 ppm, and formaldehyde at less than 100 ppb.

## Dedicated Mobile Laboratory

GE operates a mobile FTIR laboratory complete with a paired heated sampling system for time-shared testing at two locations, or simultaneous testing using two FTIR analyzers.

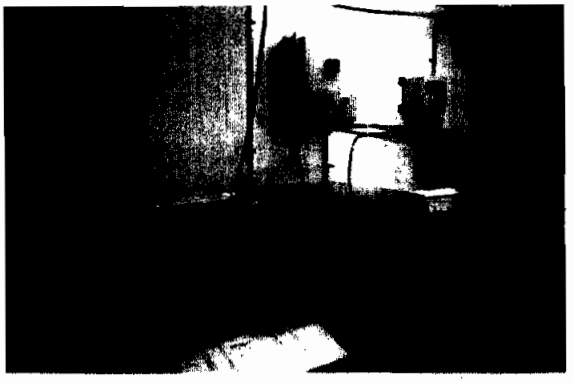

IMACC (Industrial Monitor & Control Corp.) FTIR Analyzer mounted in mobile FTIR lab

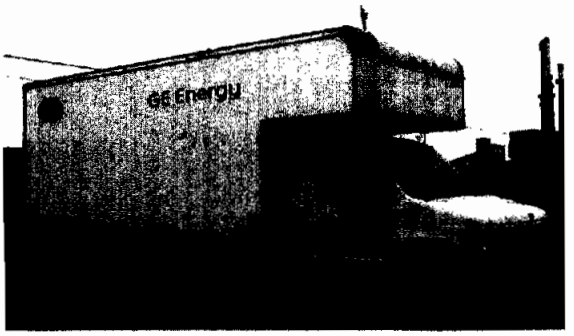


Mobile FTIR lab conducting field emissions test

## Portable FTIR Analyzer

GE also utilizes a portable, low resolution Gasmet™ FTIR analyzer (Gasmet Technologies Oy) that can be set up in a mobile lab or at a test location. This is particularly advantageous when fast response is required, or when measuring species whose sample transport is a challenge—such as measuring ammonia slip from a coal-fired facility using selective catalytic reduction (SCR) for $NO_x$ control.

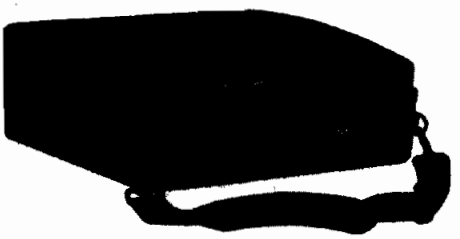

# Extractive FTIR Air Emissions Testing



## Successful Applications

Because extractive FTIR can measure so many compounds over a wide range of concentrations, potential applications are numerous. The examples below illustrate the industries where GE has successfully used FTIR testing:

- Coal-Fired Utility: Measurement of criteria pollutants (CO, $SO_2$, NO, $NO_2$, $N_2O$), diluents ($H_2O$, $CO_2$), HAPs (HCl, HF), and other compounds ($NH_3$, $HNO_3$)
- Ethanol Fermentation Plant: Measurement of multiple VOCs (ethanol, isopropanol, formaldehyde, acetaldehyde, acetic acid, formic acid, methyl acetate, ethyl acetate, methyl formate) and HCl
- Chemical Manufacturing: Simultaneous inlet and stack measurements at a thermal oxidizer using two FTIR analyzers to determine species-specific control efficiency for an aromatic and an organic amine compound
- Chemical Manufacturing: Characterization of an organic acetate, acrylate, and aldehyde emissions from a batch polymerization process
- Fiberglass Monufacturing: Meosurement of phenol, formaldehyde, and methanol; simultaneous inlet and stack measurements at a thermal oxidizer using two FTIR analyzers to determine control efficiency for formaldehyde
- Reciprocating Internal Combustion Engine (RICE): Measurement of formaldehyde, acrolein, and uncombusted fuel (natural gas) emissions
- Fire Research Center: Characterization of emissions of 22 compounds, including 15 VOCs, from uncontrolled combustion processes

FTIR technology is often utilized for these applications:

- Compliance ond engineering studies
- Characterization of steady-state or batch (highly variable) emissions
- Species-specific control device efficiency determination
- Measurement of very high concentration gas streams using a dilution system

## Regulatory Acceptance

The United States Environmental Protection Agency (USEPA) funded the initial development of FTIR testing in the early 1990s and currently cites three extractive FTIR tests in its reference methods, in addition to the American Society for Testing and Materials (ASTM) method used for compliance testing:

- USEPA Reference Method 318, "Extractive FTIR Method for Measurement of Emissions from the Mineral Wool and Wool Fiberglass Industries," 40CFR63
- USEPA Reference Method 320, "Measurement Of Vapor Phase Organic And Inorganic Emissions By Extractive Fourier Transform Infrared (FTIR) Spectroscopy," 40CFR63
- USEPA Reference Method 321, "Measurement of Gaseous Hydrogen Chloride Emissions At Portland Cement Kilns by Fourier Transform Infrared (FTIR) Spectroscopy," 40CFR63
- ASTM Method D6348-03, "Standard Test Method for Determination of Gaseous Compounds by Extractive Direct Interface Fourier Transform Infrared (FTIR) Spectroscopy"

FTIR test methods are unique among EPA methods because they are considered "self-validating" through the use of dynamic matrix spiking calibrations. In this technique, conducted as part of every compliance test, a compound of interest is injected into the back of the sampling probe where it mixes with the sampled gas and is transported to the analyzer. The injection is accomplished using a certified gas cylinder and a calibrated mass flow meter, with the spike injected at a dilution ratio of at least 10:1. This calibration certifies that the compound can be measured in the presence of the source matrix, and can be transported through the sampling system without losses. The plot below shows typical spiking data collected in an FTIR test. The spike gas here is formaldehyde, and the spike tracer (used to determine the dilution ratio) is $SF_6$. The spike was recovered at 98.8% of the expected volue; well within the method required 70-130% recovery.

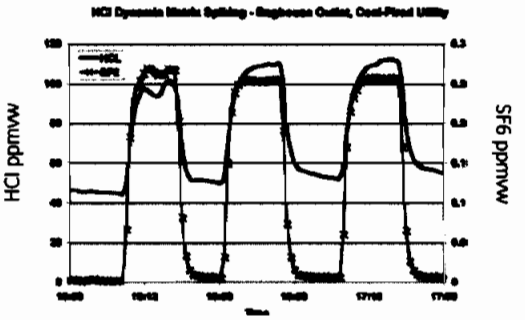

# Extractive FTIR Air Emissions Testing

technical overview

Extractive FTIR testing has also been incorporated in numerous Maximum Achievable Control Technology (MACT) standards, and is increasingly being included in facility permits as the mandated testing methodology.

## Cost-Effective Emissions Testing

The cost of extractive FTIR testing is, as for all air emissions testing methods, dependent on the scope of work and project duration. Certainly, when there is a need to measure a single compound like HCl, manual testing will be less costly; however, the manual method data will not provide as low a detection limit or time-resolved emissions data. Similarly, a VOC test conducted using Method 25A (flame ionization detector) will be less costly, but will not provide information on the compounds being emitted or accurate source emissions (unless response factors are measured).

FTIR delivers considerable cost advantage when used to measure multiple components, thereby replacing several manual ond/or instrumental test methods ond the respective personnel. And, with FTIR deployed on-site, tests can be conducted while process variations are under study, thereby avoiding costly retests later on.

## GE Expertise and Focus on Quality

As with any advanced measurement technology, good results come from proper source testing, expert spectral interpretation, and meticulous data analysis. With GE's FTIR, sample collection is performed by skilled technicians with a minimum of five years experience in FTIR testing. Sample integrity is rigorously monitored through our quality assurance (QA) calibrations and matrix spike validation process. GE's own Six Sigma (6σ) process ensures data quality. And o 19-year veteran of FTIR technology, an experienced spectroscopist who participated in the original EPA-sponsored research to develop the methodology, conducts our interpretation.

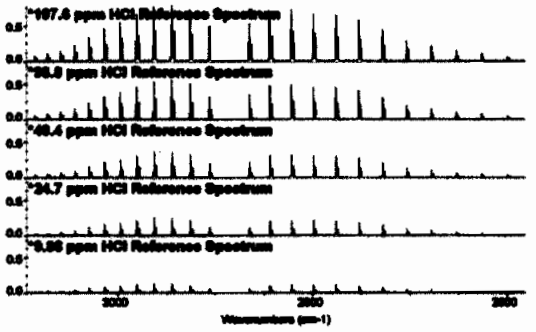


ISO 9001 Accredited Quality System

For more information contact your GE Energy sales representative at 800.821.2222 or visit us on the web at ge-energy.com/airquality.



GEA-14569 (04/06)

Environ. Sci. Technol. 2007, 41, 6940–6946

# Origin, Occurrence, and Source Emission Rate of Acrolein in Residential Indoor Air

VINCENT Y. SEAMAN,[†] DEBORAH H. BENNETT,[‡] AND THOMAS M. CAHILL*[,§]

*Departments of Environmental Toxicology and Public Health, University of California, Davis, Davis, California, and Department of Integrated Natural Sciences, Arizona State University at the West Campus, P.O. Box 37100, Phoenix, Arizona 85069*

Acrolein, a volatile, unsaturated aldehyde, is a known respiratory toxicant and one of the 188 most hazardous air pollutants identified by the U.S. EPA. A newly developed analytical method was used to determine residential indoor air concentrations of acrolein and other volatile aldehydes in nine homes located in three California counties (Los Angeles, Placer, Yolo). Average indoor air concentrations of acrolein were an order of magnitude higher than outdoor concentrations at the same time. All homes showed similar diurnal patterns in indoor air concentrations, with acrolein levels in evening samples up to 2.5 times higher than morning samples. These increases were strongly correlated with temperature and cooking events, and homes with frequent, regular cooking activity had the highest baseline (morning) acrolein levels. High acrolein concentrations were also found in newly built, uninhabited homes and in emissions from lumber commonly used in home construction, suggesting indoor contributions from off-gassing and/or secondary formation. The results provide strong evidence that human exposure to acrolein is dominated by indoor air with little contribution from ambient outdoor air.

## Introduction

Acrolein, a highly reactive α,β-unsaturated aldehyde, is a common constituent of both indoor and outdoor air (*1*, *2*). Acrolein is a known pulmonary toxicant (*3*–*8*) and has been shown to act synergistically with other carcinogens in the development of lung cancer (*9*). Epidemiological studies have implicated acrolein in the exacerbation of asthma in children (*10*) and high rates of lung cancer in women exposed to cooking fumes (*11*). A recent risk assessment of acrolein in ambient air suggests that acrolein could be associated with decreased respiratory function in the United States (*12*).

Acrolein is produced by the incomplete combustion of organic material as well as the oxidation of atmospheric chemicals such as 1,3-butadiene, a primary component of motor vehicle exhaust. The U.S. Environmental Protection Agency (EPA) estimates that about 75% of ambient acrolein originates from mobile sources, with the remainder from agriculture, industrial processes, tobacco smoke, and forest fires (*13*). Using emission data from 1996 to model ambient air concentrations, the EPA estimated average acrolein concentrations of 0.119 $\mu g/m^3$ (national) and 0.157 $\mu g/m^3$ (California), which are well above the EPA Reference Concentration (RfC) of 0.02 $\mu g/m^3$ (*14*). A more recent study projected the average concentration of acrolein in ambient air in California to be 0.36 $\mu g/m^3$ (*15*), which is more than twice the EPA estimate. The California Air Resources Board (CARB) reported that the statewide average ambient concentrations in 2004, 2005, and 2006 were 1.21, 1.37, and 1.35 $\mu g/m^3$, respectively, based on routine air monitoring of acrolein using a canister sampling method (stated method minimum detection limit = 0.3 $\mu g/m^3$)(*16*). Although the modeling estimates and measurements are not in close agreement, they all report ambient acrolein levels well above the EPA RfC.

Less is known about indoor sources of acrolein, which include heated cooking oil, cigarette smoke, incense, candles, and wood-burning fireplaces (*1*, *2*, *17*). Carbonyls can also be formed by the oxidation of volatile organic compounds (VOCs) which off-gas from home furnishings, building materials, carpeting, wood finish, glues and adhesives, and paints (*18*–*20*). The formation of acrolein and other unsaturated aldehydes by these processes, however, is complex and not well understood at this time. Numerous attempts to quantify residential indoor acrolein levels have either been unsuccessful or have provided conflicting and/or inconsistent results (*20*–*26*). These studies have reported higher indoor levels of numerous other volatile carbonyls than those outdoors, however the methods used have failed to generate reproducible results for acrolein. These methods also require extended sampling periods (24–48 h or longer) and thus do not provide maximum exposure concentrations or diurnal fluctuations. Therefore, while it is generally accepted that indoor concentrations of many VOCs are higher than outdoor levels, the values for acrolein are uncertain. It is also clear that traditional methods for measuring carbonyls are not suitable for acrolein. A method recently developed by the authors has the capability to detect low $ng/m^3$ concentrations of acrolein and other carbonyls using a sampling period of 10 min (*27*). This method is useful for determining the concentrations of acrolein found indoors and the temporal fluctuations due to human activities and stationary sources.

The objective of this research was to quantify the indoor and outdoor concentrations of acrolein in nine homes in three different California counties and in a number of unoccupied, newly constructed houses. These data were then used to establish the source emission rates for acrolein in a typical home and to identify possible sources of these compounds. In addition to acrolein, over 30 other volatile carbonyls were similarly measured (see Table S1, Supporting Information). A variety of building materials and furnishings, such as wood, particleboard, adhesive, carpet, paint, and drywall, were also analyzed to identify potential sources of indoor carbonyls.

## Materials and Methods

**Selection of Sampling Locations.** Three non-smoking residential homes were selected as a convenience sample in each of three California counties (Yolo, Placer, and Los Angeles) to reflect semi-rural, suburban, and urban environments. The locations of the homes sampled were chosen to provide a variety of internal and external environments (Table 1). Two of the homes in Placer County (PL-01,02) were located in the same housing tract and were of similar size, construc-

* Corresponding author e-mail: tmcahill@asu.edu.
[†] Department of Environmental Toxicology, University of California, Davis.
[‡] Department of Public Health, University of California, Davis.
[§] Arizona State University.



10.1021/es0707299 CCC: $37.00 
Published on Web 09/18/2007

**TABLE 1. Physical and Environmental Characteristics of the Homes**

| | | | | | | | temp (°C) | | | | RH (%) | | | |
|---|---|---|---|---|---|---|---|---|---|---|---|---|---|---|
| | | | | | | | a.m. | | p.m. | | a.m. | | p.m. | |
| house | type | location | area ($m^2$) | volume ($m^3$) | AER ($h^{-1}$) | cooking | in | out | in | out | in | out | in | out |
| YO-01 | condominium | Davis[a] | 158 | 578 | 0.12 | p.m.[d] | 17 | 16 | 18 | 15 | 72 | 89 | 69 | 86 |
| YO-02 | apartment | Davis[a] | 80 | 133 | 0.23 | a.m. p.m.[d] | 19 | 18 | 19 | 17 | 79 | 80 | 79 | 80 |
| YO-03 | house, 1-story | Davis[a] | 182 | 500 | 0.14 | a.m.[d]p.m.[d] | 19 | 12 | 17 | 14 | 52 | 78 | 54 | 79 |
| LA-01 | house, 2-story | Glendale[b] | 186 | 527 | 0.23 | p.m.[d] | 20 | 25 | 19 | 15 | 56 | 49 | 64 | 75 |
| LA-02 | house, 1-story | Arcadia[b] | 194 | 531 | 0.19 | p.m.[d] | 17 | 12 | 22 | 16 | 73 | 83 | 55 | 68 |
| LA-03 | duplex, lower | Los Angeles[b] | 34 | 82 | 2.23 | p.m.[d] | 18 | 15 | 19 | 18 | 68 | 68 | 72 | 72 |
| PL-01 | house, 2-story | Roseville[c] | 207 | 756 | 0.13 | | 16 | 12 | 19 | 15 | 79 | 100 | 69 | 71 |
| PL-02 | house, 2-story | Roseville[c] | 214 | 782 | 0.10 | a.m. | 18 | 12 | 19 | 15 | 75 | 100 | 72 | 71 |
| PL-03 | house, 1-story | Fair Oaks[c] | 186 | 510 | 0.26 | p.m. | 21 | 13 | 22 | 18 | 59 | 82 | 54 | 100 |

[a] Yolo County, semi-rural. [b] Los Angeles County, urban. [c] Placer County, suburban. [d] Cooking occurred prior to/during air sampling.

tion, and age, thus differences in indoor air quality would likely be due to furnishings and/or occupant activities.

Indoor and outdoor measurements were also made in six newly built, unoccupied homes. These homes were tested to detect carbonyls arising from building materials, fixtures, and furnishings in the absence of human habitation. Four were model homes in Sacramento, CA, which were completely furnished and decorated but had no residents. Two were newly built, unoccupied houses in Davis, CA, complete with carpeting, paint, and cabinets, but no furniture or decorative items.

**House Characterization.** The homeowners were asked to complete a questionnaire before and after sampling, detailing physical characteristics of their home and personal activities that might affect carbonyl emissions. All sampling and analysis protocols were approved by the Institutional Review Board of the University of California, Davis.

The air exchange rate (AER) for each home was determined using the perfluorocarbon (PFT) technique, which is based on a continual release of tracer gas and uptake by diffusion samplers (capillary adsorption tubes or CATs) (*28*). The perfluorocarbon sources were placed in the test homes 24 h prior to the placement of the CATs to allow the indoor PFT concentrations to equilibrate. A single CAT was then placed in each home 1 m above the floor and within 2 m of the air sampling equipment. The sampling locations were similar in all of the homes, and were at least 2 m from windows, doors, fireplaces. A second CAT was placed in two of the homes (YO-01, LA-03) for quality control purposes. AER measurements took place the same day that air sampling was being conducted and the CAT analysis was performed according to the PFT method cited.

**Sample Collection.** An initial intensive sampling set was conducted in house YO-01 to assess diurnal fluctuations in a typical home. Samples were collected every 2 h for two separate 24-h periods 1 month apart. This experiment was designed to ensure that indoor concentrations do not fluctuate widely and thus a house could be characterized by a pair of samples in the morning and evening.

In the nine residential homes, indoor and outdoor air samples were collected twice during a 24 h period in January 2006. The first set of samples was taken in the morning between 7 and 9 a.m., while the second set was in the evening between 5 and 7 p.m. (after any evening cooking). The uninhabited houses (i.e., the new and model homes) were only sampled during the morning time period due to access limitations. Duplicate samples were collected simultaneously at each measuring event by placing two sets of mist chambers side-by-side. Temperature and relative humidity were recorded for each sampling event.

Carbonyl sample collection and analysis was conducted using previously described methods (*27*). Briefly, two sets of mist chambers (each set = two mist chambers stacked in series), each containing a 0.1 M bisulfite solution that traps aldehydes and other carbonyls, were placed on a cart such that the mist chamber air intake was 1 m above the floor. This height was selected as it represents the breathing zone for a person in the seated position. Each set of mist chambers was connected to a small, portable pump and ambient air was pulled through at a rate of 19 $L \cdot min^{-1}$ for 10 min. After the samples were collected, the solutions were transferred to a test tube containing hydrogen peroxide (to oxidize the bisulfite and liberate the carbonyls), pentafluorohydroxylamine (PFBHA) (to derivatize the free carbonyls), and hexane (to extract the PFBHA-derivatives from the aqueous solution). The samples were allowed to react for 4 days at room temperature and the derivatives were then extracted in hexane, concentrated by nitrogen evaporation, and quantified by gas chromatography–negative chemical ion mass spectrometry. Acrolein-$d_4$ and benzaldehyde-$d_6$ were used as internal standards, and were added to the bisulfite solution as field-positive controls (matrix spikes) prior to sample collection. Acrolein-$d_4$ was used for the quantification of acrolein and other unsaturated aldehydes, while benzaldehyde-$d_6$ was used to quantify the saturated and aromatic aldehydes.

Duplicate samples were collected simultaneously at each measuring event using the two sets of mist chambers placed side-by-side. Two field blanks were collected at each site (one indoor and one outdoor) by adding 10 mL of sodium bisulfite and 10 $\mu$L of the labeled matrix spike to separate mist chambers, waiting 10 min, and transferring the solution to a reaction tube. The blanks were then stored and processed in the same manner as the samples.

**Emissions from Building Materials.** Several common building materials were tested to determine if they could be primary sources of carbonyls. The synthetic building materials consisted of a wood adhesive, interior latex paint, nylon carpet pieces, particleboard, and drywall. Five different species of lumber, namely Douglas fir (*Pseudotsuga menziesii*), pine (50:50 mixture of *Pinus ponderosa* and *Pinus lambertiana*), redwood (*Sequoia sempervirens*), "yellow poplar" (*Liriodendron tulipifera*), and red oak (*Quercus rubra*), were purchased at a local lumber yard and tested. To the best of our knowledge, none of the lumber samples were treated with preservatives or other chemicals by the retailer or wholesale supplier and were the grade commonly used in home construction. In addition, a fresh wood sample was collected from a living redwood tree and analyzed immediately to determine emissions from wood prior to lumber processing and aging.

In each case, 10 g of the material was sealed in a round-bottom flask. The latex paint was brushed onto aluminum foil (~750 $cm^2$ surface area) and allowed to dry for 24 h before

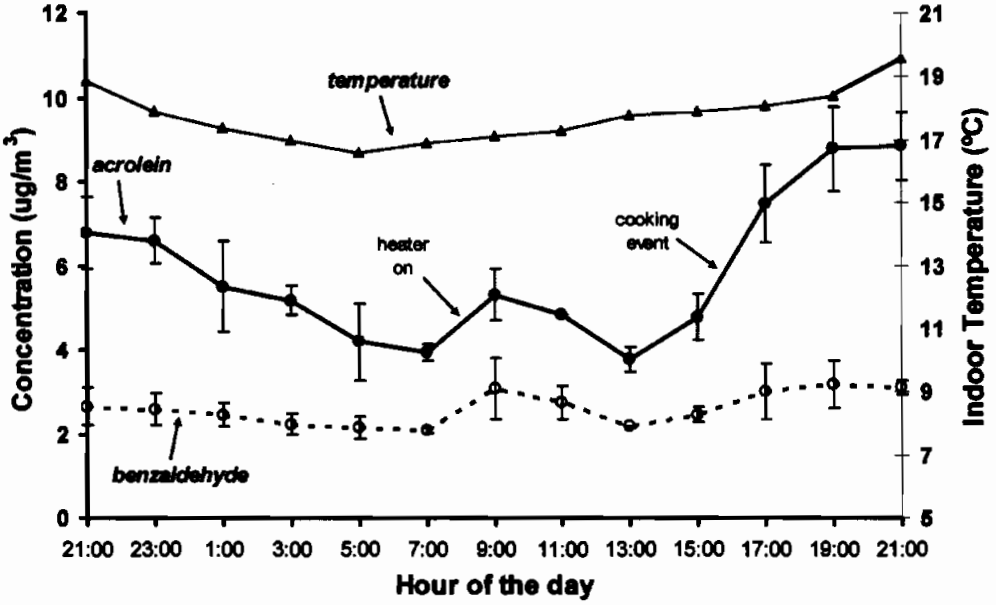


**FIGURE 1. Indoor diurnal cycles of acrolein, benzaldehyde, and temperature over two 24 h periods in house YO-01. On each day, a heater ran from 7:30 to 8:00 in the morning and a cooking event occurred from 16:00 to 16:30 in the evening. The temperature ranged from 18 °C in the morning to 20 °C in the evening.**

being peeled off, cut into strips, and put in the flask. The wood adhesive was dried directly in the flask with a stream of air for 24 h before sample collection. The wood, drywall, and particleboard samples were whittled into shavings or small pieces with a stainless steel knife. The samples were stored in the sealed flasks for 24 h before sample collection. Purified nitrogen gas was then pumped through each flask and into a pair of mist chambers for 10 min at 19 L/min as per the standard sample collection procedure. The mist chamber solutions were extracted and analyzed in the same manner as the air samples. It should be noted that there was no attempt to determine the surface areas of the materials, except for the latex paint, thus quantitative comparisons by surface area are not possible. In addition, this sampling procedure will not volatilize all the chemicals from the substrates, so the results represent a qualitative measure of chemicals that are emitted from the different substrates. Finally, the use of nitrogen as the carrier gas limits the chemical species collected to primary emissions, thus secondary carbonyl formation via ozone and/or other oxidizers would not be seen.

## Results

**House Characterization.** The physical characteristics of the sampled homes, temperature, relative humidity (RH), and cooking activities for all test days appear in Table 1. Air exchange rates in seven of the nine homes were between 0.1 and 0.26, which are slightly lower than normally seen in the average home (0.25–0.64) (*28*). Lower AERs are more common in newer houses (five of the homes were less than 15 years old) because they have fewer air leaks and drafts than older homes. Also, the sampling was performed during cool weather, so relatively few windows and doors were open on the test days. LA-03, an older home, had an AER of 2.23 due to a very small area, windows and doors being open nearly all of the time, and a steady, strong breeze at the site.

The homes were also characterized as to the type of heating or cooking appliances used (natural gas or electric), floor coverings (carpeting, wood, or tile), recent remodeling (new furniture, paint and tile work within the past 6 months), and the use of candles, incense, or air fresheners. Fresh paint was being applied to the exterior of the house next door to LA-01 during a.m. outdoor sampling. The a.m. sampling was performed prior to any cooking except for home YO-03. Cooking prior to the p.m. sampling occurred in all but two homes. None of the inhabitants of the homes smoked tobacco products.

Winds were calm for all outdoor measurements except LA-03, a beachfront unit located on the Pacific Ocean. In the morning, a 10 mph breeze was blowing off-shore (from the east), and in the afternoon, a 12 mph wind was blowing on-shore (from the west).

**QA/QC.** The acrolein concentrations reported for each event were the average of duplicate, side-by-side measurements. The relative standard deviation (RSD) of the duplicates ranged from 0.01 to 23% (avg. = 8.9%). The two field blanks were averaged at each location and subtracted from the collected sample concentration. The effective minimum detection limits (MDL) for acrolein (0.009 $\mu g/m^3$ outdoors; 0.081 $\mu g/m^3$ indoors) were determined as the mean field blank mass plus 3 standard deviations of the blanks. This equates to three times the standard deviations of the field blanks for the blank-subtracted air concentrations. All the indoor and ambient samples were above the MDLs. The two duplicate CATs had RSDs of 0.8 and 1.1%.

**Diurnal Acrolein Concentrations.** The fluctuations of acrolein and benzaldehyde were monitored in home YO-01 over two 24 periods to assess the diurnal variation of these chemicals (Figure 1). Overall, the acrolein concentrations ranged by nearly a factor of 2 (4.8–8.8 $\mu g/m^3$) while benzaldehyde showed a much smaller diurnal variation (2.4–3.1 $\mu g/m^3$). Acrolein levels were lowest between the hours of 3 a.m. and 3 p.m., and steadily increased from 3 to 9 p.m. A central heating system (natural gas) ran from 8:00 to 8:30 a.m. on both days, and aside from a single cooking event each day at approximately 4:30 p.m., there were no other human activities during the two 24-h sampling periods. The 30 min heating periods produced small, temporary increases in both acrolein and benzaldehyde levels, while the cooking events coincided with sharp increases in the acrolein concentrations, which continued to rise for 4–5 h after the cessation of cooking. The cooking events had no discernible effect on benzaldehyde levels (Figure 1). Based on the results of the diurnal experiments, an a.m. sample (collected between

**TABLE 2. Indoor/Outdoor Concentrations of Acrolein**

| | acrolein concentration ($\mu g/m^3$) | | | | | |
|---|---|---|---|---|---|---|
| | a.m. | | | p.m. | | |
| house | indoors | outdoors | indoor/outdoor ratio | indoors | outdoors | indoor/outdoor ratio |
| YO-01 | 7.8 | 0.09 | 87 | 12.2 | 0.41 | 30 |
| YO-02 | 7.7 | 0.31 | 25 | 8.7 | 0.66 | 13 |
| YO-03 | 3.5 | 0.12 | 29 | 4.3 | 0.23 | 19 |
| average ± SD | 6.3 ± 2.4 | 0.17 ± 0.12 | 47 ± 35 | 8.4 ± 4.0 | 0.43 ± 0.22 | 21 ± 8.6 |
| LA-01 | 3.4 | 1.6 | 2.1 | 3.9 | 1.1 | 3.5 |
| LA-02 | 2.6 | 0.8 | 3.3 | 6.5 | 1.7 | 3.8 |
| LA-03 | 2.5 | 1.7 | 1.5 | 5.9 | 0.4 | 15 |
| average ± SD | 2.9 ± 0.5 | 1.2 ± 0.6 | 2.3 ± 0.9 | 5.5 ± 1.4 | 1.4 ± 0.5 | 7.4 ± 6.6 |
| PL-01 | 2.2 | 0.17 | 13 | 3.5 | 0.45 | 7.8 |
| PL-02 | 4.0 | 0.17 | 24 | 6.1 | 0.45 | 14 |
| PL-03 | 2.1 | 0.27 | 7.8 | 3.1 | 0.15 | 21 |
| average ±S D | 2.8 ± 1.1 | 0.20 ± 0.06 | 15 ± 8.3 | 4.2 ± 1.6 | 0.35 ± 0.17 | 14 ± 6.6 |
| average (all homes) | 4.0 ± 2.2 | 0.58 ± 0.64 | 21 ± 27 | 6.0 ± 2.9 | 0.62 ± 0.49 | 14 ± 8.5 |
| model home #1 | 4.5 | 0.40 | 11 | | | |
| model home #2 | 5.5 | 0.31 | 18 | | | |
| model home #3 | 5.4 | 0.68 | 7.9 | | | |
| model home #4 | 4.5 | 0.72 | 6.3 | | | |
| average ± SD | 5.0 ± 0.6 | 0.53 ± 0.20 | 11 ± 6.3 | | | |
| new home #1 | 3.0 | 0.84 | 3.6 | | | |
| new home #2 | 3.2 | 0.52 | 6.2 | | | |
| average ±SD | 3.1 ± 0.1 | 0.68 ± 0.23 | 4.9 ± 1.8 | | | |

7 and 9 a.m.) and a p.m. sample (collected between 5 and 7 p.m.) would reflect the daily minimum and maximum concentrations of acrolein inside the home. An average of the a.m. and p.m. samples in this study represents a reasonable estimate of the 24-h average for carbonyls.

**Indoor/Outdoor Acrolein Concentrations.** Outdoor concentrations of acrolein ranged from 0.09 to 1.7 $\mu g/m^3$ and were consistent within each geographical area, with similar values in Yolo and Placer Counties and higher levels in Los Angeles County (Table 2). The indoor acrolein concentrations (2.1−12.2 $\mu g/m^3$) were approximately 10 times higher than the outdoor concentrations, and were similar in all the homes except YO-01 and YO-02 (Table 2). These two houses had both a.m. and p.m. acrolein concentrations that were approximately twice that of the other homes. There were no apparent relationships between indoor acrolein levels and the type of house heating or cooking appliances (natural gas or electric), floor coverings (carpeting, wood, or tile), recent remodeling (new furniture, paint and tile work in the past 6 months), or the use of candles, incense, and air fresheners. There was a strong correlation (Pearson correlation, $r = 0.72$, $p < 0.05$) between temperature and the a.m.−p.m. changes in indoor acrolein levels, but not outdoor concentrations of acrolein ($r = 0.06$). The relative humidity had a moderate inverse correlation with the a.m.−p.m. acrolein changes both inside ($r = -0.52$, $p < 0.15$) and outside ($r = -0.54$, $p < 0.15$). However, this may be the result of the negative correlation between relative humidity and temperature.

Indoor acrolein concentrations in the unoccupied model and new homes were also similarly elevated compared to the outside air. The new homes had indoor a.m. acrolein levels (3.0 $\mu g/m^3$) comparable to thos of the occupied homes (2.9 $\mu g/m^3$ excluding YO-01 and YO-02), while the furnished model homes were nearly 70% higher (5.0 $\mu g/m^3$).

**a.m./p.m. Acrolein Concentrations.** In all homes, the indoor p.m. concentrations of acrolein were significantly higher (paired $t$-test, $P < 0.003$) than the a.m. levels (Table 2). The greatest a.m.-to-p.m. increases were in homes where cooking activities were occurring at the time of p.m. sample collection (YO-01, LA-02, LA-03), however increases also occurred in homes where no human activities occurred (the residents were absent during the day at PL-01 and PL-02).

**TABLE 3. Indoor Acrolein Source Rate**

| | source rate (mg/h) | | |
|---|---|---|---|
| house | a.m. | p.m. | avg |
| YO-01 | 0.95 | 1.46 | 1.20 |
| YO-02 | 0.31 | 0.34 | 0.33 |
| YO-03 | 0.41 | 0.48 | 0.44 |
| average ± SD | 0.56 | 0.76 | 0.66 |
| LA-01 | 0.31 | 0.48 | 0.40 |
| LA-02 | 0.27 | 0.72 | 0.50 |
| LA-03 | 0.16 | 1.04 | 0.60 |
| average ± SD | 0.25 | 0.75 | 0.50 |
| PL-01 | 0.34 | 0.52 | 0.43 |
| PL-02 | 0.41 | 0.86 | 0.73 |
| PL-03 | 0.33 | 0.53 | 0.43 |
| average ± SD | 0.33 | 0.53 | 0.43 |
| average ± SD (all homes) | 0.41 ± 0.23 | 0.72 ± 0.20 | 0.56 ± 0.27 |

Outdoor acrolein concentrations also increased at six of the nine home sites from a.m. to p.m., although the increases and resultant levels were much less dramatic than those seen indoors.

**Acrolein Source Strength of Homes.** The acrolein source emission rate or source strength ($S$) of each home was calculated using the following formula:

$$S = (\mathrm{AER} + k_{acr}) \times V \times (C_{in} - C_{out}) \quad (1)$$

where $S$ = source strength ($\mu g/h$), AER = air exchange rate ($h^{-1}$), $k_{acr} = 0.0935\ h^{-1}$ (indoor disappearance rate constant for acrolein, from (*29*)), $V$ = house volume ($m^3$), $C_{in}$ = indoor acrolein concentration ($\mu g/m^3$), and $C_{out}$ = outdoor acrolein concentration ($\mu g/m^3$).

The source strength was higher in the p.m. than the a.m. in all homes (Table 3). The greatest increases were seen in LA-02, where the resident baked a ham and cooked numerous dishes containing both animal and vegetable fats prior to the p.m. sampling, and LA-03, the small duplex unit where the resident was sautéing fish and vegetables on the stove during sampling. The homes with the smallest increase, YO-02 and YO-03, were characterized by both a.m. and p.m.

**TABLE 4. Acrolein Emissions from Building Materials and Wood**

| sample | acrolein emission[a] |
|---|---|
| **building material** | |
| nylon carpet | N.D. |
| wood adhesive | N.D. |
| latex paint | 0.35 ± 0.08 |
| drywall | N.D. |
| particle board | 1.0 ± 0.045 |
| **lumber species** | |
| Douglas fir | 8.1 ± 0.90 |
| pine | 5.9 ± 0.55 |
| "yellow poplar" | 1.0 ± 0.053 |
| red oak | 1.0 ± 0.14 |
| redwood lumber | 1.3 ± 0.41 |
| redwood (fresh) | N.D. |

[a] ng acrolein/g of material ($n$ = 3). N.D. = below the limit of quantification.

cooking. The overall average source rate for acrolein was 0.56 ± 0.27 mg/h and the increase from a.m. to p.m. (>175%) is highly significant (paired $t$-test, $P < 0.003$).

**Indoor/Outdoor Concentrations of Other Carbonyls.** While this research focused on acrolein concentrations, many other carbonyls were also detected and quantified (see Table S1, Supporting Information). For almost all compounds, the levels in indoor air were higher than those outdoors. Furaldehyde, benzaldehyde, and the $C_5$–$C_{10}$ $n$-aldehydes were found in the greatest concentrations.

**Aldehyde Emissions from Building Materials.** The acrolein emission data from building materials appears in Table 4. The pine and Douglas fir wood, which are commonly used for framing houses, had the highest acrolein emission rates. "Yellow poplar", oak, redwood, and particleboard, which consists of wood particles and adhesives, also emitted moderately high concentrations of acrolein. Interestingly, no acrolein emissions were detected from the fresh redwood. Trace amounts of acrolein were produced by the latex paint, but none were produced by the drywall, construction adhesive, and nylon carpet samples. Overall, the lumber samples appeared to give greater direct aldehyde emissions compared to synthetic materials. We again note that because the surface areas of the samples were not determined and no attempt was made to quantify secondary emissions from reactions of VOCs with ozone or other oxidants, so these conclusions are at best a partial description of the building materials emissions.

In addition to acrolein, the building materials emitted a variety of other volatile carbonyls. The interior latex paint emitted large amounts of glycolaldehyde, benzaldehyde, and glyoxal, but only traces of other aldehydes. The $n$-aldehydes were among the most abundant compounds detected in the pine and fir samples. The red oak samples were associated with a definite odor and emitted large amounts of furaldehyde and 2,4-hexadienal. The drywall, construction adhesive, and nylon carpet samples showed little or no aldehyde emission. The quantitative results for all of the aldehydes are presented in Tables S2 and S3, Supporting Information.

## Discussion

The major finding of this study was that indoor concentrations of acrolein, one of the top hazardous air pollutants (HAPS) identified by the U.S. EPA and a known pulmonary toxicant, were 3–40 times higher than outdoor concentrations measured at the same time. The indoor concentrations ranged from 2.1 to 12.2 $\mu g/m^3$, and are consistent with previously published indoor values (*1*, *26*), although they were higher than those found in the RIOPA study (*24*). Outdoor concentrations, which averaged 0.63 $\mu g/m^3$ (0.09–1.7 $\mu g/m^3$), were highest in Los Angeles and are similar to the CARB ambient monitoring values and others reported in the literature (*1*, *2*, *24*). This value is more than four times higher than the EPA estimated average for California (0.157 $\mu g/m^3$)(*14*) providing evidence that the EPA model significantly underestimates ambient levels of acrolein. Outdoor concentrations increased from a.m. to p.m. at six of the nine home sites. The higher a.m. concentrations at the remaining three homes can possibly be explained by weather (evening rain at PL-03), geography (off-shore wind blowing off of Los Angeles in a.m., on-shore wind blowing off the ocean in p.m. at LA-03), and environmental sources (fresh paint applied adjacent to LA-01 in a.m.). There was no apparent relationship between the indoor and outdoor acrolein levels. In fact, the homes with the lowest indoor levels were located in Los Angeles, which was the area with the highest outdoor levels (Table 2). This would suggest that indoor acrolein levels are the result of indoor production and emissions and are not normally influenced by the outdoor air. Although the sample size was relatively small ($n$ = 9), the homes varied in their location, style, size, age, and occupants and thus should be an adequate representation of common residences. The strong correlation between the indoor a.m.–p.m. levels of acrolein and temperature suggests that a combination of fixed sources, such as off-gassing from wood, combined with human activities such as cooking, account for the high indoor levels of acrolein.

Off-gassing of acrolein from indoor sources is also supported by the fact that during the diurnal measurements at YO-01 the changes in acrolein levels coincided with changes in temperature while benzaldehyde, a much less volatile compound, showed only a slight temperature dependence. This pattern was seen in all of the homes, as a.m. to p.m. increases in acrolein concentrations occurred even in the absence of human activity (PL-02). The high quantities of acrolein emitted by pine and fir lumber along with the elevated acrolein concentrations found in the new, unoccupied homes both provide evidence that off-gassing from wood is a potential source of indoor acrolein. The observation that no acrolein was detected in the freshly cut redwood sample, while the redwood lumber had significant acrolein emissions, suggests that acrolein is a decomposition product which is released as the wood ages. This would also explain prolonged emissions by wood products used in home construction. The fact that the model homes (fully furnished and decorated) had indoor acrolein concentrations averaging 1.5× greater than those of the new homes (no furniture or decorative items) indicates that primary emissions of acrolein from furniture and/or secondary formation via oxidation of other emitted VOC's may also be occurring.

Numerous studies have shown that acrolein is produced by heated animal and vegetable oils (*11*, *30*–*32*). During the diurnal measurements at YO-01, it was noted that cooking events coincided with a noticeable "spike" in the indoor acrolein concentration (Figure 1). The residents of the homes with the highest a.m. and p.m. levels of indoor acrolein (YO-01 and YO-02) reported cooking stir-fried meals on a daily basis. One possible explanation for this is that acrolein may accumulate in indoor air when large amounts are produced on a continual basis. The greatest a.m.-to-p.m. increases were in homes where cooking activities were occurring at the time of p.m. sample collection (YO-01, LA-02, LA-03). These observations provide strong evidence that cooking is a significant source of acrolein in occupied homes.

It is evident from these data that indoor acrolein concentrations in residential homes are the result of both fixed sources and human activities. The nearly twofold increase in the source rate from a.m. to p.m. (0.41–0.72 mg/h) reflects the contributions of human activities and increased

fixed source emissions throughout the day. The overall average indoor source rate for acrolein was 0.56 ± 0.27 mg/h.

The concentrations of acrolein determined in this study contrast with those of the recent RIOPA study that sampled 234 homes (*24*). The RIOPA study found no statistically significant indoor/outdoor differences for acrolein, although all 9 of the other compounds quantified showed higher concentrations indoors. The median indoor acrolein concentration was reported as 0.59 $\mu g/m^3$ compared to a median outdoor concentration of 0.46 $\mu g/m^3$ (*24*). However, both these median values are close to the reported limit of detection of 0.14 $\mu g/m^3$ (*33*) and only 68% of the outdoor samples and 71% of the indoor samples were above the detection limit (*24*). Therefore, the failure of the RIOPA data to identify a significant indoor−outdoor difference in Acrolein concentrations may have been due to difficulties associated with quantifying values near the limit of detection. In contrast, the current study sampled a more limited number of houses (9 active homes and 6 model/new houses). However, the analytical method was able to detect acrolein in all the indoor and outdoor samples at concentrations that were 61 and 67 times greater than the limit of detection, respectively, which resulted in very precise quantification of acrolein with an average difference between field replicates of 8.9%. The precise acrolein measurements combined with multiple replicates per house resulted in statistically significant differences in indoor and outdoor acrolein concentrations despite a smaller sample set of houses. The acrolein results presented here are consistent with those of the other 9 carbonyls quantified in the RIOPA study which all showed statistically higher concentrations indoors.

The observed indoor acrolein concentrations result from direct acrolein emission and possibly the oxidation of other volatile indoor chemicals. The data collected from the houses cannot differentiate between primary acrolein emission and secondary formation. However, the increase in acrolein concentrations after cooking suggests a significant contribution from primary emissions. The sources of the background concentrations which occur in the absence of human activity are likely numerous and complex. Wood used for framing and construction is a probable primary source for acrolein and other aldehydes, which were also found indoors in elevated concentrations. The oxidation of other organic chemicals may also be source of acrolein that should be investigated.

These results suggest that human exposure to acrolein will be dominated by indoor exposure because people commonly spend more time indoors than outdoors. The identification of specific primary and secondary sources of indoor acrolein could be used to develop mitigation measures. In light of these findings, the rationale of regulating ambient air concentrations of acrolein to reduce human exposures is questionable and efforts should be focused on understanding sources in the indoor environment.

## Acknowledgments

We are indebted to Skip Huckaby for providing technical expertise in making and optimizing the mist chambers, Lissa and Mike Phlegar for making the model homes available for sample collection; and Kathy Fitzgerald for providing access to the newly constructed homes. We also thank all of our participants for allowing us to use their homes for this study. The chemical analyses and air exchange rate data were generated at the Harvard School of Public Health by Robert A. Weker (currently with MIT, Department of Environment, Health and Safety).

## Supporting Information Available

Table S1 contains the indoor and outdoor concentrations of carbonyls in Yolo, Los Angeles, and Place Counties. Table S2 provides the carbonyl emission data from common building materials. Table S3 details the carbonyls emitted from different species of lumber. This material is available free of charge via the Internet at http://pubs.acs.org.

## Literature Cited

(1) CICAD. *Concise International Chemical Assessment Document (Acrolein)*; World Health Organization, 2002; p 43.
(2) Ghilarducci, D. P.; Tjeerdema, R. S. Fate and effects of acrolein. *Rev. Environ. Contam. Toxicol.* **1995**, *144*, 95−146.
(3) Agency for Toxic Substances and Disease Registry. *A Toxicological Profile for Acrolein*; U.S. Public Health Service, USPHS: Washington, DC, 1990.
(4) Alarie, Y. Sensory Irritation by Airborne Chemicals. *CRC Crit. Rev. Toxicol.* **1973**, *2*, 2999−363.
(5) Grafstrom, R. C.; Dypbukt, J. M.; Willey, J. C.; Sundqvist, K.; Edman, C.; Atzori, L.; Harris, C. C. Pathobiological Effects of Acrolein in Cultured Human Bronchial Epithelial-Cells. *Cancer Res.* **1988**, *48* (7), 1717−1721.
(6) Kehrer, J. P.; Biswal, S. S. The molecular effects of acrolein. *Toxicol. Sci.* **2000**, *57* (1), 6−15.
(7) Monteil, C.; Le Prieur, E.; Buisson, S.; Morin, J. P.; Guerbet, M.; Jouany, J. M. Acrolein toxicity: comparative in vitro study with lung slices and pneumocytes type II cell line from rats. *Toxicology* **1999**, *133* (2−3), 129−138.
(8) Prabhu, S. D.; Srivastava, S.; Chandrasekar, B.; Yan, G.; Bolanowski, D.; Ortines, R.; Ping, P. P.; Bhatnagar, A. Chronic exposure to acrolein, an environmental Aldehydic pollutant, causes myocardial oxidative stress, inflammation and dilated cardiomyopathy. *Circulation* **2003**, *108* (17), 58−58.
(9) Biswal, S.; Maxwell, T.; Rangasamy, T.; Kehrer, J. P. Modulation of benzo a pyrene-induced p53 DNA activity by acrolein. *Carcinogenesis* **2003**, *24* (8), 1401−1406.
(10) Leikauf, G. D. Hazardous air pollutants and asthma. *Environ. Health Perspect.* **2002**, *110*, 505−526.
(11) Yu, I. T. S.; Chiu, Y. L.; Au, J. S. K.; Wong, T. W.; Tang, J. L. Dose-response relationship between cooking fumes exposures and lung cancer among Chinese nonsmoking women. *Cancer Res.* **2006**, *66* (9), 4961−4967.
(12) Woodruff, T. J.; Wells, E. M.; Holt, E. W.; Burgin, D. E.; Axelrad, D. A. Estimating risk from ambient concentrations of acrolein across the United States. *Environ. Health Perspect.* **2007**, *115* (3), 410−415.
(13) U.S. Environmental Protection Agency. *Toxicological Review of Acrolein*; Environmental Protection Agency: Washington, DC, 2003.
(14) U.S. Environmental Protection Agency. *National-Scale Air Toxics Assessment*; Environmental Protection Agency: Washington, DC, 2002.
(15) Morello-Frosch, R. A.; Woodruff, T. J.; Axelrad, D. A.; Caldwell, J. C. Air toxics and health risks in California: The public health implications of outdoor concentrations. *Risk Anal.* **2000**, *20* (2), 273−291.
(16) California Air Resources Board. *Aerometric Data Analysis and Management system (ADAM), Air Toxics Summary*; www.arb.ca.gov/adam/toxics.
(17) Ho, S. S. H.; Yu, J. Z. Concentrations of formaldehyde and other carbonyls in environments affected by incense burning. *J. Environ. Monitor.* **2002**, *4* (5), 728−733.
(18) Morrison, G. C.; Nazaroff, W. W. Ozone interactions with carpet: Secondary emissions of aldehydes. *Environ. Sci. Technol.* **2002**, *36* (10), 2185−2192.
(19) Hess-Kosa, K. *Indoor Air Quality*; Lewis Publishers: Boca Raton, FL, 2002; p 300.
(20) Zhang, J. F.; He, Q. C.; Lioy, P. J. Characteristics of Aldehydes - Concentrations, Sources, and Exposures for Indoor and Outdoor Residential Microenvironments. *Environ. Sci. Technol.* **1994**, *28* (1), 146−152.
(21) Feng, Y. L.; Zhu, J. P. Separation and determination of carbonyl compounds in indoor air using two-step gradient capillary electrochromatography. *Anal. Sci.* **2004**, *20* (12), 1691−1695.
(22) Highsmith, V. R.; Zweidinger, R. B.; Merrill, R. G. Characterization of Indoor and Outdoor Air Associated with Residences Using Woodstoves - a Pilot-Study. *Environ. Int.* **1988**, *14* (3), 213−219.

(23) Lindstrom, A. B.; Proffitt, D.; Fortune, C. R. Effects of modified residential construction on indoor air quality. *Indoor Air* **1995**, *5* (4), 258−269.
(24) Liu, W.; Zhang, J.; Zhang, L.; Turpin, B. J.; Weisel, C. P.; Morandi, M. T.; Stock, T. H.; Colome, S.; Korn, L. R. Estimating contributions of indoor and outdoor sources to indoor carbonyl concentrations in three urban areas of the United States. *Atmos. Environ.* **2006**, *40* (12), 2202−2214.
(25) Meininghaus, R.; Bastin, E.; Bourder, S.; Cicolella, A.; Granier, D.; Gonzalez-Flesca, N. *Indoor and outdoor aldehyde concentrations in a medium-sized French town*; International Conference on Air Pollution IX, Ancona, Italy, 2001; Latini, G., Brebbia, C. A., Eds.; Ancona, Italy, 2001; pp 263−273.
(26) Gilbert, N. L.; Guay, M.; Miller, J. D.; Judek, S.; Chan, C. C.; Dales, R. E. Levels and determinants of formaldehyde, acetaldehyde, and acrolein in residential indoor air in Prince Edward Island, Canada. *Environ. Res.* **2005**, *99* (1), 11−17.
(27) Seaman, V. Y.; Charles, M. J.; Cahill, T. M. A sensitive method for the quantification of acrolein and other volatile carbonyls in ambient air. *Anal. Chem.* **2006**, *78* (7), 2405−2412.
(28) Dietz, R. N.; Goodrich, R. W.; Cote, E. A.; Wieser, F. Detailed Description and Performance of a Passive Perfluorocarbon Tracer System for Building Ventilation and Air Exchange Measurements. In *Measured Air Leakage of Buildings*, Trechel, H. R., Ed.; American Society for Testing and Materials: Philadelphia, PA, 1986; Vol. STP 904, pp 203−253.
(29) Seaman, V. Y. The Origin and Occurrence of Acrolein in Ambient Air. University of California, Davis, Davis, CA, 2006.
(30) Casella, I. G.; Contursi, M. Quantitative analysis of acrolein in heated vegetable oils by liquid chromatography with pulsed electrochemical detection. *J. Agric. Food Chem.* **2004**, *52* (19), 5816−5821.
(31) Svendsen, K.; Jensen, H. N.; Sivertsen, I.; Sjaastad, K. Exposure to cooking fumes in restaurant kitchens in Norway. *Ann. Occup. Hyg.* **2002**, *46* (4), 395−400.
(32) Umano, K.; Shibamoto, T. Analysis of Acrolein from Heated Cooking Oils and Beef Fat. *J. Agric. Food Chem.* **1987**, *35* (6), 909−912.
(33) Weisel, C. P.; Zhang, J. F.; Turpin, B. J.; Morandi, M. T.; Colome, S.; Stock, T. H.; Spektor, D. M.; Korn, L.; Winer, A.; Alimokhtari, S.; Kwon, J.; Mohan, K.; Harrington, R.; Giovanetti, R.; Cui, W.; Afshar, M.; Maberti, S.; Shendell, D. Relationship of Indoor, Outdoor and Personal Air (RIOPA) Study: Study design, methods and quality assurance/control results. *J. Exposure Anal. Environ. Epidemiol.* **2005**, *15* (2), 123−137.

*Received for review March 26, 2007. Revised manuscript received July 30, 2007. Accepted July 31, 2007.*

ES0707299